Supporting Information

Fluoride-Ion-Catalyzed Synthesis of Ladder-type Conjugated Benzobisbenzofurans via Intramolecular Nucleophilic Aromatic Substitution Reaction under Metal-free and Mild Conditions

*Katsutoshi Sekino,[†] Naoki Shida,[†] Ryosuke Shiki,[†] Natsuki Takigawa,[†] Hiroki Nishiyama,[†] Ikuyoshi Tomita,[†] Shinsuke Inagi[†‡]**

[†]Department of Chemical Science and Engineering, School of Materials and Chemical Technology, Tokyo Institute of Technology, 4259 Nagatsuta-cho, Midori-ku, Yokohama 226-8502, Japan, Tel: +81-45-924-5407, Fax: +81-45-924-5407
E-mail: inagi@cap.mac.titech.ac.jp
[‡]PRESTO, Japan Science and Technology Agency (JST), 4-1-8 Honcho, Kawaguchi, Saitama 332-0012, Japan

Contents

Experimental

1. General considerations

All reagents and dehydrated solvents were obtained from commercial source and used without further purification unless otherwise noted. ^{1}H, ^{13}C and ^{19}F NMR spectra were recorded on JEOL JNM-ECP300 (^{1}H: 300 MHz, ^{19}F: 282.23 MHz) spectrometer, Bruker Advance III HD400 (^{1}H: 400.13 MHz, ^{19}F: 376.31 MHz) spectrometer and Bruker Advance III HD500 (^{13}C: 125.72 MHz) spectrometer using $CDCl_3$ as a solvent. Silicon oil bath was used as a heat source for the reactions. The chemical shifts for ^{1}H, ^{13}C and ^{19}F NMR spectra are given in δ (ppm) relative to internal TMS, $CDCl_3$, and monofluorobenzene respectively. Fourier transform infrared (FT-IR) spectra were obtained on SHIMADZU IRTracer-100. High-resolution mass spectra (HRMS) were obtained on a JEOL JMS-700 spectrometer or a Bruker Daltonics micrOTOF II spectrometer. The cyclic voltammetry (CV) measurements were performed using ALS/DY2325 BI-POTENTIOSTAT. All CV measurements were carried out in the three-electrode system equipped with a Pt disk working electrode (ϕ = 1 mm), a Pt plate counter electrode (10 mm × 10 mm) and a SCE reference electrode in CH_2Cl_2 solution of *n*-Bu_4NPF_6 (0.1 M) at scan rate of 100 mVs^{-1}. UV-vis absorption spectra were recorded in $CHCl_3$ a SHIMADZU UV-1800. Fluorescence (FL) spectra were obtained on a SHIMADZU RF-6000 spectrophotometer. The single crystals suitable for X-ray diffraction were obtained by a $CHCl_3$ solution at room temperature. The single crystal X-ray analyses were carried out on a Rigaku XtaLAB Synergy-DW (with) Hybrid Photon Counting (HPC) detector (Cu Kα radiation, λ= 1.54184 Å). An empirical absorption correction was carried out by the MULTI-SCAN method. The structures were solved by the SHELXT (SHELX2014) using OLEX2 software. The non-hydrogen atoms were refined anisotropically. Hydrogen atoms were refined using the riding model. All calculations were performed using Gaussian 16 software. Geometry optimizations and frequency calculations were performed for all compounds at the B3LYP or ωB97XD level of theory using 6-31G(d) or def2TZVP basis set for all atoms. Single point calculations were performed at B3LYP, ωB97XD or B3LYP-D3 level of theory using 6-311G+(2df,2p) basis set for all atoms. In specific cases, the solvation of DMF was taken into account with the polarizable continuum model (PCM) using the integral equation formalism variant. Ground states and transition states were confirmed by frequencies analysis (no imaginary frequencies and one imaginary frequency, respectively). IRC analyses of transition states led to postulated ground states. Elemental analyses were carried out at J-SCIENCE MICRO CORDER JM10 for C, H and N, Elementar Vario micro cube for O, and Yanaco HSU-20+ICS-1100 for F.

2. Synthesis

2-1. Synthesis of 1a-1c

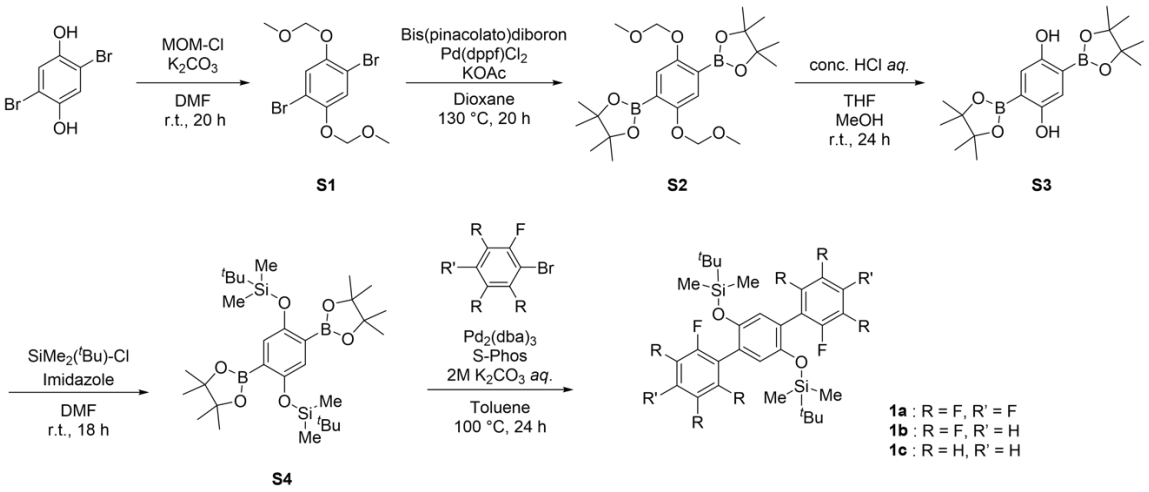

Scheme S1. Synthesis of **1a-c**

*Synthesis of 1,4-dibromo-2,5-bis(methoxymethoxy)benzene (**S1**)*

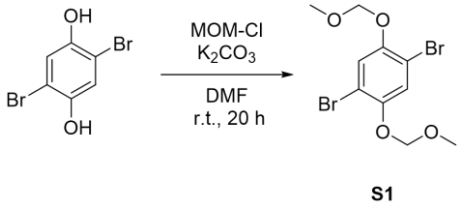

To a DMF solution (15 mL) of 2,5-dibromohydroquinone (500.0 mg, 1.87 mmol) was added successively K_2CO_3 (2.064 g, 14.9 mmol) and chloromethyl methyl ether (0.42 mL, 5.60 mmol) at 0 °C under an argon atmosphere. The mixture was stirred at room temperature for 20 h. After quenching by addition of distilled water, the resulting mixture was extracted with Et_2O. The organic layer was washed with distilled water and dried over anhydrous Na_2SO_4. After filtration and removal of the solvent, the residue was purified by silica gel column chromatography using hexane/ethyl acetate (9/1) to give a white solid (544.7 mg, 82%).

S1: white solid; ^{1}H NMR (400.13 MHz, $CDCl_3$, ppm): δ = 7.37 (s, 2H, Ar), 5.17 (s, 4H, OC*H*$_2$OCH$_3$), 3.52 (s, 6H, OCH$_2$OC*H*$_3$); ^{13}C NMR (125.72 MHz, $CDCl_3$, ppm): δ = 149.5 (s, Ar), 121.2 (s, Ar), 112.2 (s, Ar), 96.0 (s, O*C*H$_2$OCH$_3$), 56.6 (s, OCH$_2$O*C*H$_3$).

*Synthesis of 2,2'-(2,5-bis(methoxymethoxy)-1,4-phenylene)bis(4,4,5,5-tetramethyl-1,3,2-dioxaborolane) (**S2**)*

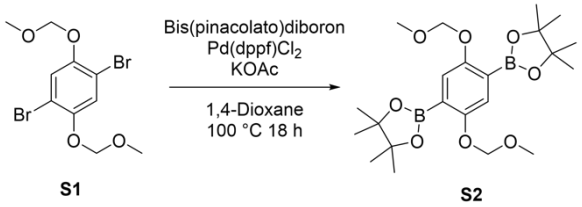

A solution of **S1** (3.300 g, 9.27 mmol), dried KOAc (5.458 g, 55.6 mmol), bis(pinacolato)diboron (5.179 g, 20.4 mmol) and [1,1'-bis(diphenylphosphino)ferrocene]dichloropalladium(II) (678.2 mg, 0.93 mmol) in 1,4-dioxane (70 mL) was stirred at 100 °C for 20 h under an argon atmosphere. After quenching by addition of distilled water, the resulting mixture was extracted with ethyl acetate. The organic layer was washed with distilled water and dried over anhydrous Na_2SO_4. After filtration over celite and the removal of the solvent, black oily product was obtained (8.512 g). Bis(pinacolato)diboron-derived residue remained as an inseparable impurity under any chromatographic conditions, so crude material was used for the next reaction.

S2: ^{1}H NMR (300 MHz, $CDCl_3$, ppm): δ = 7.29 (s, 2H, Ar), 5.15 (s, 4H, OC*H*$_2$OCH$_3$), 3.53 (s, 6H, OCH$_2$OC*H*$_3$), 1.26 (s, 24H, OC(C*H*$_3$)$_2$); HRMS (ESI) calcd for $C_{22}H_{36}B_2NaO_8$ ($[M + Na]^+$) *m/z* 473.2494, found 473.2489.

*Synthesis of 2,5-bis(4,4,5,5-tetramethyl-1,3,2-dioxaborolan-2-yl)benzene-1,4-diol (**S3**)*

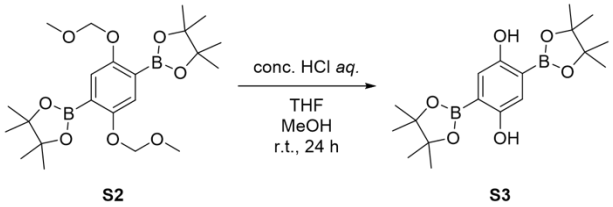

To a THF (32 mL) and MeOH (18 mL) solution of **S2** (8.512 g, crude material) was added conc. HCl aq. (10.0 mL, 120 mmol) under an argon atmosphere. The mixture was stirred at room temperature for 24 h. After addition of ice water, the resulting mixture was extracted with CH_2Cl_2. The organic layer was washed with distilled water and dried over anhydrous Na_2SO_4. After filtration and removal of the solvent, black oily product was obtained (2.882 g). Bis(pinacolato)diboron-derived residue remained as an inseparable impurity under any chromatographic conditions, so crude material was used for the next reaction.

S3: ^{1}H NMR (300 MHz, $CDCl_3$, ppm): δ = 7.30 (s, 2H, O*H*), 7.11 (s, 2H, Ar), 1.26 (s,

24H, OC(CH_3)$_2$); HRMS (ESI) calcd for $C_{18}H_{28}B_2NaO_6$ ([M + Na]$^+$) *m/z* 385.1970, found 385.1964.

*Synthesis of ((2,5-bis(4,4,5,5-tetramethyl-1,3,2-dioxaborolan-2-yl)-1,4-phenylene)bis(oxy))bis(tert-butyldimethylsilane) (**S4**)*

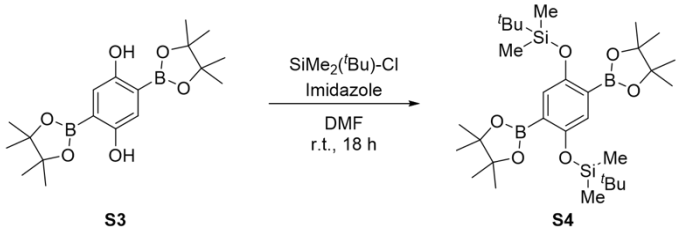

S3 **S4**

To a DMF solution (40 mL) of **S3** (2.882 g, crude material) and imidazole (3.597 g, 52.8 mmol) was added *tert*-butyldimethylchlorosilane (3.514 g, 23.3 mmol) under an argon atmosphere. The mixture was stirred at room temperature for 18 h. After quenching by addition of distilled water, the resulting mixture was extracted with $CHCl_3$. The organic layer was washed with distilled water and dried over anhydrous Na_2SO_4. After filtration and removal of the solvent, the residue was purified by silica gel column chromatography using hexane/$CHCl_3$/ethyl acetate (16/2/1) and washed with hexane to give a white solid (1.189 g, total yield of 22% over 3 steps from **S1**).

S4: white solid; m.p. 213.7–214.7 °C; ^{1}H NMR (300 MHz, $CDCl_3$, ppm): δ = 7.07 (s, 2H, Ar), 1.30 (s, 24H, OC(CH_3)$_2$), 1.01 (s, 18H, Si(CH_3)$_2$C(CH_3)$_3$), 0.18 (s, 12H, Si(CH_3)$_2$C(CH_3)$_3$); ^{13}C NMR (125.72 MHz, $CDCl_3$, ppm): δ = 153.9 (s, Ar), 127.3 (s, Ar), 83.4 (s, O*C*(CH_3)$_2$), 26.1 (s, Si(CH_3)$_2$*C*(CH_3)$_3$), 25.1 (s, Si(CH_3)$_2$C(*C*H$_3$)$_3$), 18.5 (s, OC(*C*H$_3$)$_2$), −4.2 (s, Si(*C*H$_3$)$_2$C(CH_3)$_3$); HRMS (FAB, matrix = NBA) calcd for $C_{30}H_{56}B_2O_6Si_2$ ([M]$^+$) *m/z* 590.3802, found 590.3808; IR (KBr, cm^{-1}): 2979, 2966, 2941, 2896, 2860, 1490, 1398, 1371, 1325, 1290, 1275, 1246, 1196, 1142, 1090, 991, 964, 932, 908, 860, 841, 812, 796, 777, 692,682.

*Suzuki-coupling reaction of **S4** with arylbromide to give **1a-c***

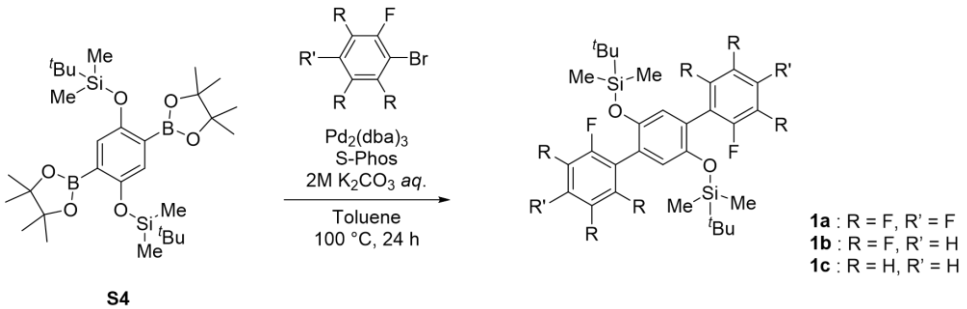

S4

To a toluene solution of tris(dibenzylideneacetone)dipalladium(0) (0.05 eq.) and 2-

dicyclohexylphosphino-2',6'-dimethoxybiphenyl (0.1 eq.) was added **S4** (1.0 eq.), bromofluorobenzene (2.5 eq.) and 2 M K_2CO_3 aq. (14 eq.) under an argon atmosphere, then the mixture was stirred at 100 °C for 24 h. After cooling to room temperature, the resulting mixture was extracted with $CHCl_3$. The organic layer was washed with distilled water and dried over anhydrous Na_2SO_4. After filtration over celite and removal of the solvent, the residue was purified by silica gel column chromatography to give the desired product.

Synthesis of 1a: Tris(dibenzylideneacetone)dipalladium(0) (15.5 mg, 17 μmol), 2-dicyclohexylphosphino-2',6'-dimethoxybiphenyl (13.9 mg, 34 μmol), **S4 (**200 mg, 0.34 mmol), bromopentafluorobenzene (214.3 mg, 0.87 mmol), 2 M K_2CO_3 aq. (2.4 mL, 4.8 mmol), and toluene (3.4 mL). Hexane/$CHCl_3$ (19/1) was used as an eluent for column chromatography to give a white solid (198 mg, 87%).

1a: white solid; m.p. 180.5–181.9 °C; ^{1}H NMR (400.13 MHz, $CDCl_3$, ppm): δ = 6.81 (s, 2H, Ar), 0.80 (s, 18H, $Si(CH_3)_2C(C\mathit{H}_3)_3$), 0.06 (s, 12H, $Si(C\mathit{H}_3)_2C(CH_3)_3$); ^{13}C NMR (125.72 MHz, $CDCl_3$, ppm): δ = 147.5 (s, Ar), 145.6-143.5 (m, *C*F), 142.0-139.7 (m, *C*F), 138.9-136.7 (m, *C*F), 122.4 (s, Ar), 120.1 (s, Ar), 112.7 (dt, *J* = 18.8 Hz, 3.7 Hz, Ar), 25.4 (s, $Si(CH_3)_2\mathit{C}(CH_3)_3$), 17.9 (s, $Si(CH_3)_2C(\mathit{C}H_3)_3$), –4.6 (s, $Si(\mathit{C}H_3)_2C(CH_3)_3$); ^{19}F NMR (376.31 MHz, $CDCl_3$, ppm): δ = –139.60 (dd, *J* = 23.1 Hz, 8.2 Hz, 4F), –155.50 (t, *J* = 20.8 Hz, 2F), –163.12 (dt, *J* = 23.7 Hz, 7.3 Hz, 4F); HRMS (FAB, matrix = NBA) calcd for $C_{30}H_{32}F_{10}O_2Si_2$ ($[M]^+$) *m/z* 670.1781, found 670.1788; IR (KBr, cm^{-1}): 2953, 2932, 2899, 2862, 1651, 1528, 1506, 1472, 1437, 1389, 1310, 1260, 1231, 1069, 993, 941, 876, 853, 802, 781, 691.

Synthesis of 1b: Tris(dibenzylideneacetone)dipalladium(0) (16.6 mg, 18 μmol), 2-dicyclohexylphosphino-2',6'-dimethoxybiphenyl (14.3 mg, 35 μmol), **S4** (201 mg, 0.34 mmol), 1-bromo-2,3,5,6-tetrafluorobenzene (194 mg, 0.85 mmol), 2 M K_2CO_3 aq. (2.4 mL, 4.8 mmol), and toluene (3.4 mL). Hexane/$CHCl_3$ (19/1) was used as an eluent for column chromatography to give a white solid (137 mg, 63% yield).

1b: white solid; m.p. 176.0–177.1 °C; ^{1}H NMR (400.13 MHz, $CDCl_3$, ppm): δ = 7.14-7.06 (m, 2H, Ar), 6.84 (s, 2H, Ar), 0.79 (s, 18H, $Si(CH_3)_2C(C\mathit{H}_3)_3$), 0.05 (s, 12H, $Si(C\mathit{H}_3)_2C(CH_3)_3$); ^{13}C NMR (125.72 MHz, $CDCl_3$, ppm): δ = 147.4 (s, Ar), 147.3-145.0 (m, *C*F), 145.3-143.0 (m, *C*F), 122.3 (s, Ar), 121.1 (s, Ar), 118.5 (t, *J* = 17.9 Hz, Ar), 105.3 (t, *J* = 21.9 Hz, Ar), 25.4 (s, $Si(CH_3)_2\mathit{C}(CH_3)_3$), 17.9 (s, $Si(CH_3)_2C(\mathit{C}H_3)_3$), –4.7 (s, $Si(\mathit{C}H_3)_2C(CH_3)_3$); ^{19}F NMR (376.31 MHz, $CDCl_3$, ppm): δ = –140.16 (ddd, *J* = 22.1 Hz, 11.9 Hz, 4.4, 4F), –140.38 (ddd, *J* = 22.1 Hz, 11.9 Hz, 5.1 Hz, 4F); HRMS (FAB, matrix

= NBA) calcd for $C_{30}H_{34}F_8O_2Si_2$ ([M]$^+$) *m/z* 634.1970, found 634.1966; IR (KBr, cm^{-1}) : 2961, 2935, 2896, 2860, 1700, 1610, 1596, 1496, 1453, 1402, 1373, 1261, 1204, 1175, 1141, 946, 888, 873, 846, 802, 781, 714, 693.

Synthesis of 1c: Tris(dibenzylideneacetone)dipalladium(0) (16.3 mg, 18 μmol), 2-dicyclohexylphosphino-2',6'-dimethoxybiphenyl (13.9 mg, 34 μmol), **S4** (200 mg, 0.34 mmol), 2-bromofluorobenzene (149 mg, 0.85 mmol), 2M K_2CO_3 aq. (2.4 mL, 4.8 mmol), and toluene (3.4 mL). Hexane/$CHCl_3$ (19/1) was used as an eluent for column chromatography to give a white solid (123 mg, 69%).

1c: white solid; m.p. 156.2–157.0 °C; ^{1}H NMR (400.13 MHz, $CDCl_3$, ppm): δ = 7.39 (t, *J* = 7.5 Hz, 2H, Ar*H*), 7.32-7.29 (m, 2H, Ar*H*), 7.52 (t, *J* = 7.5 Hz, 2H, Ar*H*), 7.12 (t, *J* = 9.0 Hz, 2H, Ar*H*), 6.84 (s, 2H, Ar*H*), 0.76 (s, 18H, $Si(CH_3)_2C(CH_3)_3$), -0.058 (s, 12H, $Si(CH_3)_2C(CH_3)_3$); ^{13}C NMR (125.72 MHz, $CDCl_3$, ppm): δ =160.2 (d, *J* = 247.3 Hz, *C*F), 147.0 (s, Ar), 132.5 (d, *J* = 3.8 Hz, Ar), 129.1 (d, *J* = 8.2 Hz, Ar), 127.9 (s, Ar), 126.5 (d, *J* = 16.0 Hz, Ar), 123.7 (d, *J* = 3.6 Hz, Ar), 122.4 (s, Ar), 115.7 (d, *J* = 22.1 Hz, Ar), 25.6 (s, $Si(CH_3)_2C(CH_3)_3$), 18.1 (s, $Si(CH_3)_2C(CH_3)_3$), –4.6 (s, $Si(CH_3)_2C(CH_3)_3$); ^{19}F NMR (376.31 MHz, $CDCl_3$, ppm): δ = –114.40 (s, 2F); HRMS (FAB, matrix = NBA) calcd for $C_{30}H_{40}F_2O_2Si_2$ ([M]$^+$) *m/z* 526.2535, found 526.2535; IR (KBr, cm^{-1}): 2950, 2930, 2888, 2860, 1700, 1616, 1579, 1514, 1480, 1448, 1390, 1363, 1253, 1233, 1198, 1105, 1047, 1025, 925, 885, 839, 826, 802, 778, 763, 707, 691, 674.

2-2. Synthesis of 1d-1f

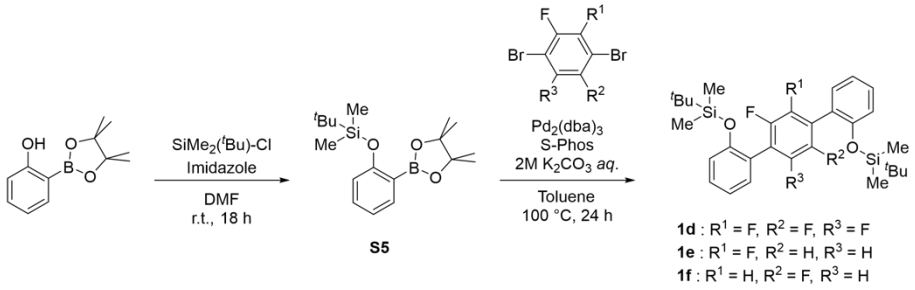

Scheme S2. Synthesis of **1d-f**

*Synthesis of tert-butyldimethyl(2-(4,4,5,5-tetramethyl-1,3,2-dioxaborolan-2-yl)phenoxy)silane (**S5**)*

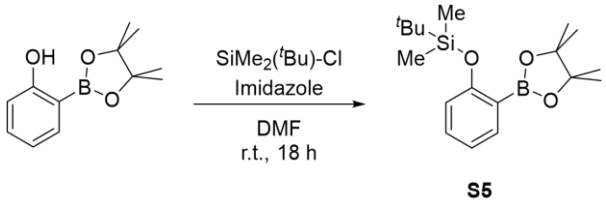

S5

To a DMF solution (30 mL) of 2-(4,4,5,5-tetramethyl-1,3,2-dioxaborolan-2-yl)phenol (2.000 g, 9.09 mmol) and imidazole (927.3 mg, 13.6 mmol) was added *tert*-butyldimethylchlorosilane (1.507 g, 10.0 mmol) under an argon atmosphere. The mixture was stirred at room temperature for 18 h. After quenching by addition of distilled water, the resulting mixture was extracted with Et_2O. The organic layer was washed with distilled water and dried over anhydrous Na_2SO_4. After filtration and removal of the solvent, the residue was purified by silica gel column chromatography using hexane/ethyl acetate (8/2) to give **S5** as colorless liquid (2.725 g, 90%).

S5: colorless oil; ^{1}H NMR (400.13 MHz, $CDCl_3$, ppm): δ = 7.69 (d, *J* = 5.8 Hz, 1H, Ar*H*), 7.28 (t, *J* = 6.9 Hz, 1H, Ar*H*), 6.92 (t, *J* = 7.3 Hz, 1H, Ar*H*), 6.78 (d, *J* = 8.2 Hz, 1H, Ar*H*), 1.32 (s, 12H, OC(C*H*$_3$)$_2$), 1.03 (s, 9H, Si(CH$_3$)$_2$C(C*H*$_3$)$_3$), 0.23 (s, 6H, Si(C*H*$_3$)$_2$C(CH$_3$)$_3$); ^{13}C NMR (125.72 MHz, $CDCl_3$, ppm): δ = 160.7 (s, Ar), 137.2 (s, Ar), 132.3 (s, Ar), 120.7 (s, Ar), 119.5 (s, Ar), 83.4 (s, O*C*(CH$_3$)$_2$), 26.0 (s, Si(CH$_3$)$_2$*C*(CH$_3$)$_3$), 25.1 (s, Si(CH$_3$)$_2$C(*C*H$_3$)$_3$), 18.5 (s, OC(*C*H$_3$)$_2$), –4.1 (s, Si(*C*H$_3$)$_2$C(CH$_3$)$_3$); HRMS (FAB, matrix = NBA) calcd for $C_{18}H_{32}BO_3Si$ ([M+H]$^+$) *m/z* 335.2208, found 335.2206; IR (KBr, neat, cm^{-1}): 3034, 2978, 2956, 2931, 2896, 2860, 1603, 1516, 1473, 1398, 1360, 1316, 1262, 1145, 1091, 963, 913, 861, 838, 800, 781, 741, 717, 672, 656.

*Suzuki-coupling reaction of **S5** with arylbromide to give **1d-f***

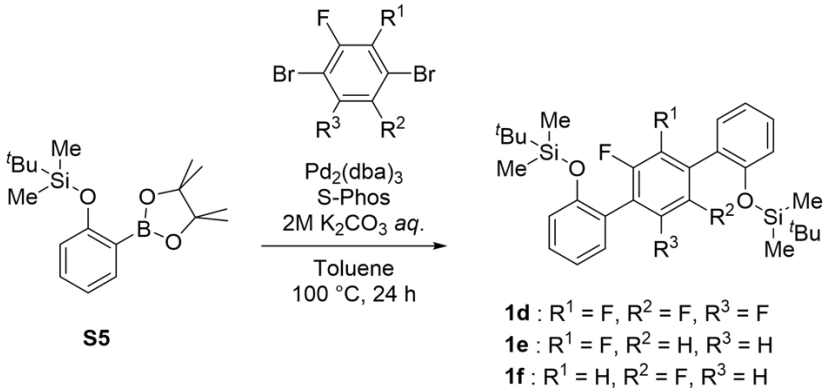

S5

1d : R^1 = F, R^2 = F, R^3 = F
1e : R^1 = F, R^2 = H, R^3 = H
1f : R^1 = H, R^2 = F, R^3 = H

To a toluene solution of tris(dibenzylideneacetone)dipalladium(0) (0.05 eq.) and 2-

dicyclohexylphosphino-2',6'-dimethoxybiphenyl (0.1 eq.) was added **S5** (2.5 eq.), dibromofluorobenzene (1.0 eq.) and 2 M K_2CO_3 aq. (14 eq.) under an argon atmosphere, then the mixture was stirred at 100 °C for 24 h. After cooling to room temperature, the resulting mixture was extracted with $CHCl_3$. The organic layer was washed with distilled water and dried over anhydrous Na_2SO_4. After filtration over celite and removal of the solvent, the residue was purified by silica gel column chromatography to give the desired product.

Synthesis of 1d: Tris(dibenzylideneacetone)dipalladium(0) (65.2 mg, 0.071 mmol), 2-dicyclohexylphosphino-2',6'-dimethoxybiphenyl (58.5 mg, 0.14 mmol), **S5** (1.000 g, 3.0 mmol), 1,4-dibromotetrafluorobenzene (438 mg, 1.4 mmol), 2M K_2CO_3 aq. (9.5 mL, 19 mmol), and toluene (14 mL). Hexane/$CHCl_3$ (19/1) was used as an eluent for column chromatography to give a white solid (756 mg, 94% yield).
1d: white solid; m.p. 163.0–164.1 °C; ^{1}H NMR (400.13 MHz, $CDCl_3$, ppm): δ = 7.38-7.33 (m, 2H, Ar), 7.30-7.24 (m, 2H, Ar), 7.10-7.04 (m, 2H, Ar), 7.10-7.04 (m, 2H, Ar), 7.01-6.97 (m, 2H, Ar), 0.85 (2s, 18H, $Si(CH_3)_2C(CH_3)_3$), 0.15 (2s, 12H, $Si(CH_3)_2C(CH_3)_3$); ^{13}C NMR (125.72 MHz, $CDCl_3$, ppm): δ = 153.8 (2s, Ar), 145.3-143.1 (m, *C*F), 132.4 (s, Ar), 131.9 (s, Ar), 130.7 (2s, Ar), 121.2 (2s, Ar), 119.5 (2d, Ar), 117.6-117.3 (m, Ar), 25.6 (2s, $Si(CH_3)_2C(CH_3)_3$), 18.1 (2s, $Si(CH_3)_2C(CH_3)_3$), –4.3 (2s, $Si(CH_3)_2C(CH_3)_3$); ^{19}F NMR (376.31 MHz, $CDCl_3$, ppm): δ = –141.99 (2s, 4F); HRMS (FAB, matrix = NBA) calcd for $C_{30}H_{39}F_4O_2Si_2$ ($[M+H]^+$) *m/z* 563.2419, found 563.2432; IR (KBr, cm^{-1}): 3063, 3036, 2964, 2937, 2895, 2859, 1602, 1581, 1517, 1465, 1447, 1410, 1363, 1317, 1283, 1259, 1139, 1096, 1041, 978, 923, 838, 800, 780, 750, 717, 664, 637.

Synthesis of 1e: Tris(dibenzylideneacetone)dipalladium(0) (15.0 mg, 0.016 mmol), 2-dicyclohexylphosphino-2',6'-dimethoxybiphenyl (12.0 mg, 0.029 mmol), **S5** (247 mg, 0.73 mmol), 1,4-dibromo-2,3-difluorobenzene (80.2 mg, 0.29 mmol), 2M K_2CO_3 aq. (2.1 mL, 4.2 mmol), and toluene (3.0 mL). Hexane/ethyl acetate (4/1) was used as an eluent for column chromatography to give a white solid (127 mg, 82% yield).
1e: white solid; m.p. 118.6–119.6 °C; ^{1}H NMR (400.13 MHz, $CDCl_3$, ppm): δ = 7.30-7.26 (m, 4H, Ar*H*), 7.13-7.12 (m, 2H, Ar*H*), 7.04 (t, *J* = 7.5 Hz, 2H, Ar*H*), 6.95 (d, *J* = 8.5 Hz, 2H, Ar*H*), 0.82 (s, 18H, $Si(CH_3)_2C(CH_3)_3$), 0.07 (s, 12H, $Si(CH_3)_2C(CH_3)_3$); ^{13}C NMR (125.72 MHz, $CDCl_3$, ppm): δ =153.3 (s, Ar), 148.5 (dd, *J* = 250.2 Hz, 15.5, Ar), 131.6 (s, Ar), 129.6 (s, Ar), 127.8-127.7 (m, *C*F), 126.8 (s, Ar), 125.8 (t, *J* = 3.4 Hz, Ar), 121.3 (s, Ar), 119.8 (s, Ar), 25.6 (s, $Si(CH_3)_2C(CH_3)_3$), 18.2 (s, $Si(CH_3)_2C(CH_3)_3$), –4.3 (s, $Si(CH_3)_2C(CH_3)_3$); ^{19}F NMR (376.31 MHz, $CDCl_3$, ppm): δ = –139.73 (s, 2F); HRMS

(FAB, matrix = NBA) calcd for $C_{30}H_{41}F_2O_2Si_2$ ([M+H]$^+$) *m/z* 527.2608, found 527.2622; IR (KBr, cm^{-1}): 3061, 3032, 2959, 2928, 2858, 1600, 1578, 1518, 1479, 1437, 1279, 1252, 929, 886, 825, 779, 751, 686.

Synthesis of 1f: Tris(dibenzylideneacetone)dipalladium(0) (27.5 mg, 0.030 mmol), 2-dicyclohexylphosphino-2',6'-dimethoxybiphenyl (24.6 mg, 0.060 mmol), **S5** (500 mg, 1.5 mmol), 1,4-dibromo-2,5-difluorobenzene (163 mg, 0.60 mmol), 2M K_2CO_3 aq. (4.2 mL, 8.4 mmol), and toluene (6 mL). Hexane/ethyl acetate (4/1) was used as an eluent for column chromatography to give a white solid (258 mg, 82% yield).
1f: white solid; m.p. 121.5–122.5 °C; ^{1}H NMR (400.13 MHz, $CDCl_3$, ppm): δ = 7.30-7.28 (m, 4H, Ar*H*), 7.12 (t, *J* = 8.0 Hz, 2H, Ar*H*), 7.04 (t, *J* = 7.4 Hz, 2H, Ar*H*), 6.94 (d, *J* = 8.4 Hz, 2H, Ar*H*), 0.84 (s, 18H, $Si(CH_3)_2C(CH_3)_3$), 0.08 (s, 12H, $Si(CH_3)_2C(CH_3)_3$); ^{13}C NMR (125.72 MHz, $CDCl_3$, ppm): δ =155.6 (dd, *J* = 244.7 Hz, 3.5 Hz, Ar), 153.3 (s, Ar), 131.6 (s, Ar), 129.6 (s, Ar), 127.0 (q, *J* = 8.3 Hz, Ar), 126.8 (s, Ar), 121.3 (s, Ar), 119.8 (s, Ar), 118.7-118.4 (m, *C*F), 25.7 (s, $Si(CH_3)_2C(CH_3)_3$), 18.2 (s, $Si(CH_3)_2C(CH_3)_3$), –4.3 (s, $Si(CH_3)_2C(CH_3)_3$); ^{19}F NMR (376.31 MHz, $CDCl_3$, ppm): δ = –121.39 (s, 2F); HRMS (FAB, matrix = NBA) calcd for $C_{30}H_{41}F_2O_2Si_2$ ([M+H]$^+$) *m/z* 527.2608, found 527.2611; IR (KBr, cm^{-1}): 3065, 2959, 2930, 2857, 1602, 1575, 1519, 1474, 1401, 1272, 1254, 1171, 1118, 1048, 921, 836, 800, 784, 761, 716, 672, 655.

2-3. Fluoride-ion-catalyzed S_NAr reaction

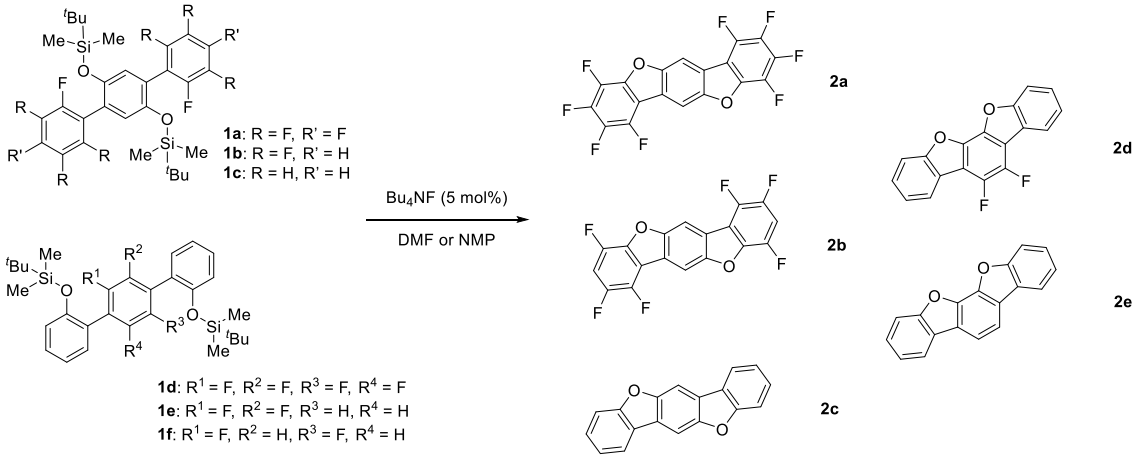

General procedure for fluoride-ion-catalyzed S_NAr

To a DMF or NMP solution of aryl silyl ether derivatives (**1a-f**) (1.0 eq.) was added 0.05 eq. of Bu_4NF (1 M in THF) under an argon atmosphere, then the mixture was stirred at each temperature and time. After cooling to room temperature, the resulting mixture was

purified respectively to give the desired product.

Synthesis of 2a: **1a** (63.4 mg, 95 μmol), 1 M Bu_4NF in THF (4.6 μL, 4.6 μmol) and DMF (2.5 mL). Reaction condition was at 80 °C for 2 h. Purification procedure was extraction with $CHCl_3$, then the organic layer was washed with distilled water and dried over anhydrous Na_2SO_4. Filtration and removal of the solvent gave a white solid (38.2 mg, 100%).
2a: white solid; m.p. 221.9–223.4 °C; ^{1}H NMR (300 MHz, $CDCl_3$, ppm): δ = 8.23 (s, 2H, Ar); ^{13}C NMR (125.72 MHz, $CDCl_3$, ppm): δ = 153.4 (s, Ar), 142.5-140.3 (m, *C*F), 142.2-140.0 (m, *C*F), 140.3-140.2 (m, *C*F), 137.4 (ddd, *J* = 248.7 Hz, 14.7 Hz, 14.7 Hz, *C*F), 134.5 (ddd, *J* = 252.8 Hz, 133.9 Hz, 4.6 Hz, *C*F), 121.7 (s, Ar), 110.4 (d, *J* = 18.5 Hz, Ar), 105.7 (s, Ar); ^{19}F NMR (282.23 MHz, $CDCl_3$, ppm): δ = –145.38 (t, *J* = 17.3 Hz, 2F), –155.24 (t, *J* = 17.3 Hz, 2F), –160.34 (t, *J* = 17.3 Hz, 2F), –163.22 (t, *J* = 20.8 Hz, 2F); HRMS (FAB, matrix = NBA) calcd for $C_{18}H_2F_8O_2$ ($[M]^+$) *m/z* 401.9927, found 401.9933; IR (KBr, cm^{-1}): 3114, 3042, 2963, 2922, 2853, 1728, 1654, 1637, 1624, 1546, 1498, 1433, 1348, 1316, 1296, 1138, 1047, 994, 885, 864, 831, 772.

Synthesis of 2b: **1b** (40.5 mg, 64 μmol), 1 M Bu_4NF in THF (3.2 μL, 3.2 μmol) and DMF (3.0 mL). Reaction condition was at 110 °C for 2 h. Purification procedure was pouring the resulting mixture into water, then the precipitate was filtered. The obtained residue was recrystallized by $CHCl_3$ to give a white solid (22.5 mg, 96%).
2b: white solid; m.p. 239.5–241.0 °C; ^{1}H NMR (400.13 MHz, $CDCl_3$, ppm): δ = 8.26 (s, 2H, Ar), 7.23-7.17 (m, 2H, Ar); ^{13}C NMR (125.72 MHz, $CDCl_3$, ppm): δ = 153.4 (s, Ar), 146.5-144.4 (m, *C*F), 144.3-142.1 (m, *C*F), 142.5-140.4 (m, *C*F), 140.8-140.7 (m, Ar), 122.7 (s, Ar), 116.6 (d, *J* = 18.1 Hz), 105.8 (s, Ar), 104.7 (dd, *J* = 24.3 Hz, 22.4 Hz, Ar); ^{19}F NMR (376.31 MHz, $CDCl_3$, ppm): δ = –137.55 (d, *J* = 19.0 Hz, 2F), –142.24 (d, *J* = 20.4 Hz, 2F), –147.63 (dd, *J* = 20.4 Hz, 20.4 Hz, 2F); HRMS (FAB, matrix = NBA) calcd for $C_{18}H_4F_6O_2$ ($[M]^+$) *m/z* 366.0115, found 366.0117; IR (KBr, cm^{-1}): 3094, 2924, 2851, 1659, 1612, 1537, 1493, 1435, 1414, 1344, 1325, 1271, 1163, 1136, 962, 907, 854, 814, 725, 679.

Synthesis of 2c from 1c: **1c** (9.9 mg, 19 μmol), 1 M Bu_4NF in THF (0.95 μL, 0.95 μmol) and NMP (3.0 mL). Reaction condition was at 200 °C for 4 h. Purification procedure was extraction with $CHCl_3$, then the organic layer was washed with distilled water and dried over anhydrous Na_2SO_4. After filtration and removal of the solvent, the crude product was reprecipitated with cold methanol to give a white solid (3.9 mg, 80%).

2c: white solid; m.p. 225.2–226.0 °C; ^{1}H NMR (400.13 MHz, $CDCl_3$, ppm): δ = 8.06 (s, 2H, Ar*H*), 8.02 (d, *J* = 8.6 Hz, 2H, Ar*H*), 7.60 (d, *J* = 8.2 Hz, 2H, Ar*H*), 7.49 (t, *J* = 7.8 Hz, 2H, Ar*H*), 7.38 (t, *J* = 7.5 Hz, 2H, Ar*H*); ^{13}C NMR (125.72 MHz, $CDCl_3$, ppm): δ = 157.4 (s, Ar), 152.9 (s, Ar), 127.6 (s, Ar), 124.7 (s, Ar), 124.3 (s, Ar), 122.8 (s, Ar), 120.9 (s, Ar), 111.9 (s, Ar), 102.7 (s, Ar); HRMS (EI) calcd for $C_{18}H_{10}O_2$ ($[M]^+$) *m/z* 258.0681, found 258.0682; IR (KBr, cm^{-1}): 3089, 3068, 3050, 3020, 2963, 2918, 2851, 1434, 1261, 1225, 1219, 1143, 1099, 1048, 1018, 929, 869, 864, 854, 804, 761, 741, 686; elemental analysis (%): calcd. ($C_{18}H_{10}O_2$): C 83.70, H 3.90, O 12.39; found: C 84.22, H 4.01, N 0.10, O 11.98.

Synthesis of 2d: **1d** (53.5 mg, 95 μmol), 1 M Bu_4NF in THF (4.8 μL, 4.8 μmol) and DMF (2.5 mL). Reaction condition was at 90 °C for 3 h. Purification procedure was extraction with $CHCl_3$, then the organic layer was washed with distilled water and dried over anhydrous Na_2SO_4. After filtration and removal of the solvent, the crude product was purified by silica gel column chromatography using hexane/$CHCl_3$ (1/1) to give a white solid (27.7 mg, 99%).
2d: white solid; m.p. 279.0–280.0 °C; ^{1}H NMR (400.13 MHz, $CDCl_3$, ppm): δ = 8.16 (d, *J* = 7.8 Hz, 2H, Ar*H*), 7.70 (d, *J* = 8.2 Hz, 2H, Ar*H*), 7.56 (t, *J* = 7.7 Hz, 2H, Ar*H*), 7.46 (t, *J* = 7.5 Hz, 2H, Ar*H*); ^{13}C NMR (125.72 MHz, $CDCl_3$, ppm): δ = 156.6 (s, Ar), 140.9 (dd, *J* = 248 Hz, 16 Hz, *C*F), 136.3 (t, *J* = 4.7 Hz, Ar), 128.0 (s, Ar), 124.0 (s, Ar), 122.8 (s, Ar), 122.5 (s, Ar), 114.1 (dd, *J* = 13 Hz, 7.8 Hz, Ar), 112.2 (s, Ar); ^{19}F NMR (376.31 MHz, $CDCl_3$, ppm): δ = −152.30 (s, 2F); HRMS (FAB, matrix = NBA) calcd for $C_{18}H_8F_2O_2$ ($[M]^+$) *m/z* 294.0492, found 294.0496; IR (KBr, cm^{-1}): 3444, 2921, 2854, 1510, 1449, 1418, 1308, 1261, 1211, 1147, 1088, 1017, 992, 894, 827, 744; elemental analysis (%): calcd. ($C_{18}H_8F_2O_2$): C 73.47, H 2.74, F 12.91, O 10.87; found: C 73.08, H 3.05, F 12.56. F prevented detection of O.

Synthesis of 2e: **1e** (50.0 mg, 95 μmol), 1 M Bu_4NF in THF (4.7 μL, 4.7 μmol) and DMF (2.5 mL). Reaction condition was at 100 °C for 3 h. Purification procedure was extraction with $CHCl_3$, then the organic layer was washed with distilled water and dried over anhydrous $MgSO_4$. After filtration and removal of the solvent, the crude product was reprecipitated with cold methanol to give a white solid (24.0 mg, 98%).
2e: white solid; m.p. 184.6–185.5 °C; ^{1}H NMR (400.13 MHz, $CDCl_3$, ppm): δ = 8.03 (d, *J* = 7.6 Hz, 2H, Ar*H*), 7.93 (s, 2H, Ar*H*), 7.71 (d, *J* = 8.2 Hz, 2H, Ar*H*), 7.52 (t, *J* = 4.2 Hz, 2H, Ar*H*), 7.41 (t, *J* = 7.5 Hz, 2H, Ar*H*); ^{13}C NMR (125.72 MHz, $CDCl_3$, ppm): δ = 156.7 (s, Ar), 140.9 (s, Ar), 127.3 (s, Ar), 124.8 (s, Ar), 124.7 (s, Ar), 123.4 (s, Ar), 120.8

(s, Ar), 115.3 (s, Ar), 112.2 (s, Ar); HRMS (EI) calcd for $C_{18}H_{10}O_2$ ($[M]^+$) *m/z* 258.0681, found 258.0675; IR (KBr, cm^{-1}): 3057, 3050, 3044, 3090, 2932, 2880, 2863, 1450, 1433, 1425, 1311, 1255, 1185, 1079, 937, 924, 822, 744; elemental analysis (%): calcd. ($C_{18}H_{10}O_2$): C 83.70, H 3.90, O 12.39; found: C 83.23, H 3.94, O 12.02.

Synthesis of 2c from 1f: **1f** (50.0 mg, 95 μmol), 1 M Bu_4NF in THF (4.7 μL, 4.7 μmol) and NMP (2.0 mL). Reaction condition was at 200 °C for 5 h. Purification procedure was extraction with $CHCl_3$, then the organic layer was washed with distilled water and dried over anhydrous Na_2SO_4. After filtration and removal of the solvent, the crude product was reprecipitated with cold methanol to give a white solid (21.0 mg, 86%). Isolated product showed identical spectra to **2c**.

3. Comparison of reaction conditions

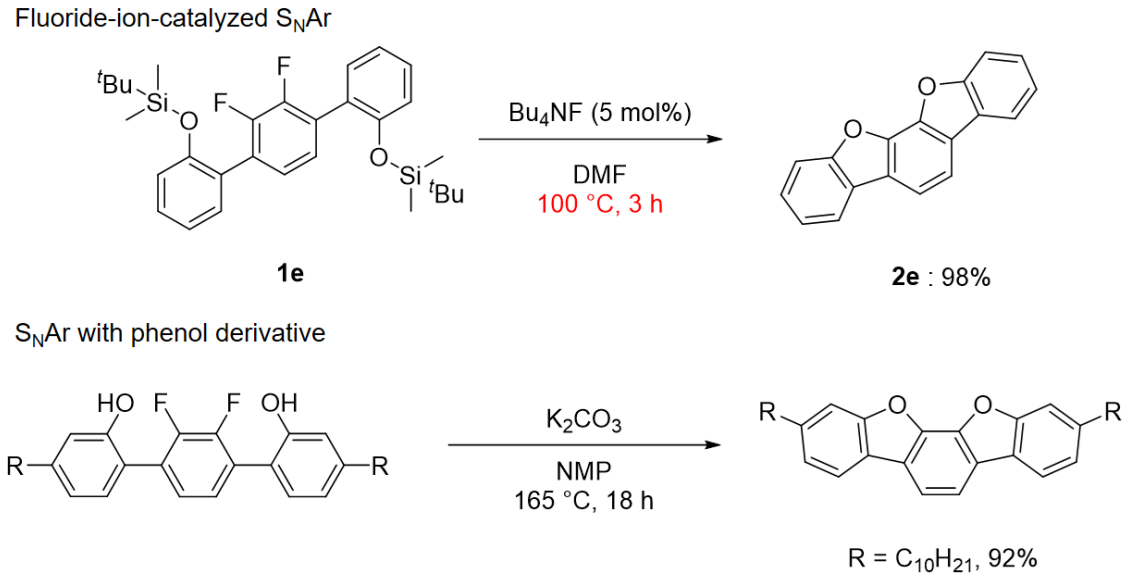

Figure S1. Comparison of reaction condition of fluoride-ion-catalyzed S_NAr vs. S_NAr with phenol derivative.[1]

4. Single crystal X-ray diffraction

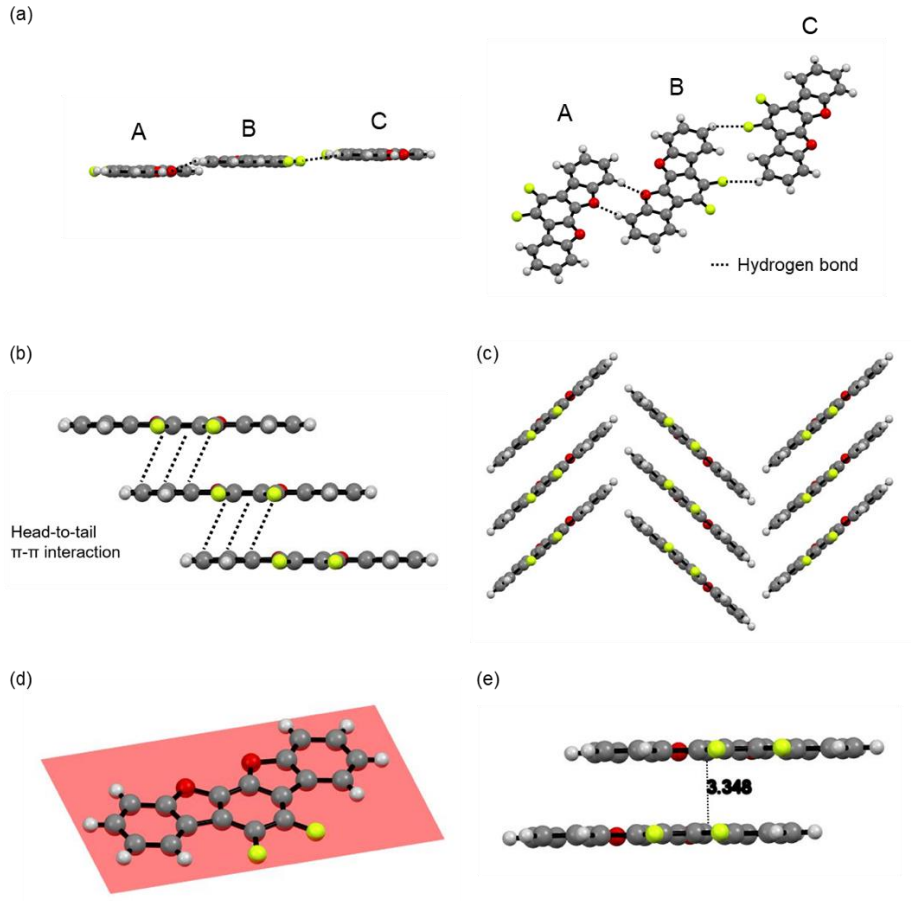

Figure S2. Structure of **2d** obtained by single crystal X-ray analysis.

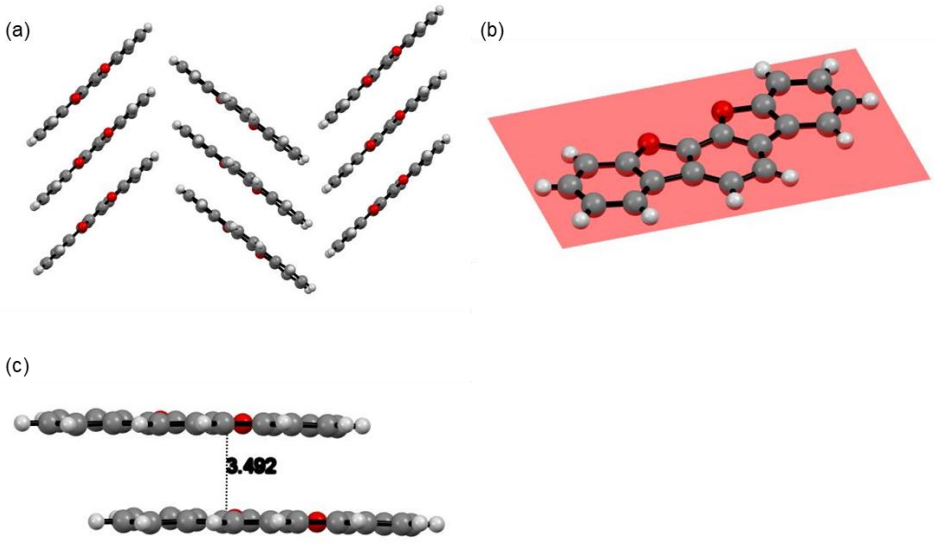

Figure S3. Reported crystal structure of **2e**.[2]

Table S1. Crystallographic data of **2d**.

Crystal data	2d
CCDC	1974979
Empirical Formula	C18H8F2O2
Formula Weight	294.24
h, k, lmax	27, 5, 33
Crystal System	monoclinic
Space Group	I 1 2/a 1
a, Å	21.8335(15)
b, Å	4.5675(2)
c, Å	26.5713(18)
α, deg	90
β, deg	112.747(8)
γ, deg	90
Volume, Å	2443.7(3)
Dcalcd, g cm^{-3}	1.600
Z	8
F(000)	1200.0
Data Collection	Data Collection
Temperature, K	90
2θ max, deg	76.254
Tmin/Tmax	0.724/1.000
Refinement	Refinement
No. of Observed Data	2442
No. of Parameters	199
R, wR2	0.0420, 0.1317
S	1.156

5. Energy diagrams of fluoride-ion-catalyzed S_NAr reaction

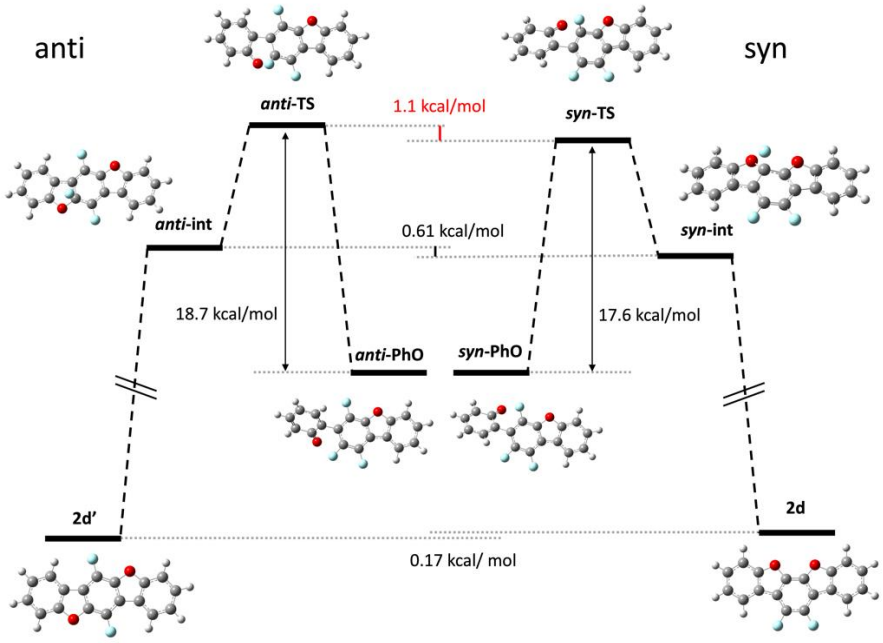

Figure S4. Energy diagram of S_NAr reaction calculated at B3LYP/6-311G+(2df,2p) level.

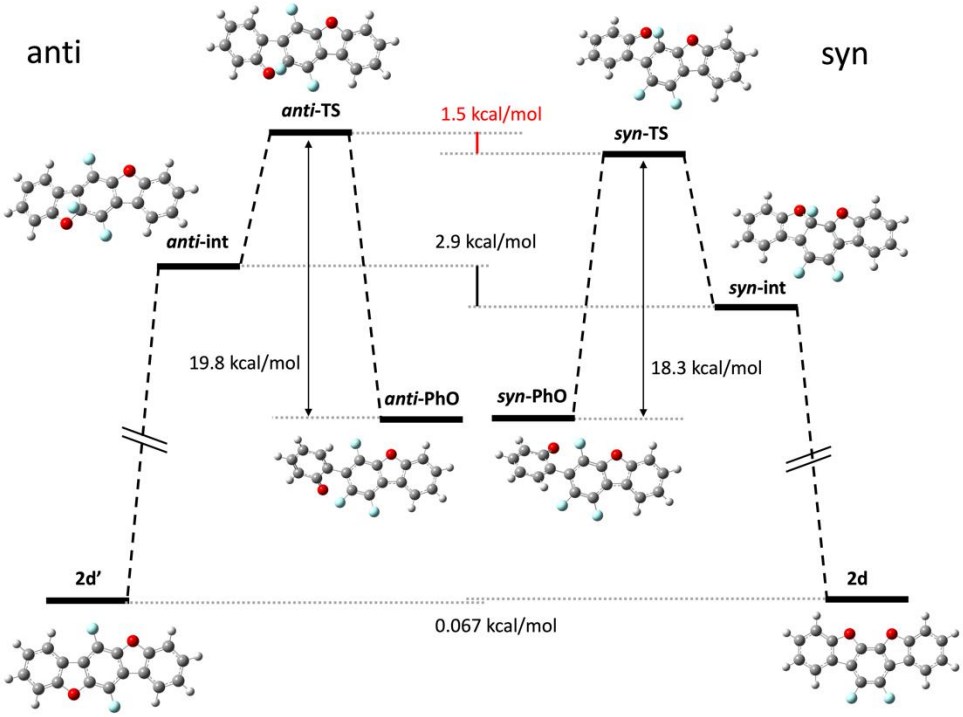

Figure S5. Energy diagram of S_NAr reaction calculated at ωB97XD/6-311G+(2df,2p) level.

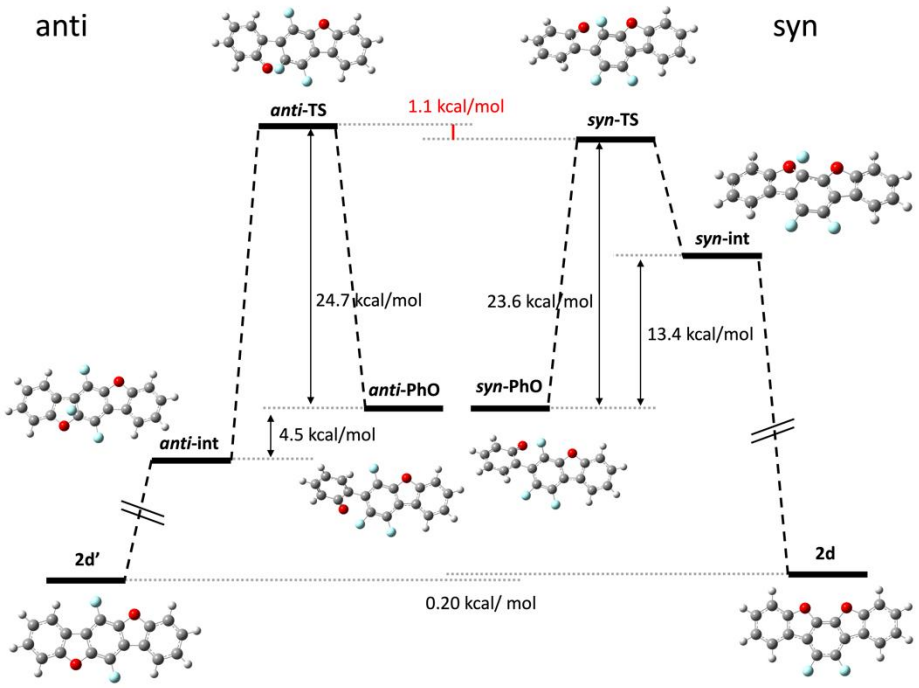

Figure S6. Energy diagram of S_NAr reaction calculated at B3LYP-D3/6-311G+(2df,2p) level with DMF solvation.

6. Mulliken charge profile

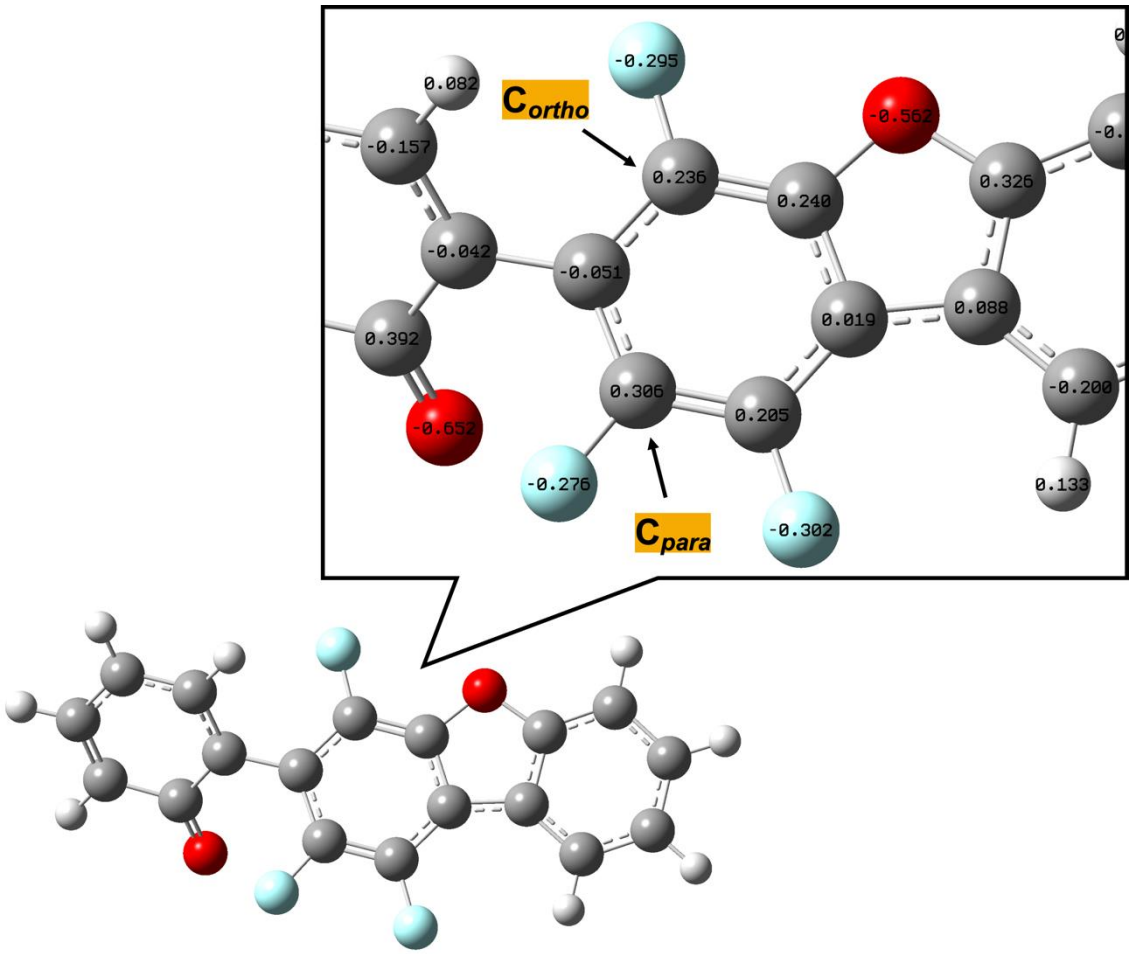

Figure S7. Mulliken atomic charges of one-sided cyclized *anti* product of **1d** calculated at B3LYP/6-31G(d) level.

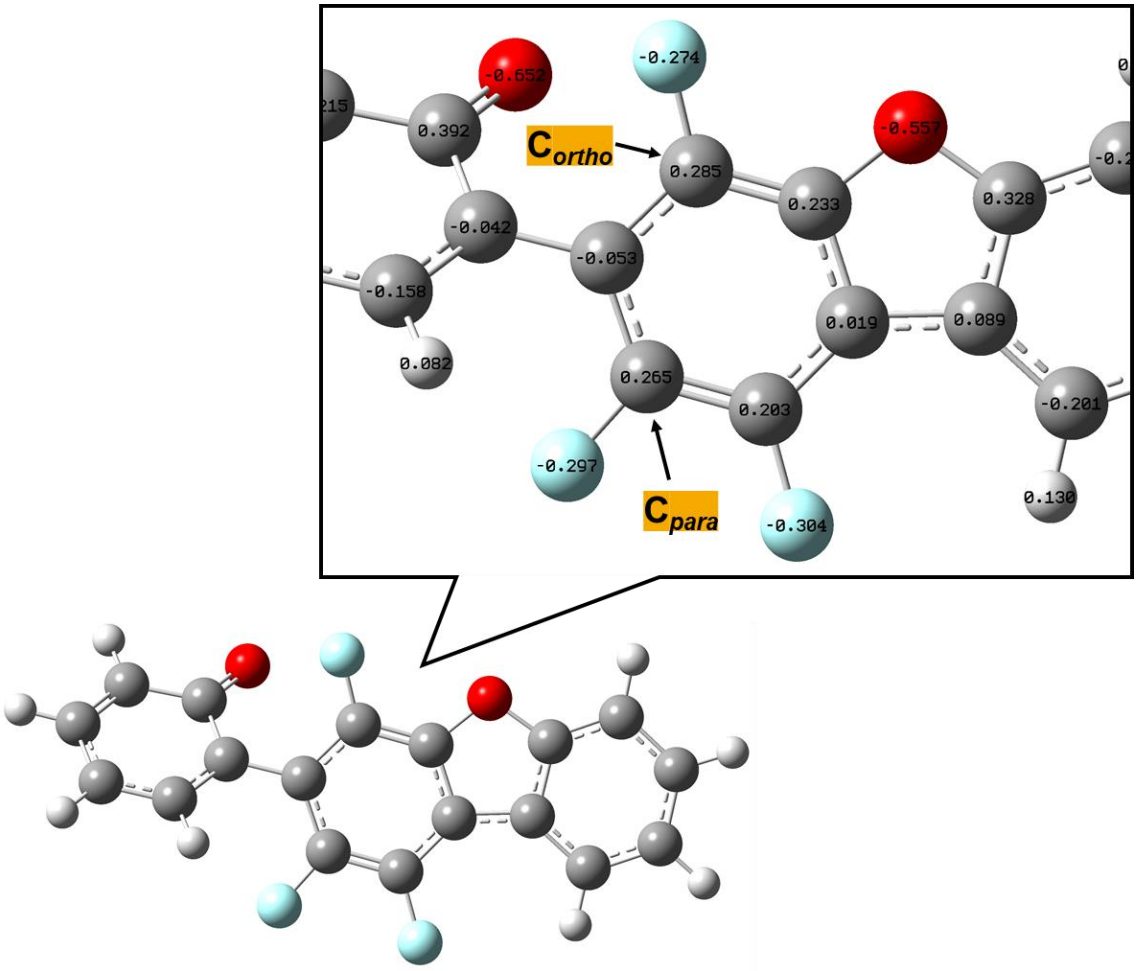

Figure S8. Mulliken atomic charges of one-sided cyclized *syn* product of **1d** calculated at B3LYP/6-31G(d) level.

7. Cyclization of 1d at higher temperature

Fluoride-ion-catalyzed cyclization of **1d** was also performed at a higher temperature. To an NMP solution (2.5 mL) of **1d** (53.4 mg, 95 μmol) was added 0.05 eq. of Bu_4NF (1 M in THF, 4.8 μL, 4.8 μmol) under an argon atmosphere. The mixture was stirred at 200 °C for 3 h. After cooling to room temperature, the mixture was extracted with $CHCl_3$, then the organic layer was washed with distilled water and dried over Na_2SO_4. **2d** was obtained in 96% yield determined by ^{19}F NMR using benzotrifluoride as an internal standard.

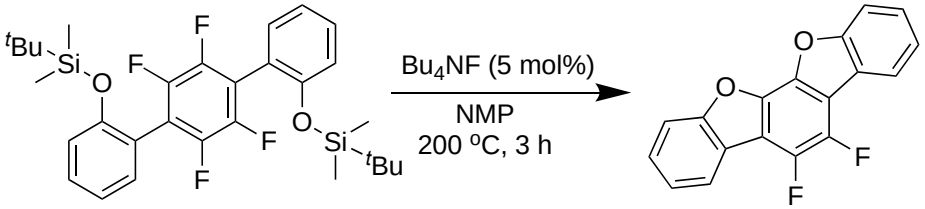

1d **2d** 96%

Scheme S3. Synthesis of **2d** at 200 °C. The yield of **2d** was determined by ^{19}F NMR using benzotrifluoride as an internal standard.

8. Optical properties

Table S2. Optical properties of **2a-e** measured in $CHCl_3$.

Compound	λ_{max}^{abs} a) [nm]	λ_{onset}^{abs} [nm]	λ_{ex} b) [nm]	λ_{max}^{em} [nm]	SS c) [nm]	ϕ_F d)
2a	312	340	312	352	5.0	0.57
2b	311	350	311	348	5.0	0.58
2c	329	350	314	359	7.0	0.64
2d	316	325	300	342	16	0.25
2e	317	325	303	335	4.5	0.44

a) Wavelength for the largest absorption. b) **2c-e** were excited at the second maximum absorption peak to avoid self-absorption. c) Stokes shift. d) Internal quantum efficiency.

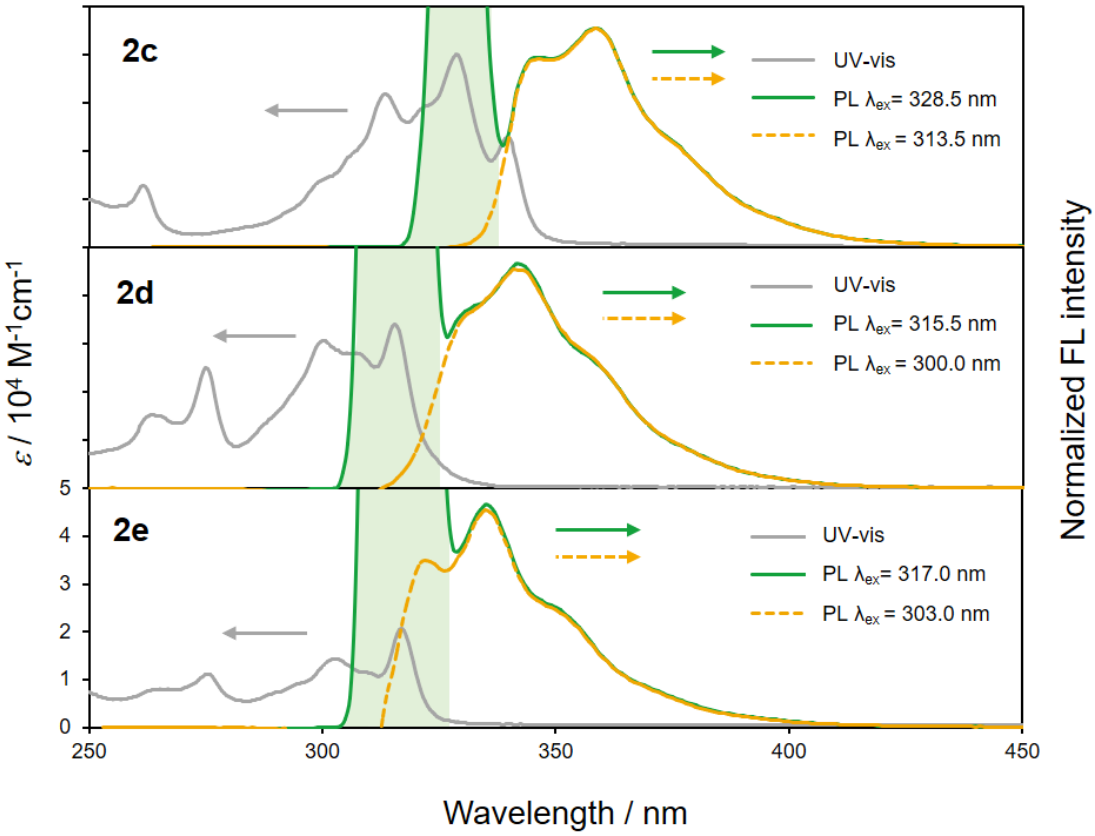

Figure S9. Absorption (gray) and fluorescence (green, yellow) spectra of **2c-e** recorded with $CHCl_3$ as a solvent. Fluorescence spectra were collected under the excitation at maximum absorption wavelength (green) or second maximum absorption wavelength (yellow).

Table S3. Optical properties of **2a-e** measured in toluene.

Compound	λ_{max}^{abs} a) [nm]	λ_{onset}^{abs} [nm]	λ_{ex} b) [nm]	λ_{max}^{em} [nm]	SS c) [nm]	ϕ_F d)
2a	314	343	314	354	9.0	0.62
2b	313	343	313	364	7.0	0.68
2c	329	347	314	359	10	0.75
2d	317	327	302	344	19	0.39
2e	318	325	304	337	9.0	0.74

a) Wavelength for the largest absorption. b) **2c-e** were excited at the second maximum absorption peak to avoid self-absorption. c) Stokes shift. d) Internal quantum efficiency.

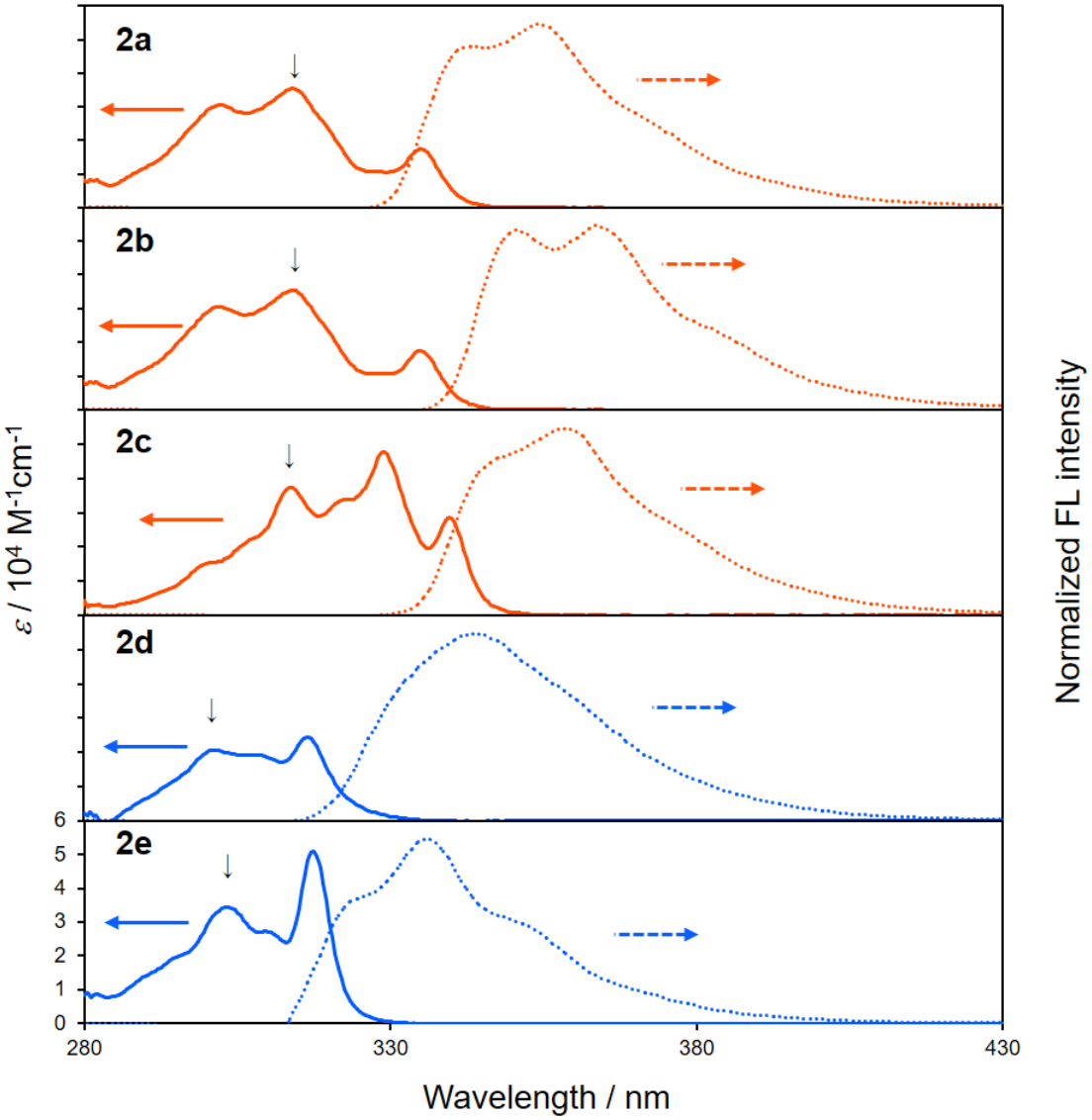

Figure S10. Absorption (solid line) and FL (dashed line) spectra of **2a-e** recorded with toluene as a solvent. Black arrows indicate the excitation wavelength for FL measurement measured in toluene.

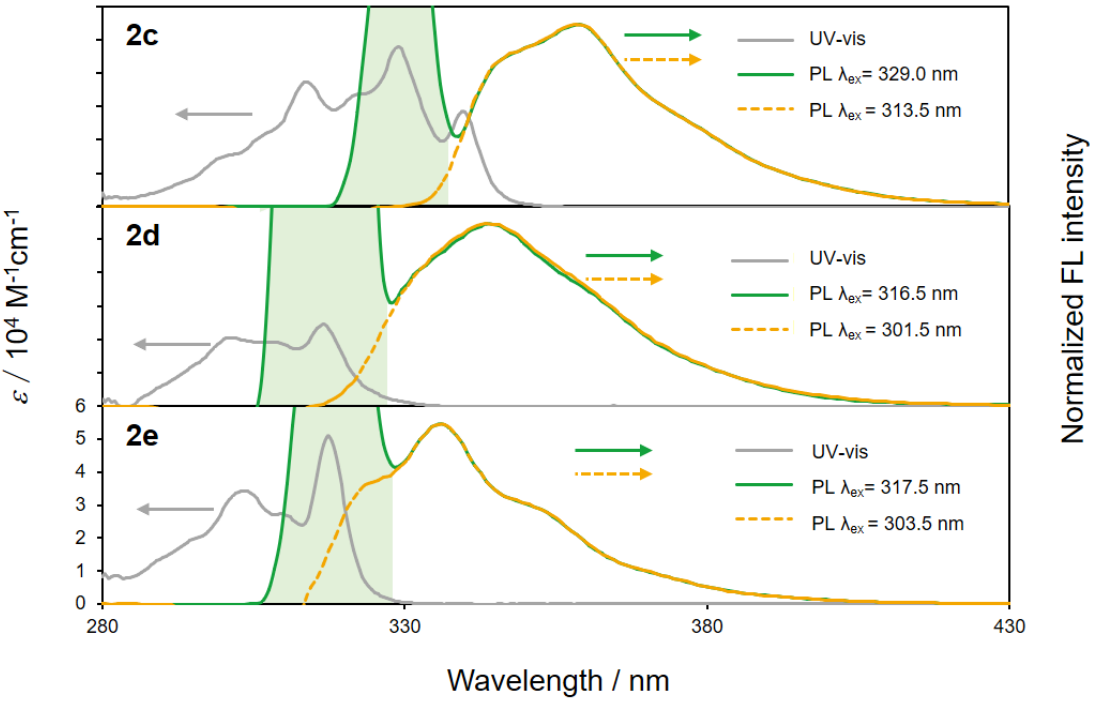

Figure S11. Absorption (gray) and fluorescence (green, yellow) spectra of **2c-e**. Fluorescence spectra were collected under the excitation at maximum absorption wavelength (green) or second maximum absorption wavelength (yellow) measured in toluene.

9. Electrochemical properties

The electrochemical properties were evaluated by cyclic voltammetry (CV) measurement (Figure S11). All the compound **2a-e** showed irreversible redox behavior in 0.1 M Bu_4NPF_6/CH_2Cl_2. In **2a**-**2d**, the oxidation peak top and reduction peak top were not observed due the overlap with background current. Oxidation and reduction voltammograms were collected independently.

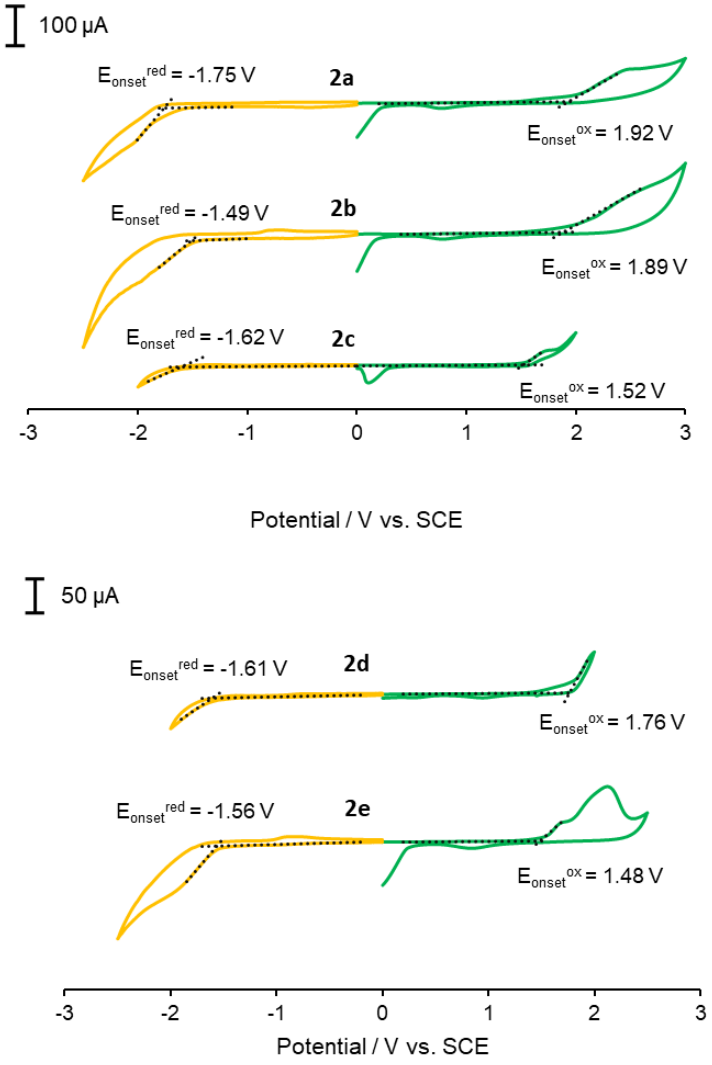

Figure S12. Cyclic voltammograms of 3 mM **2a-e** in 0.1 M Bu_4NPF_6/CH_2Cl_2 at a scan rate of 100 mV/s.

10. Orbital energy levels simulated at B3LYP-D3/def2TZVP level of theory

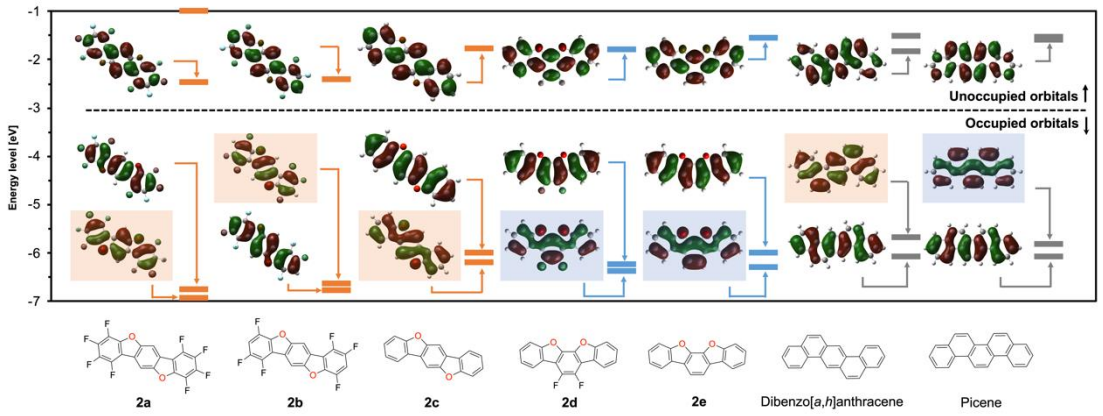

Figure S13. Orbital energy levels around frontier orbital of **2a-e**, dibenzo[*a*,*h*]anthracene and picene simulated at B3LYP-D3/def2TZVP level of theory. MOs of HOMO-1, HOMO, LUMO are described (iso value = 0.02).

11. TD DFT simulations for 2a-c

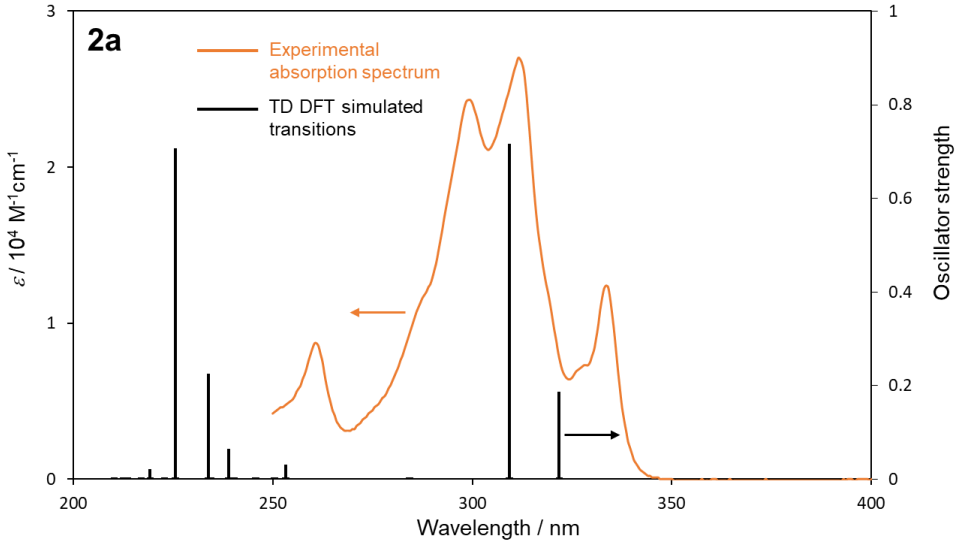

Figure S14. Absorption spectrum of **2a** and oscillator strength calculated by DFT method at the B3LYP/6-311G+(2df,2p) level.

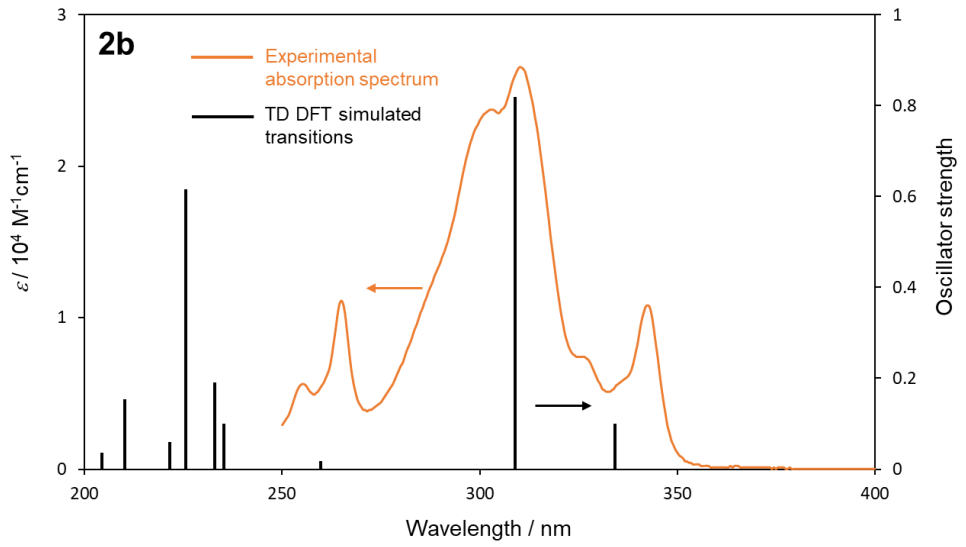

Figure S15. Absorption spectrum of **2b** and oscillator strength calculated by DFT method at the B3LYP/6-311G+(2df,2p) level.

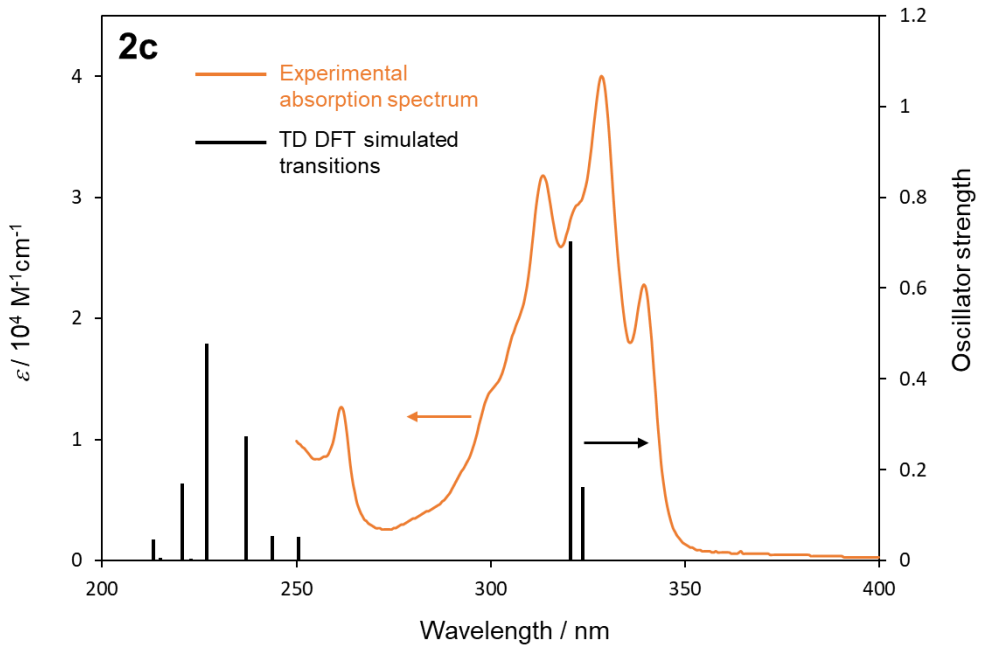

Figure S16. Absorption spectrum of **2c** and oscillator strength calculated by DFT method at the B3LYP/6-311G+(2df,2p) level.

Table S4. Summary of simulated transitions of **2a-c** calculated by DFT method at the B3LYP/6-311G+(2df,2p) level.

Compounds	λ[nm][a)]	f[b)]	Contribution
2a	321.76	0.1863	HOMO-1→LUMO (0.52022) HOMO→LUMO (-0.44048) HOMO→LUMO+1 (0.14715)
	309.29	0.7163	HOMO-1→LUMO (0.43684) HOMO→LUMO (0.53338)
2b	334.28	0.0993	HOMO-1→LUMO (-0.21702) HOMO-1→LUMO+2 (-0.12477) HOMO→LUMO (0.65337)
	308.87	0.8197	HOMO-1→LUMO (0.65510) HOMO→LUMO (0.22107) HOMO→LUMO+2 (0.10346)
2c	323.63	0.1611	HOMO-1→LUMO (0.62207) HOMO→LUMO (0.28253) HOMO→LUMO+2 (0.12764)
	320.61	0.7029	HOMO-1→LUMO (-0.28054) HOMO→LUMO (0.63264)

a) λ : Wavelength, b) f : Oscillator strength.

12. NMR charts

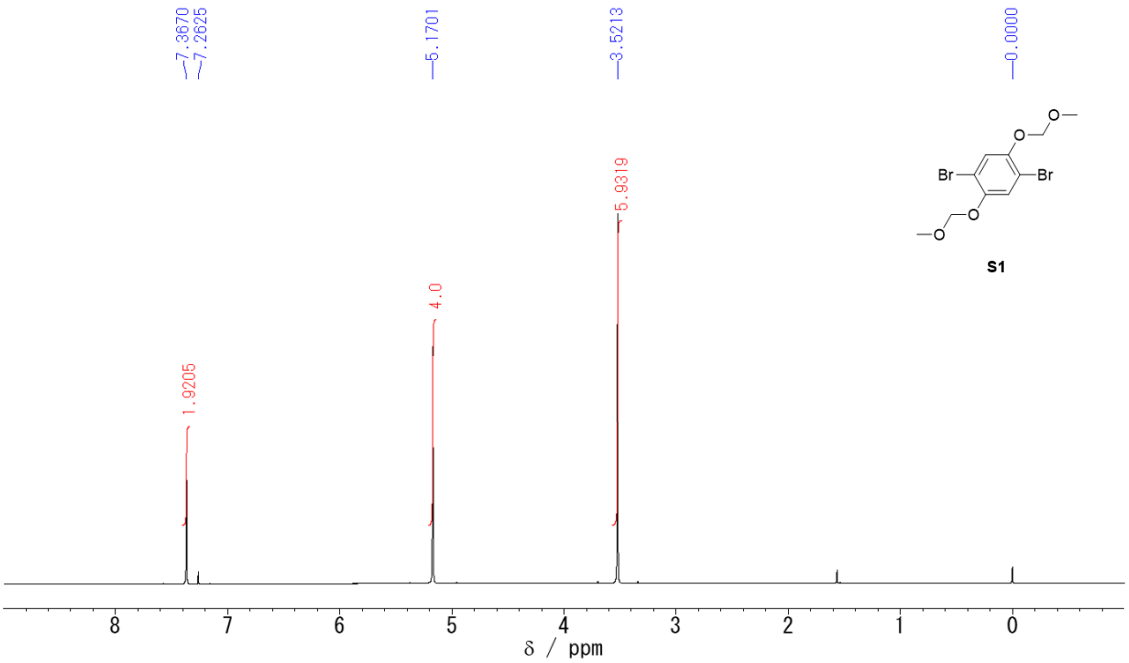

Figure S17. ^{1}H NMR spectrum (400.13 MHz, $CDCl_3$) of **S1**.

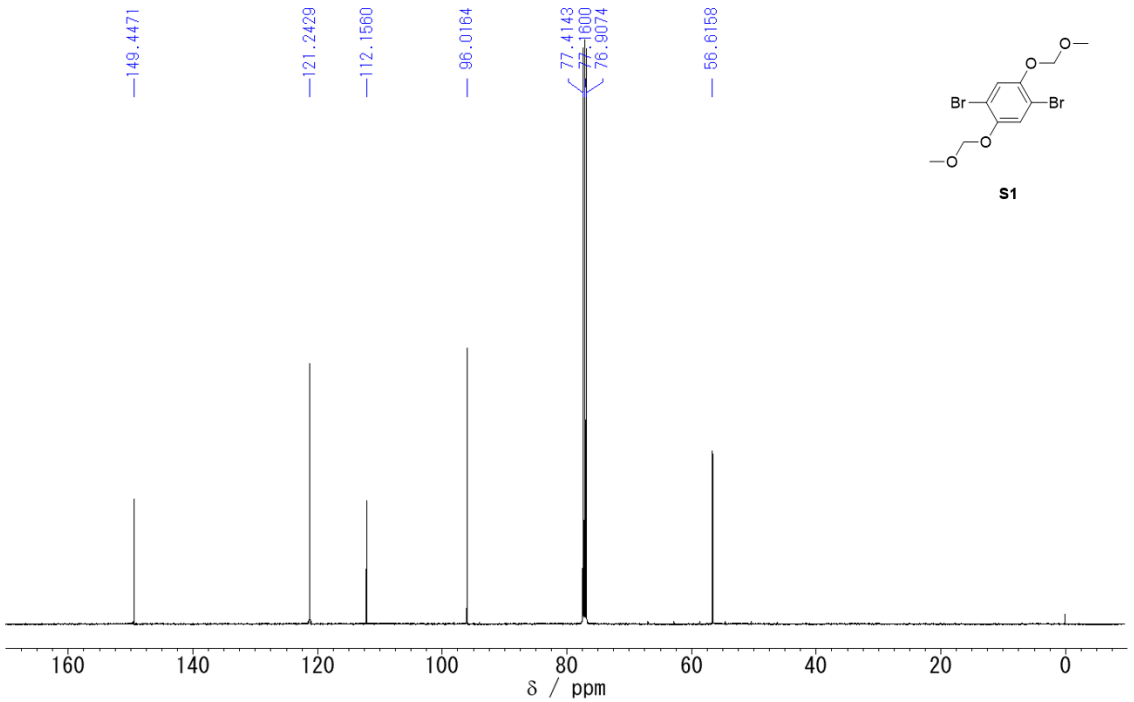

Figure S18. ^{13}C{^{1}H} NMR spectrum (125.72 MHz, $CDCl_3$) of **S1**.

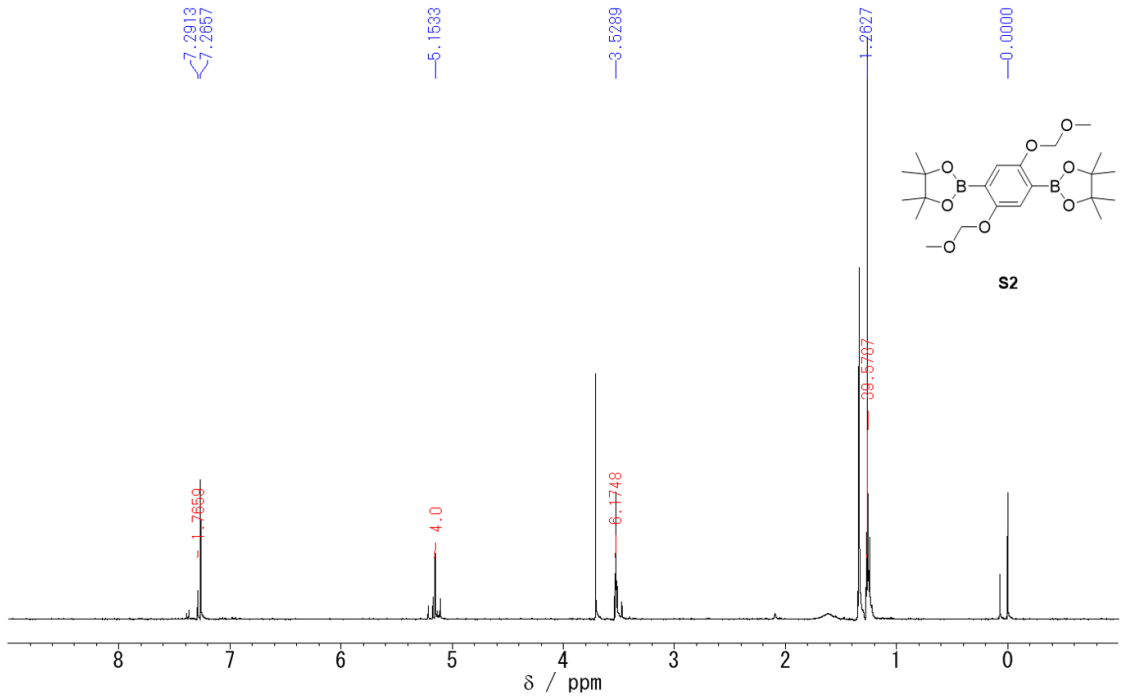

Figure S19. ^{1}H NMR spectrum (300 MHz, $CDCl_3$) of **S2**.

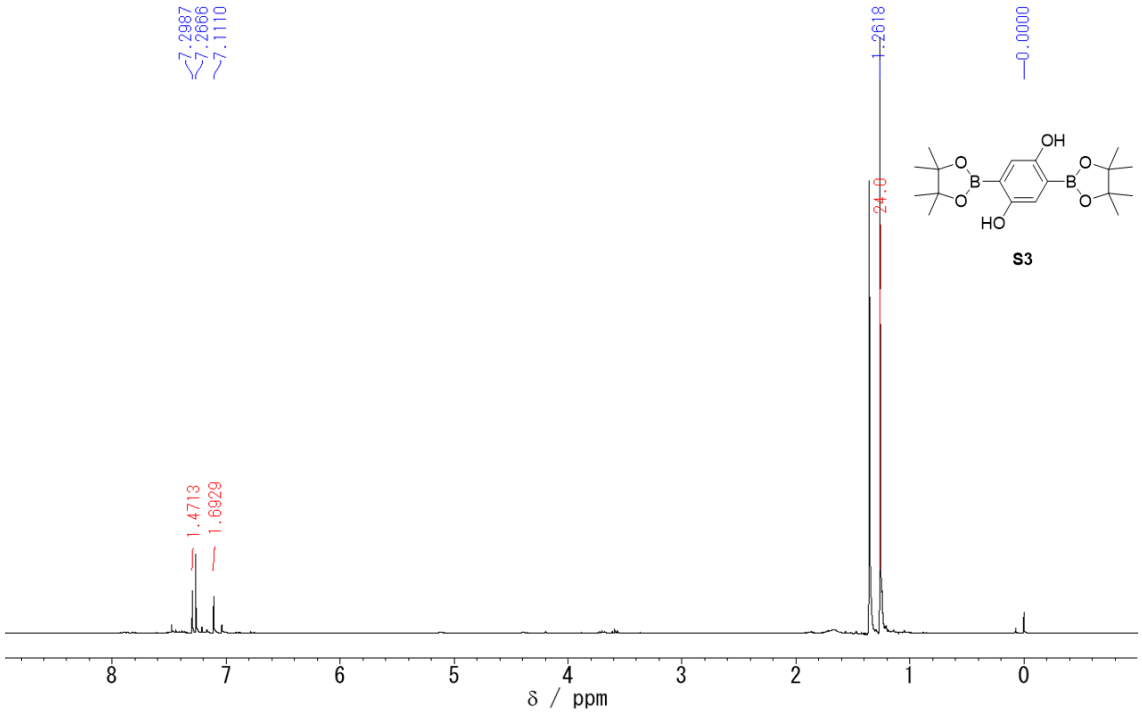

Figure S20. ^{1}H NMR spectrum (300 MHz, $CDCl_3$) of **S3**.

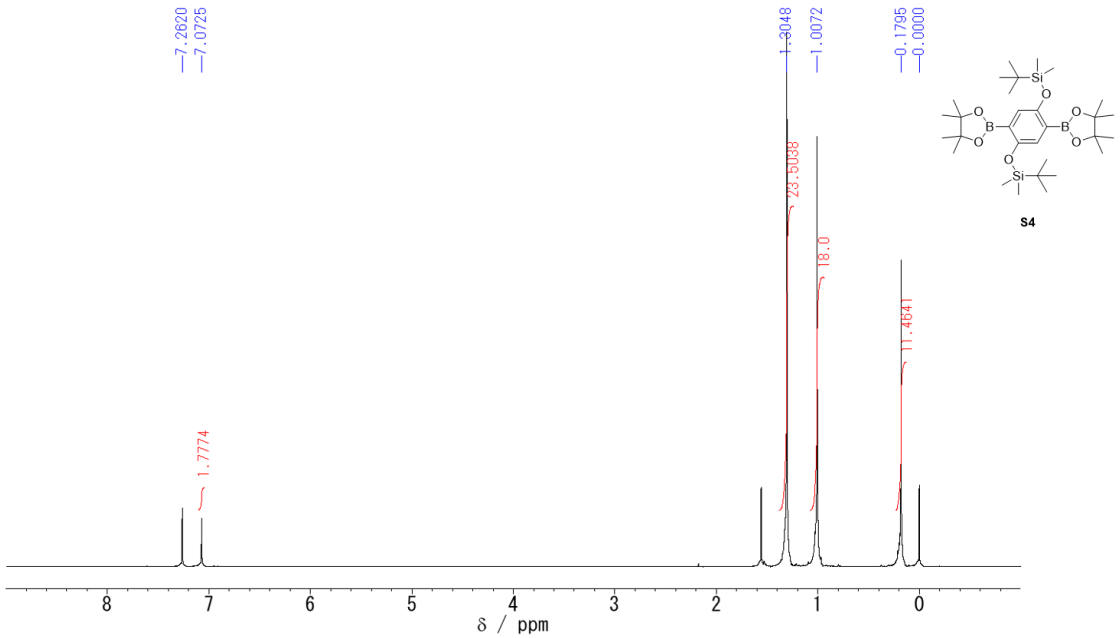

Figure S21. ^{1}H NMR spectrum (300 MHz, $CDCl_3$) of **S4**.

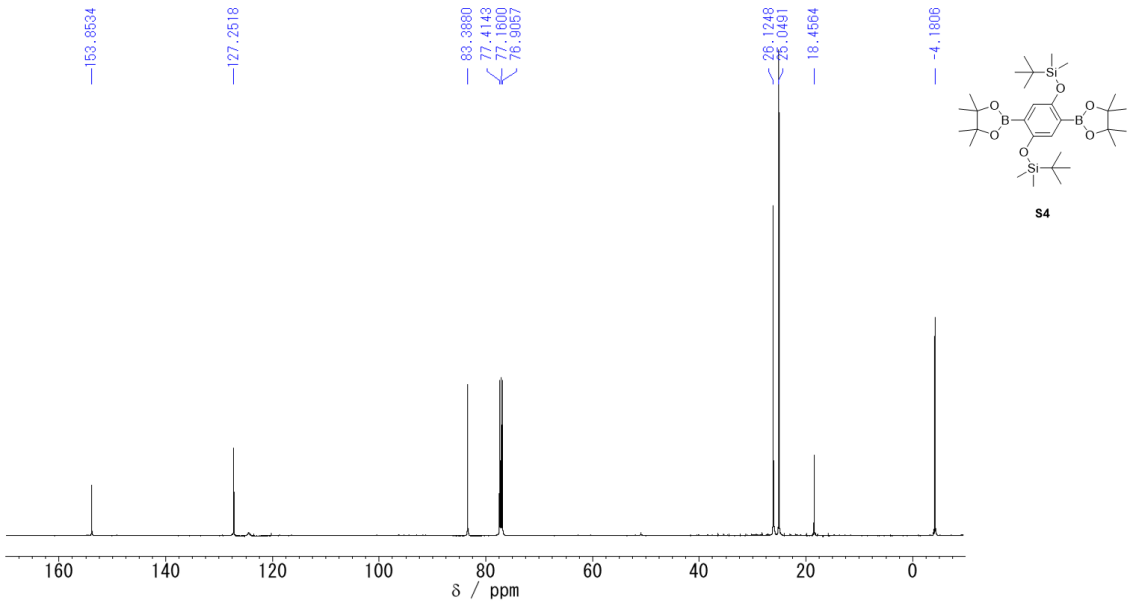

Figure S22. $^{13}C\{^{1}H\}$ NMR spectrum (125.72 MHz, $CDCl_3$) of **S4**.

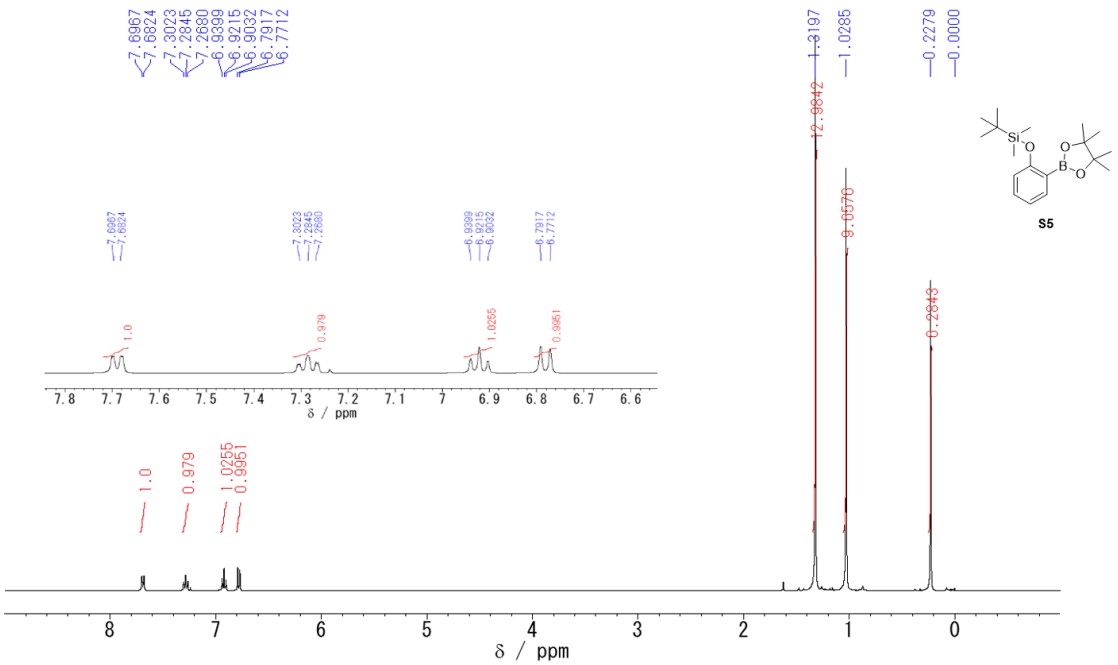

Figure S23. ^{1}H NMR spectrum (400.13 MHz, $CDCl_3$) of **S5**.

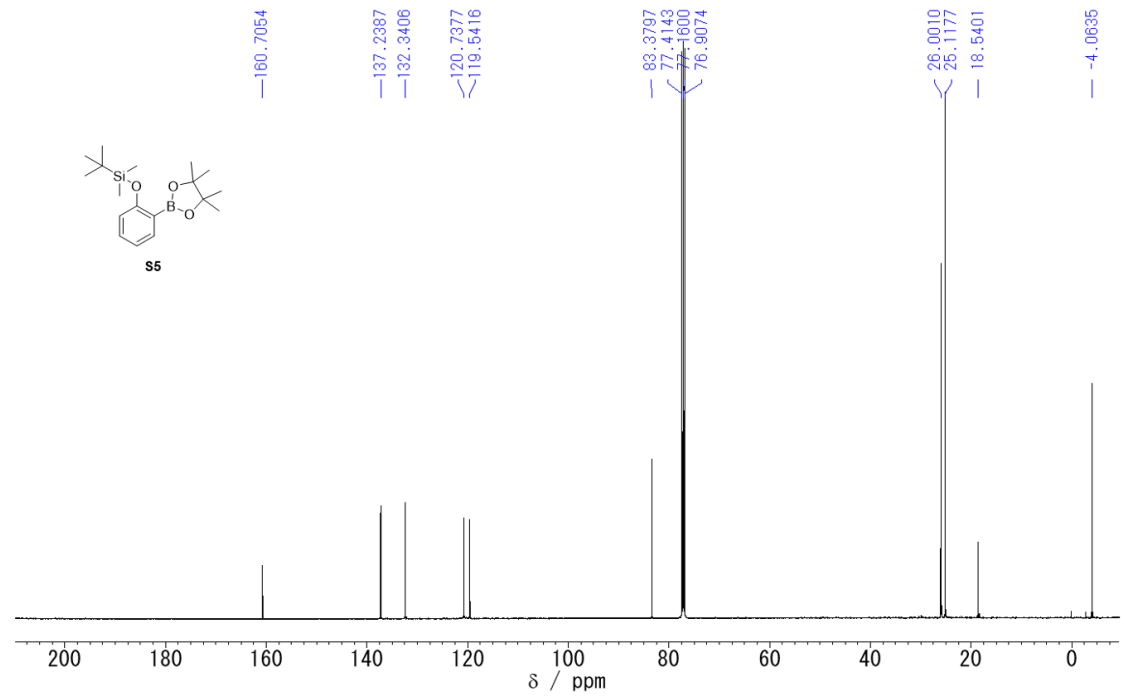

Figure S24. $^{13}C\{^{1}H\}$ NMR spectrum (125.72 MHz, $CDCl_3$) of **S5**.

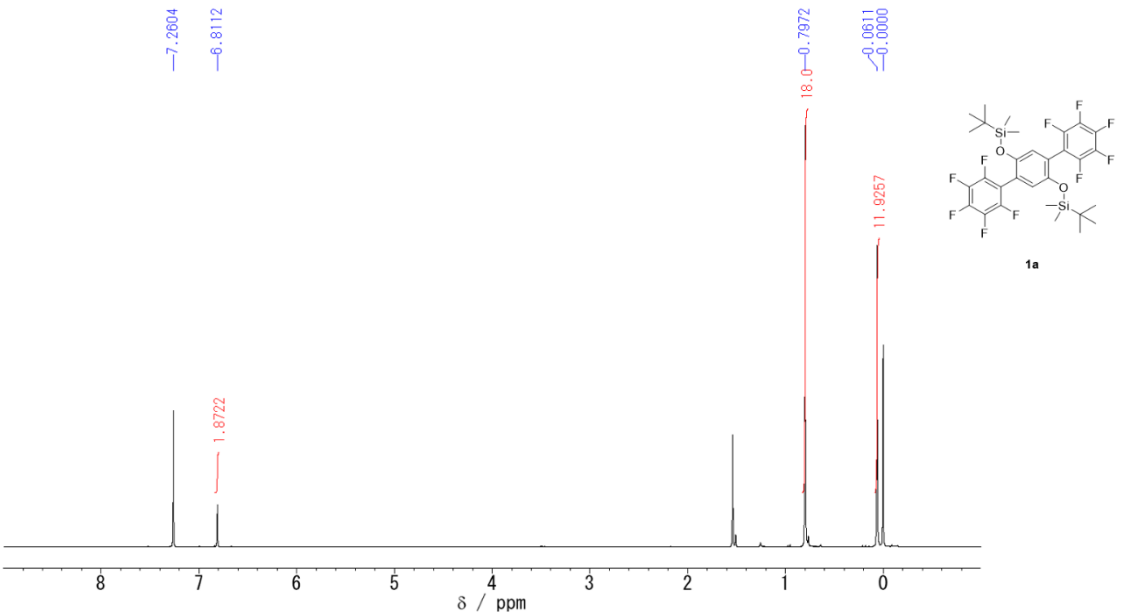

Figure S25. ^{1}H NMR spectrum (400.13 MHz, $CDCl_3$) of **1a**.

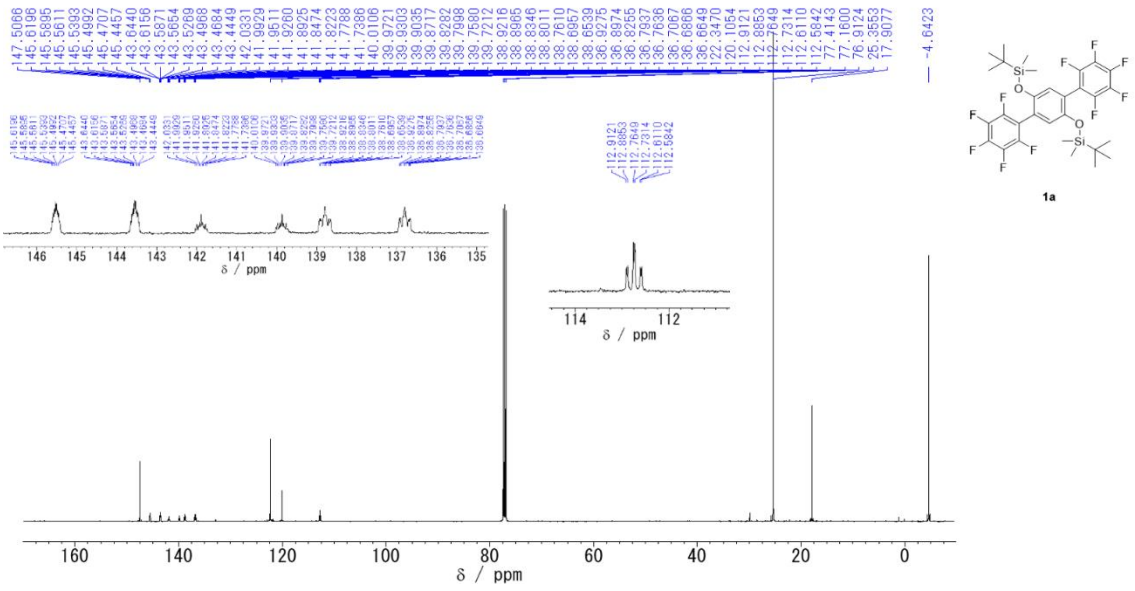

Figure S26. ^{13}C{^{1}H} NMR spectrum (125.72 MHz, $CDCl_3$) of **1a**.

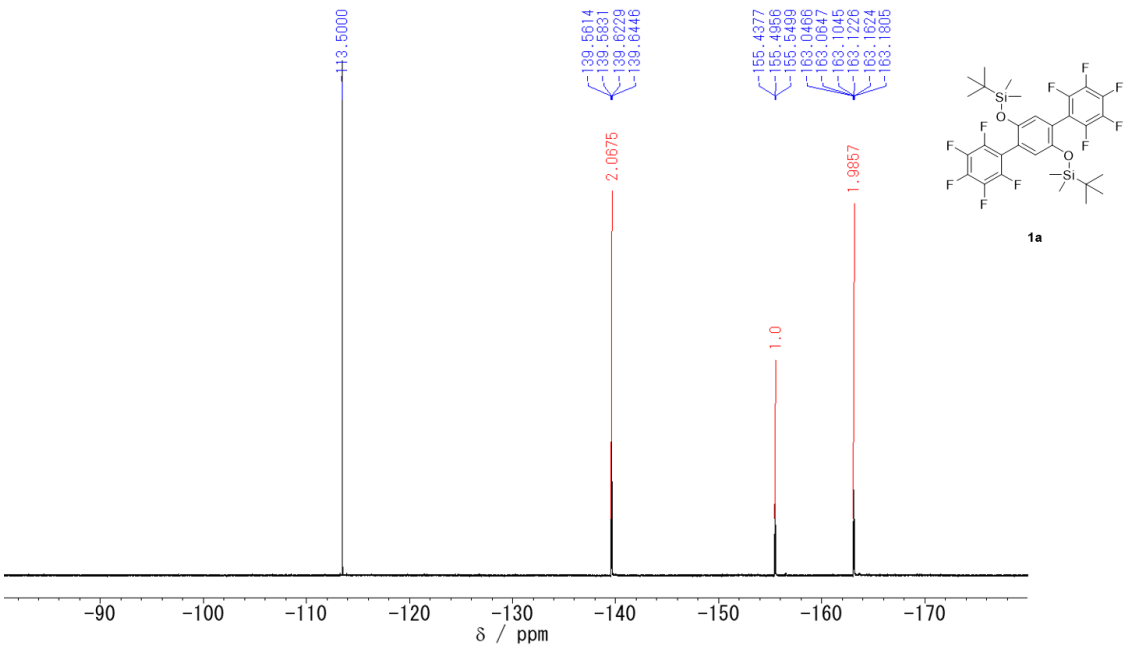

Figure S27. $^{19}F\{^{1}H\}$ NMR spectrum (376.31 MHz, $CDCl_3$) of **1a**.

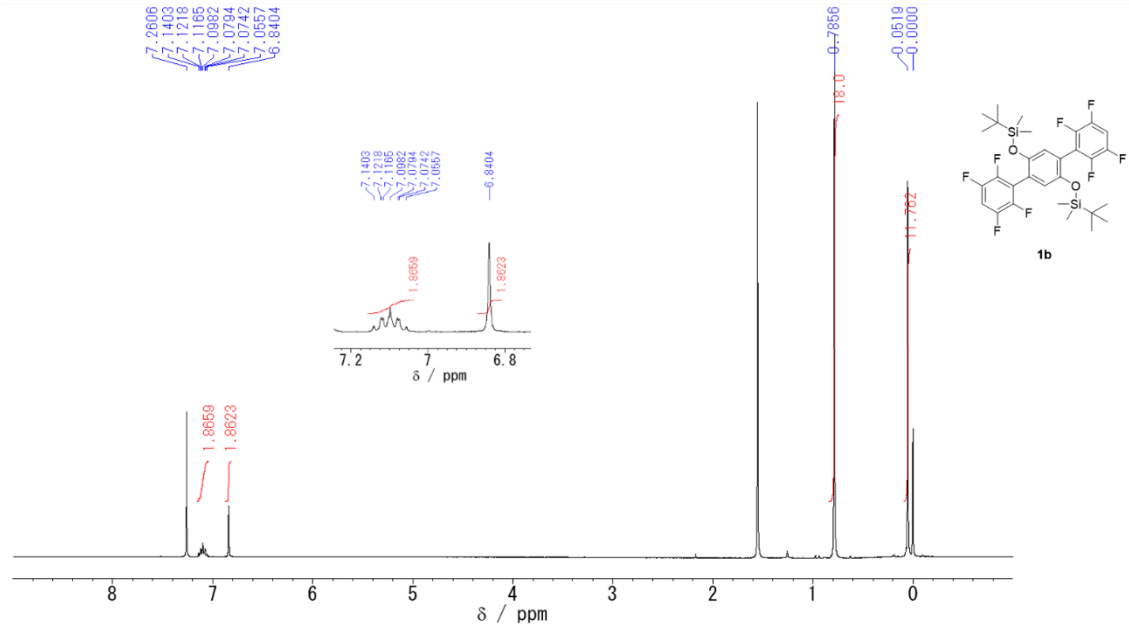

Figure S28. ^{1}H NMR spectrum (400.13 MHz, $CDCl_3$) of **1b**.

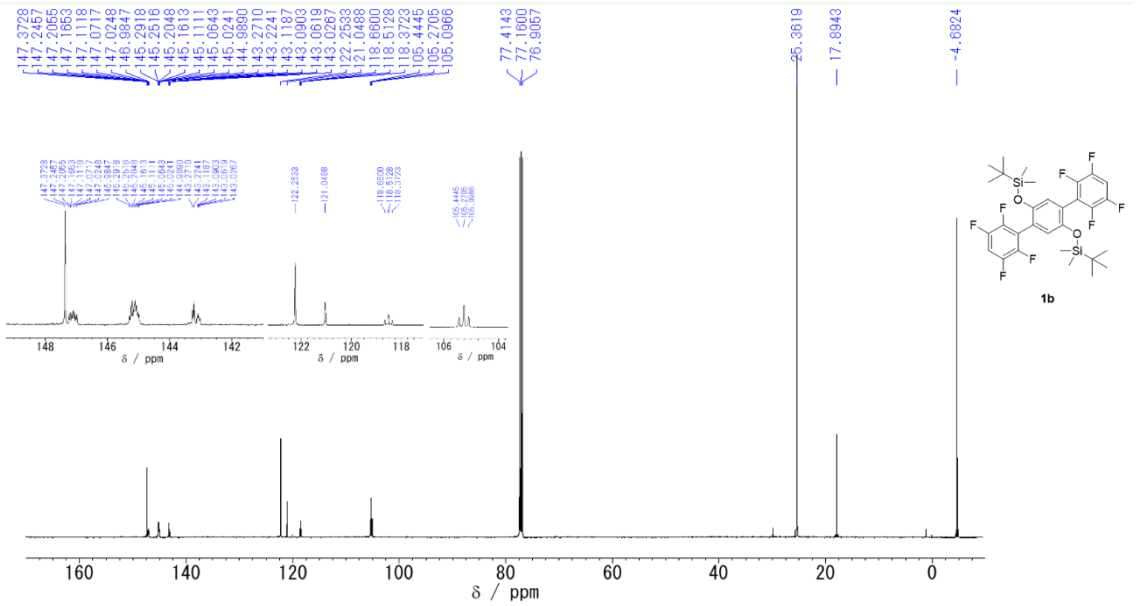

Figure S29. $^{13}C\{^{1}H\}$ NMR spectrum (125.72 MHz, $CDCl_3$) of **1b**.

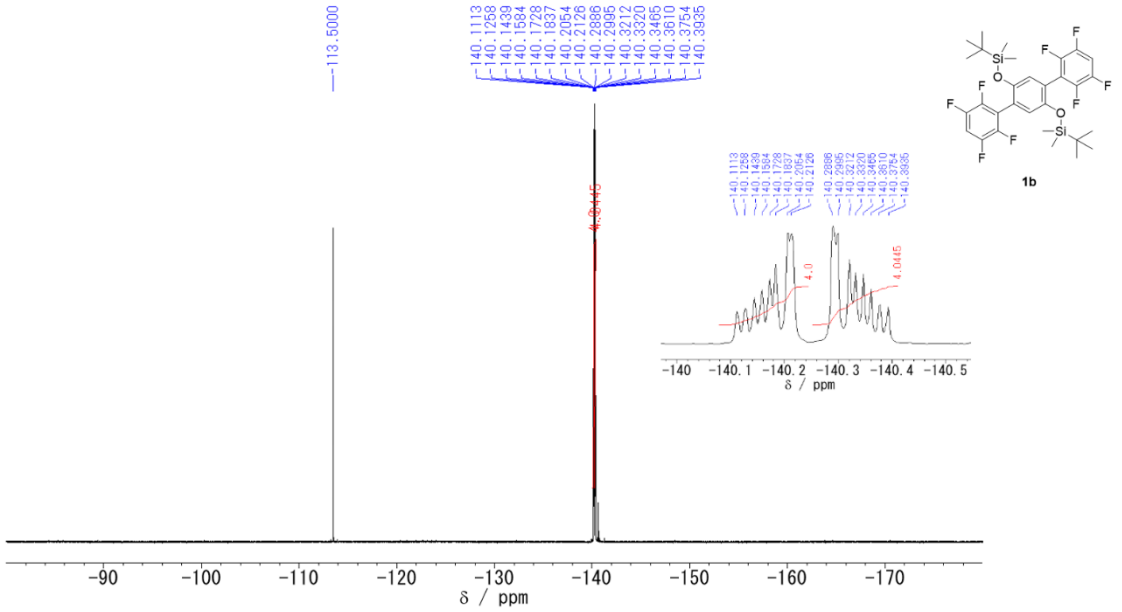

Figure S30. $^{19}F\{^{1}H\}$ NMR spectrum (376.31 MHz, $CDCl_3$) of **1b**.

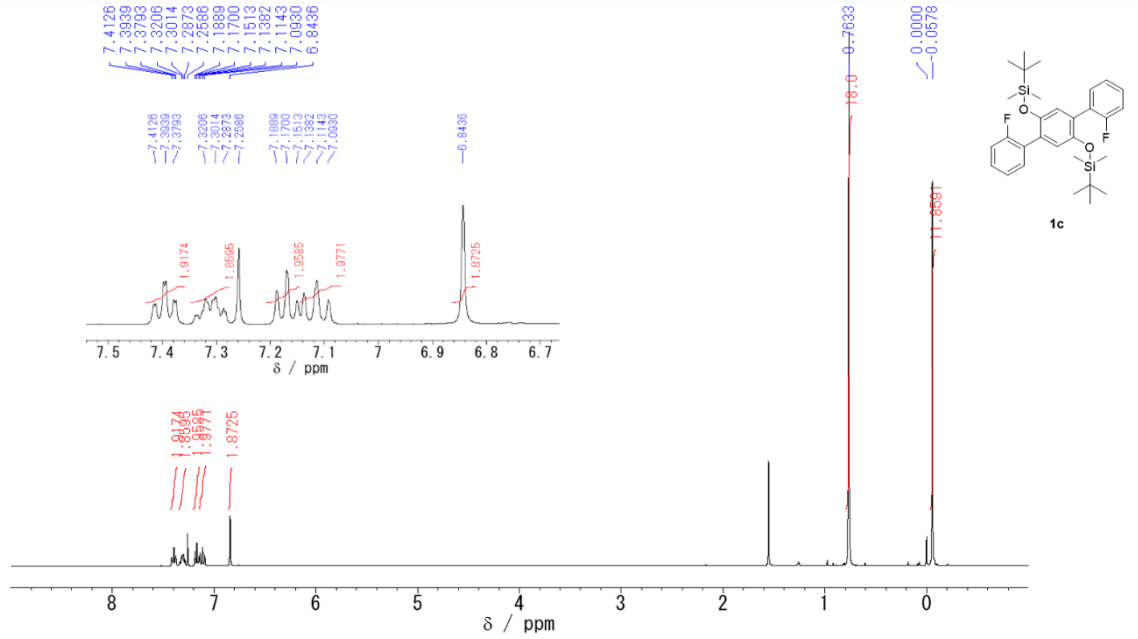

Figure S31. ^{1}H NMR spectrum (400.13 MHz, $CDCl_3$) of **1c**.

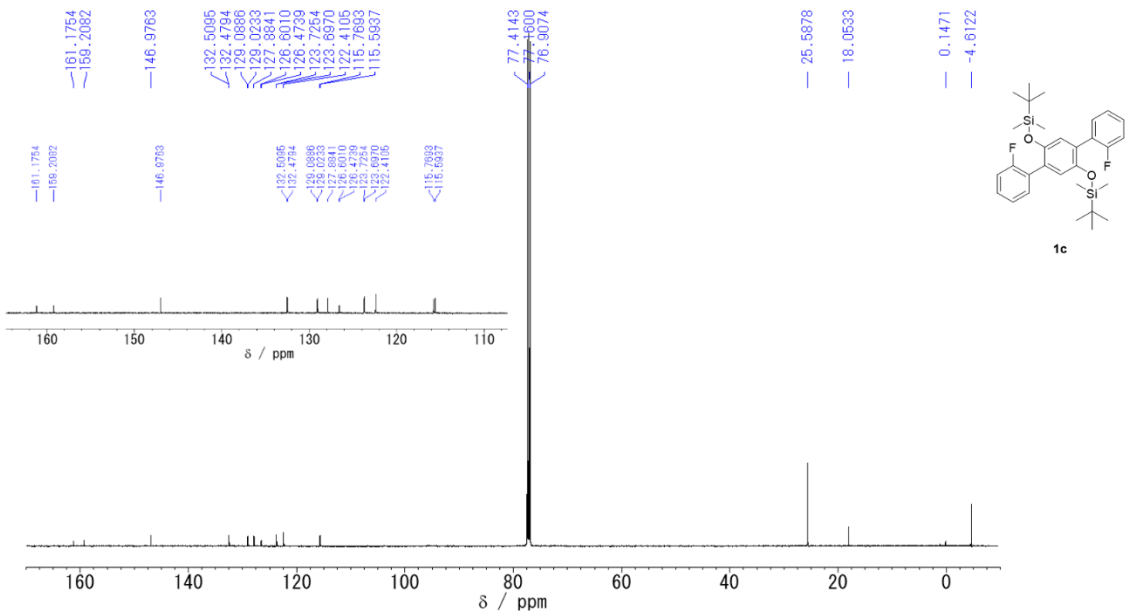

Figure S32. $^{13}C\{^{1}H\}$ NMR spectrum (125.72 MHz, $CDCl_3$) of **1c**.

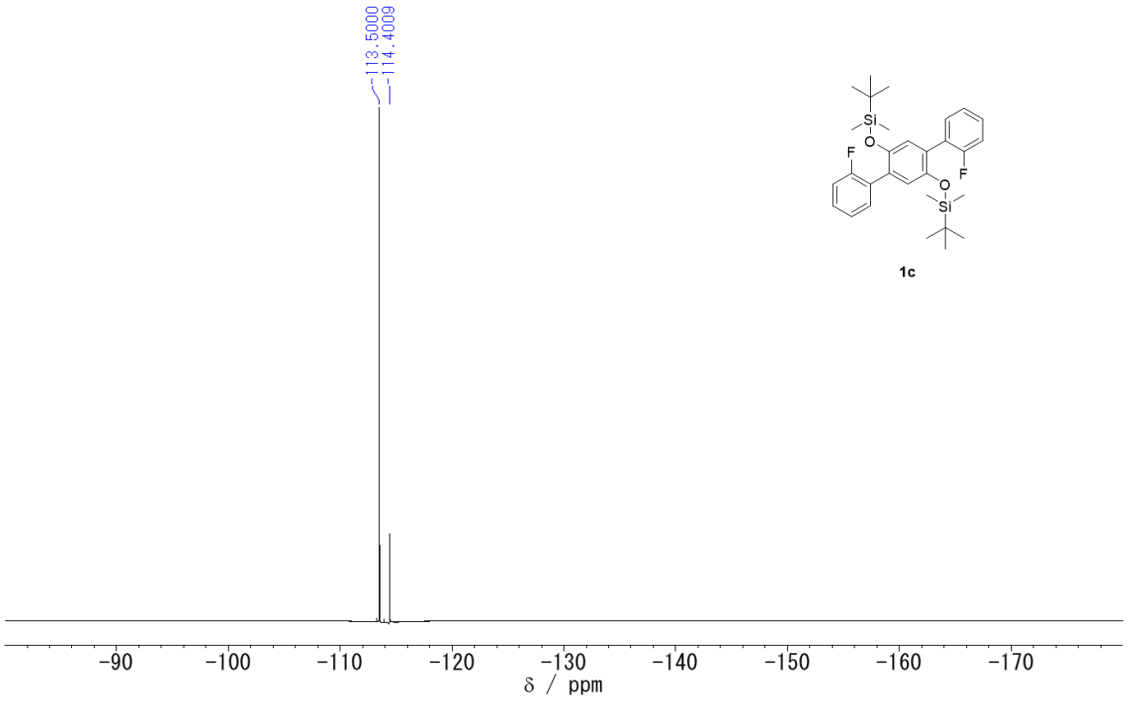

Figure S33. $^{19}F\{^{1}H\}$ NMR spectrum (376.31 MHz, $CDCl_3$) of **1c**.

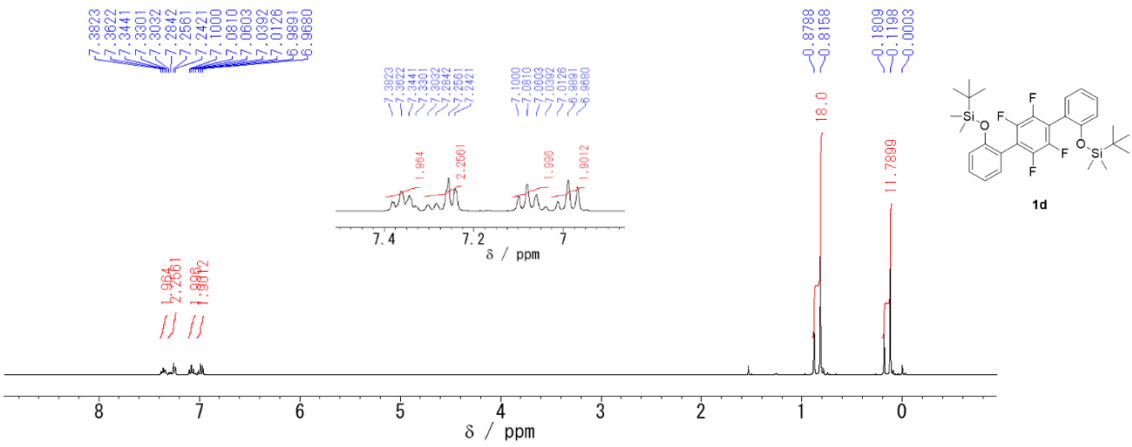

Figure S34. ^{1}H NMR spectrum (400.13 MHz, $CDCl_3$) of **1d**.

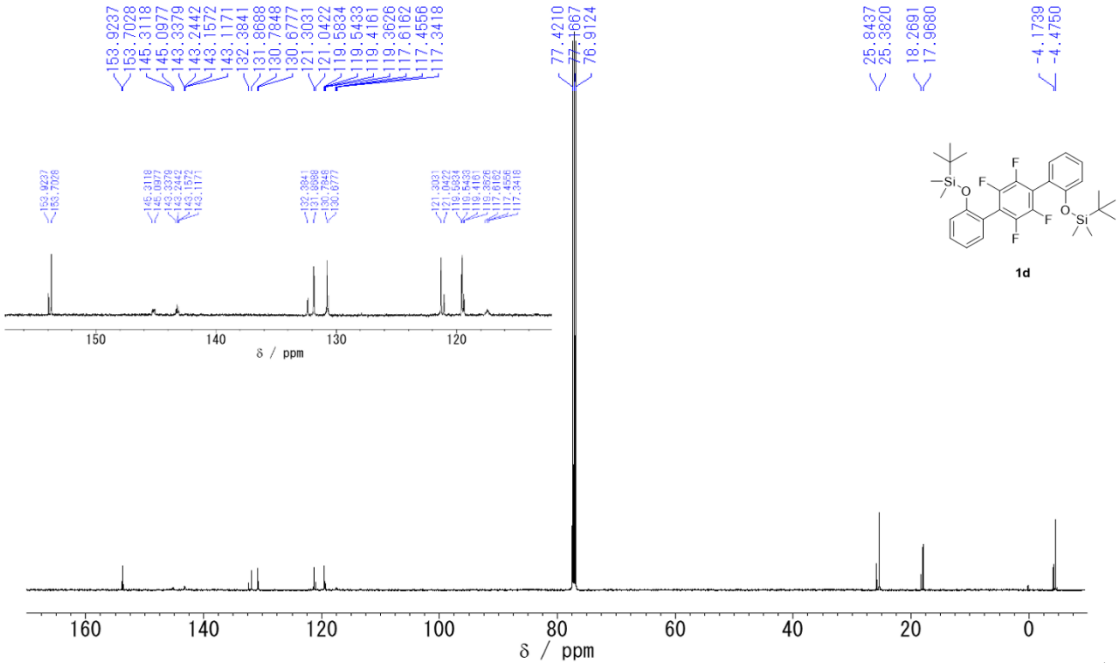

Figure S35. $^{13}C\{^{1}H\}$ NMR spectrum (125.72 MHz, $CDCl_3$) of **1d**.

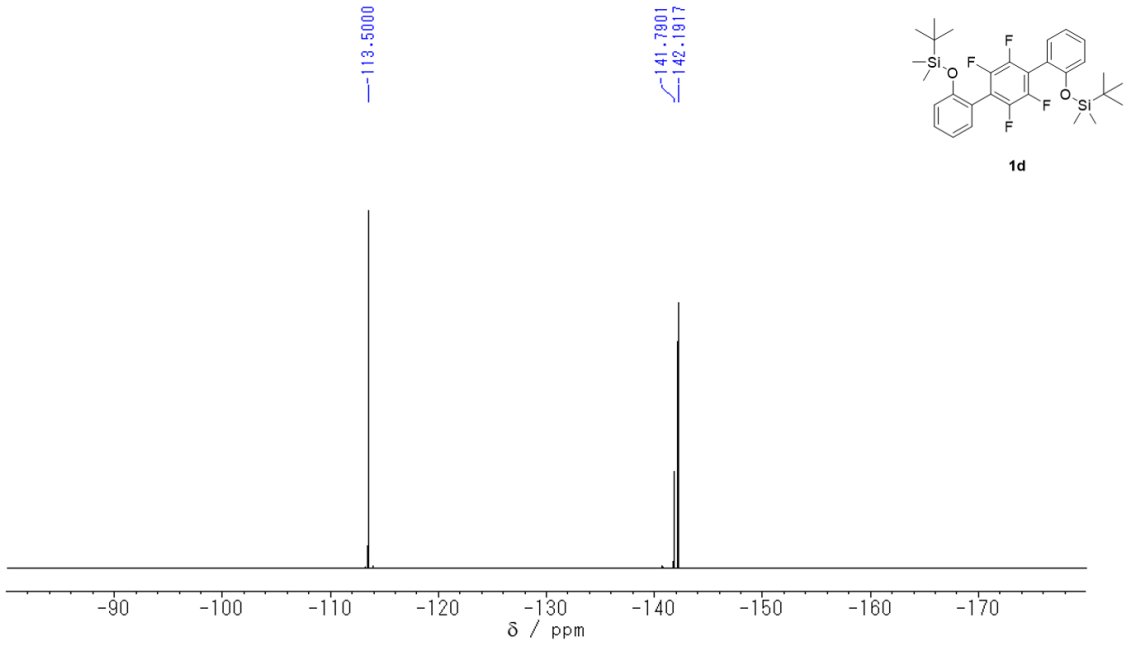

Figure S36. $^{19}F\{^{1}H\}$ NMR spectrum (376.31 MHz, $CDCl_3$) of **1d**.

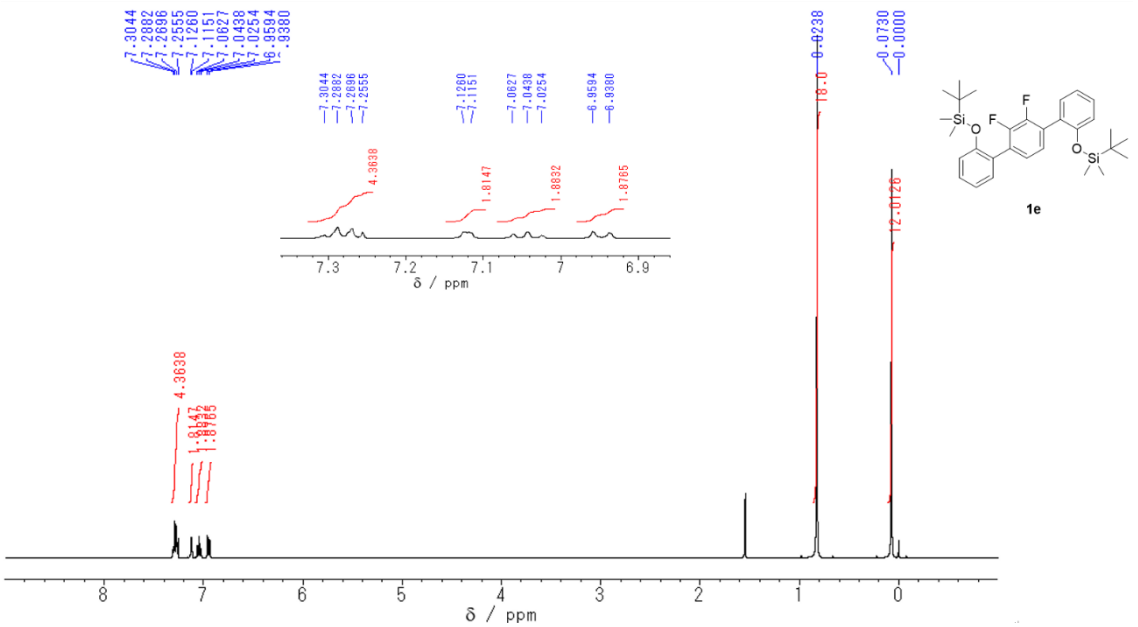

Figure S37. ^{1}H NMR spectrum (400.13 MHz, $CDCl_3$) of **1e**.

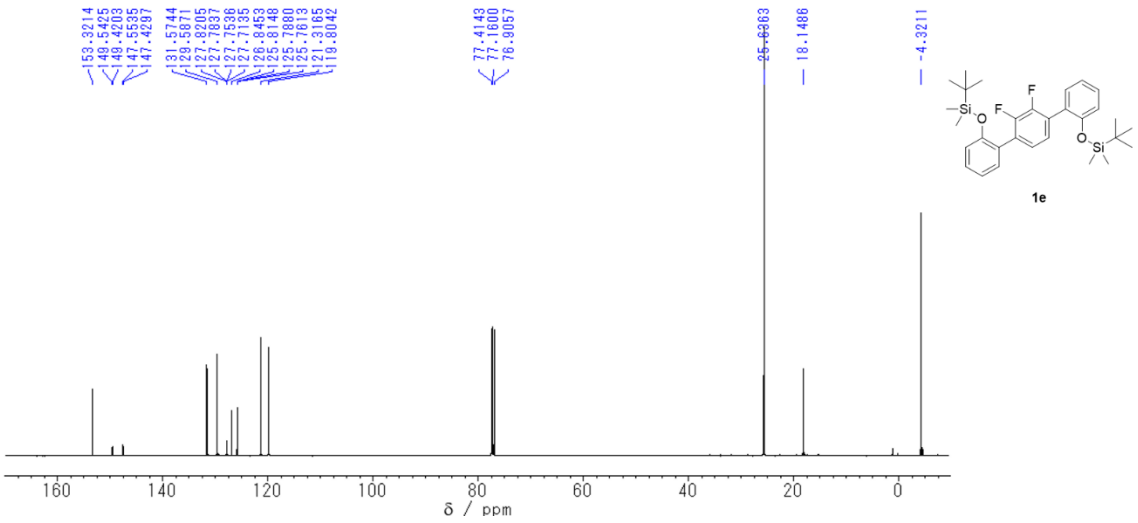

Figure S38. $^{13}C\{^{1}H\}$ NMR spectrum (125.72 MHz, $CDCl_3$) of **1e**.

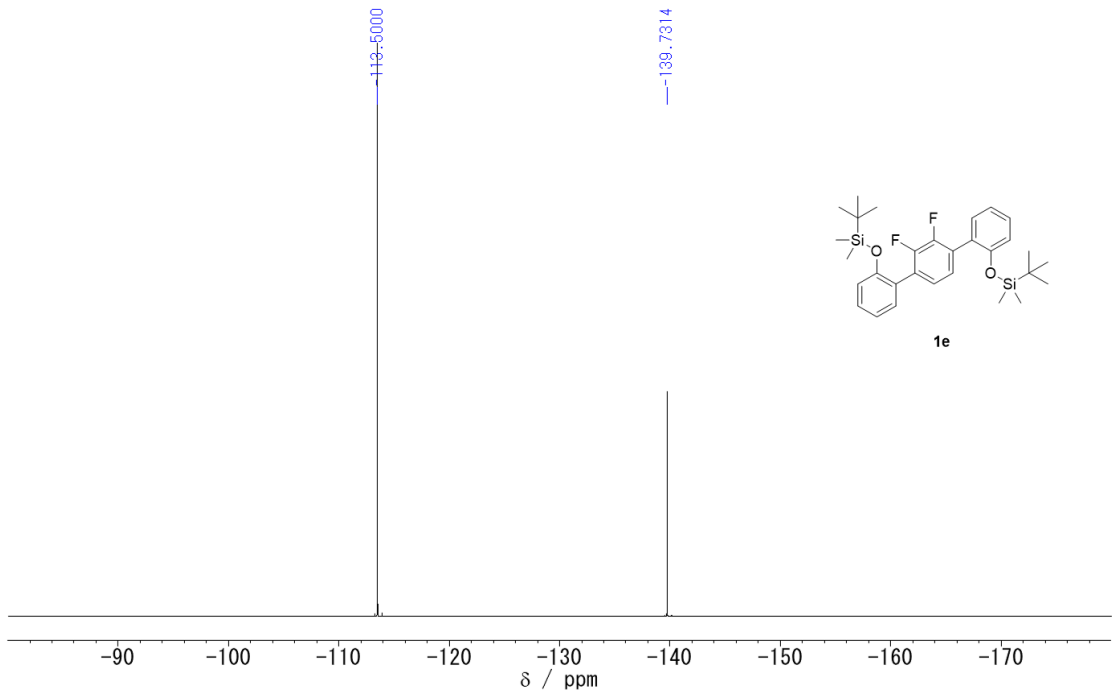

Figure S39. $^{19}F\{^{1}H\}$ NMR spectrum (376.31 MHz, $CDCl_3$) of **1e**.

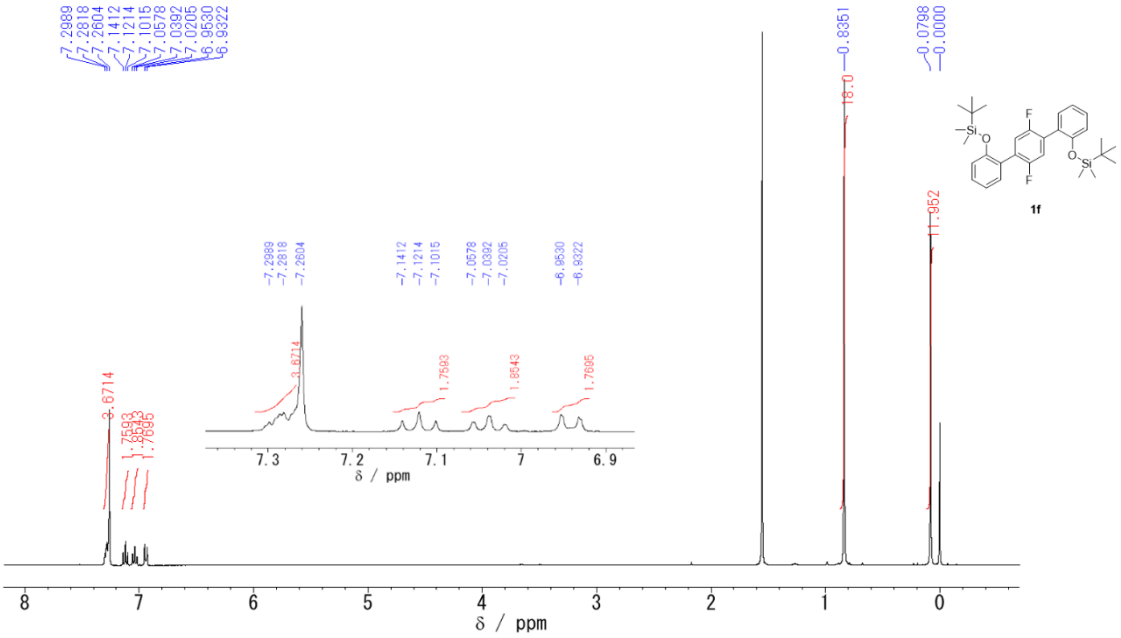

Figure S40. ^{1}H NMR spectrum (400.13 MHz, $CDCl_3$) of **1f**.

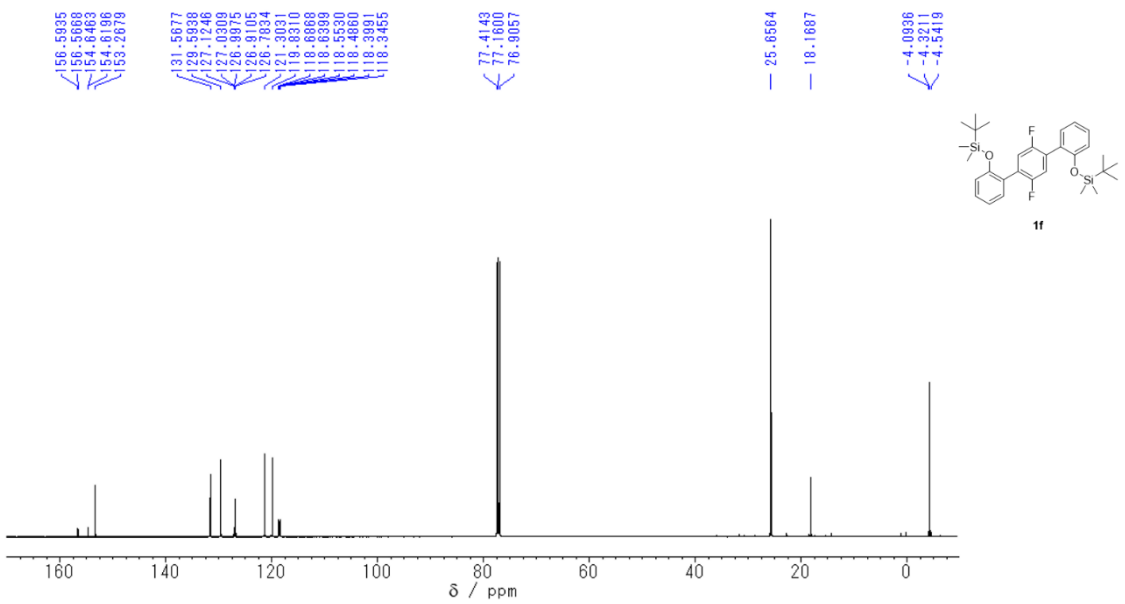

Figure S41. $^{13}C\{^{1}H\}$ NMR spectrum (125.72 MHz, $CDCl_3$) of **1f**.

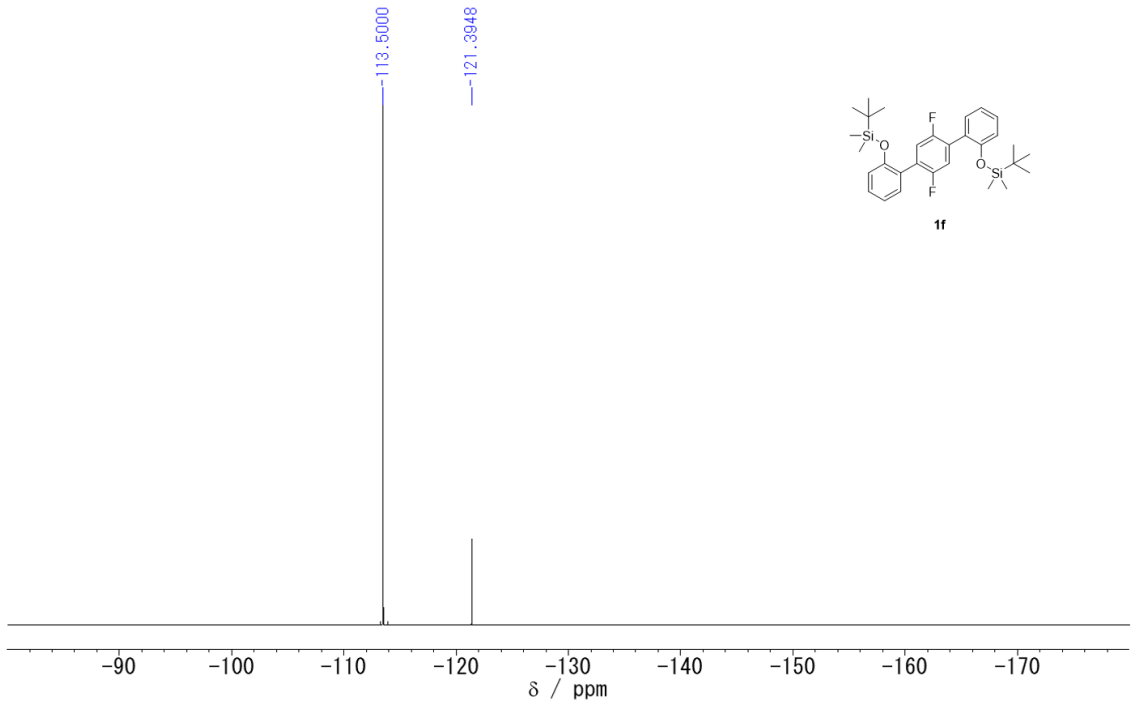

Figure S42. $^{19}F\{^{1}H\}$ NMR spectrum (376.31 MHz, $CDCl_3$) of **1f**.

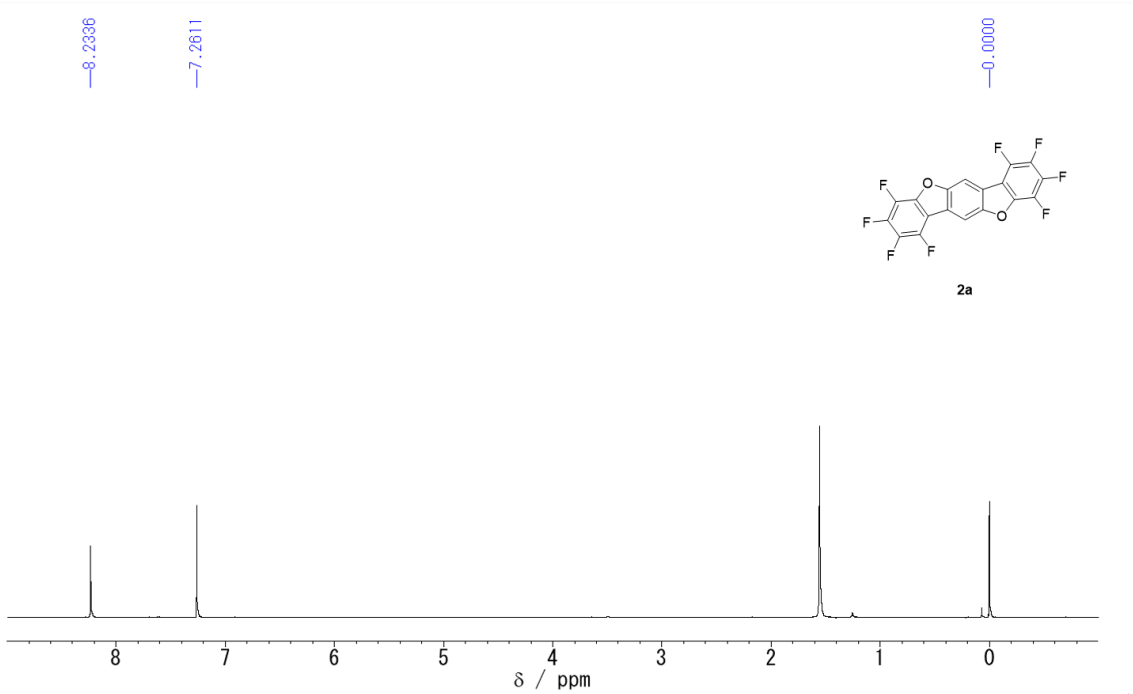

Figure S43. ^{1}H NMR spectrum (300 MHz, $CDCl_3$) of **2a**.

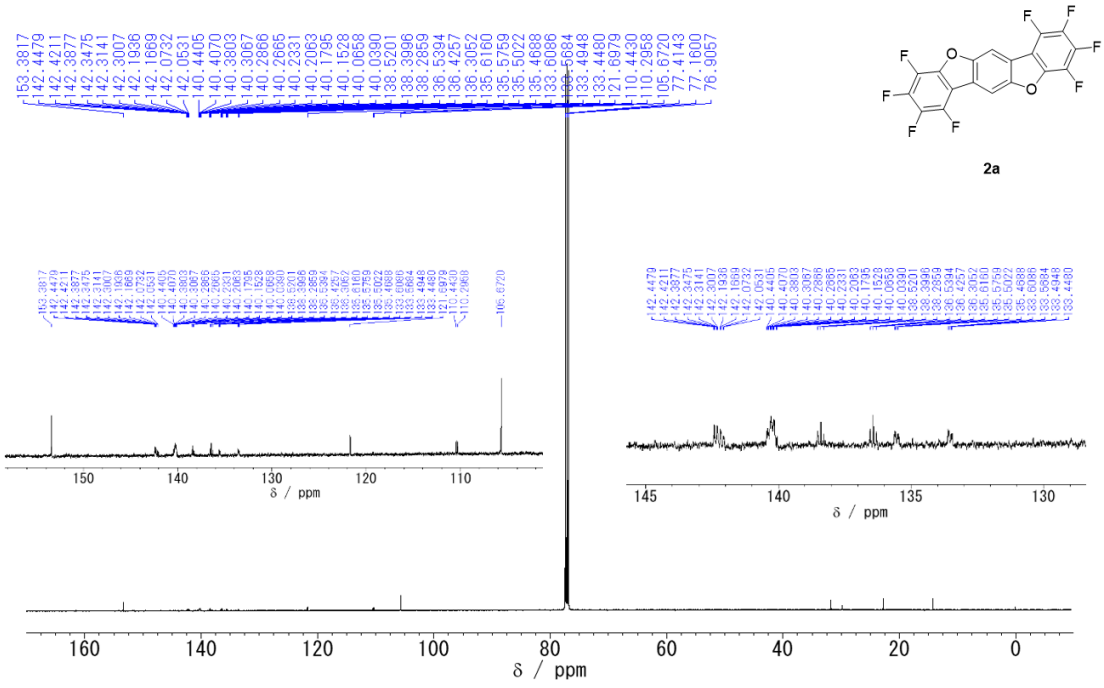

Figure S44. $^{13}C\{^{1}H\}$ NMR spectrum (125.72 MHz, $CDCl_3$) of **2a**.

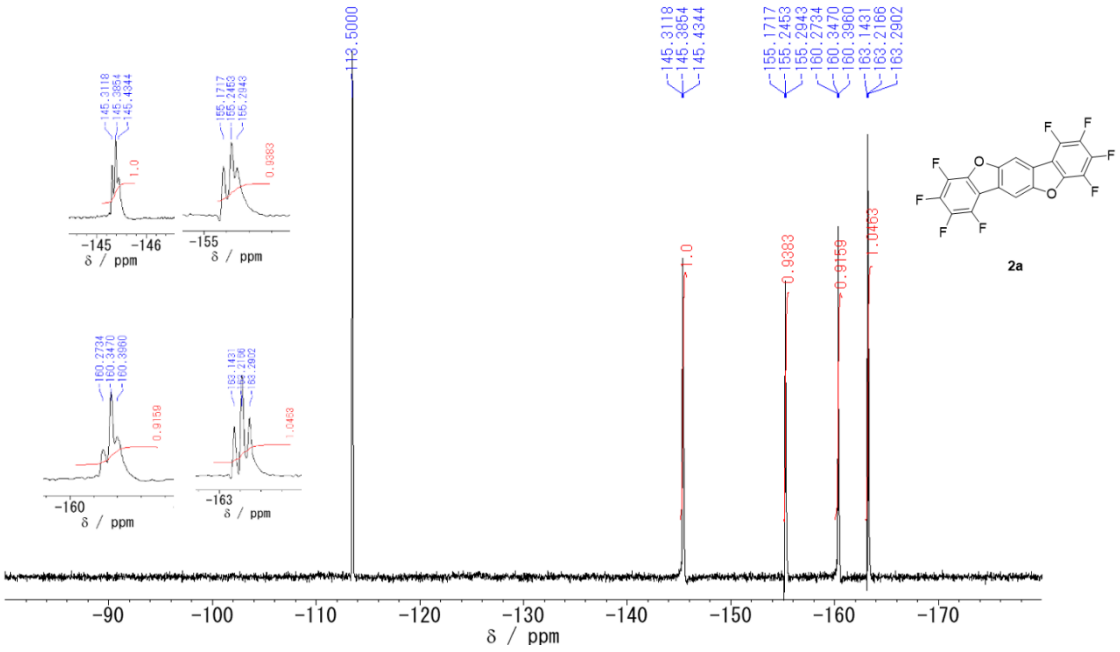

Figure S45. $^{19}F\{^{1}H\}$ NMR spectrum (282.23 MHz, $CDCl_3$) of **2a**.

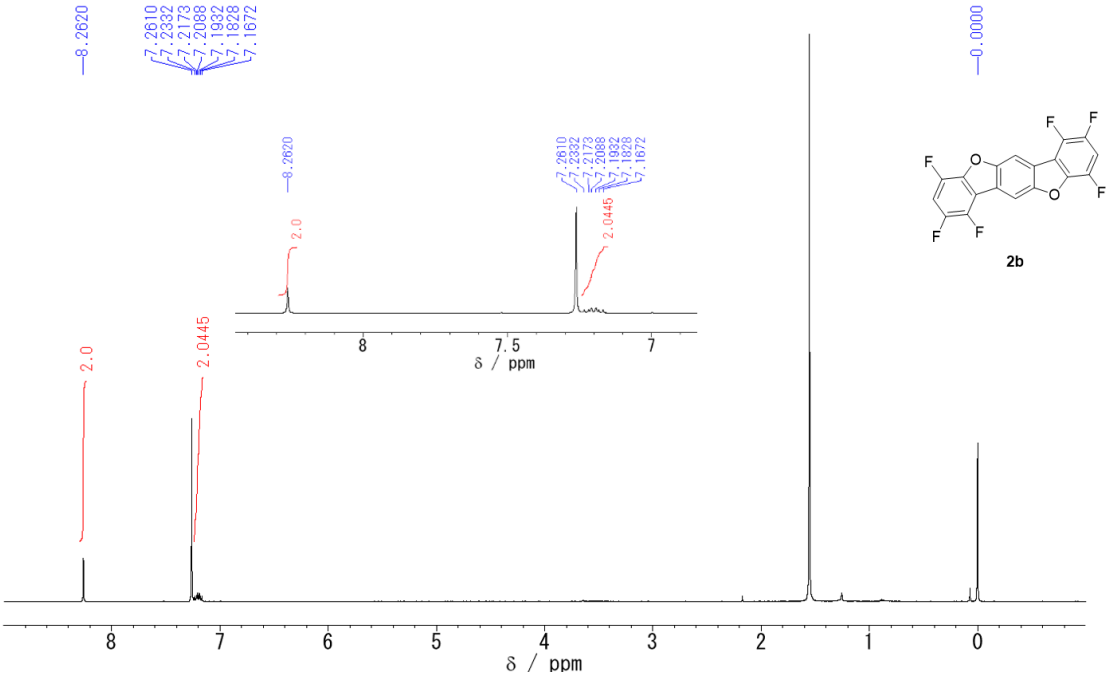

Figure S46. ^{1}H NMR spectrum (400.13 MHz, $CDCl_3$) of **2b**.

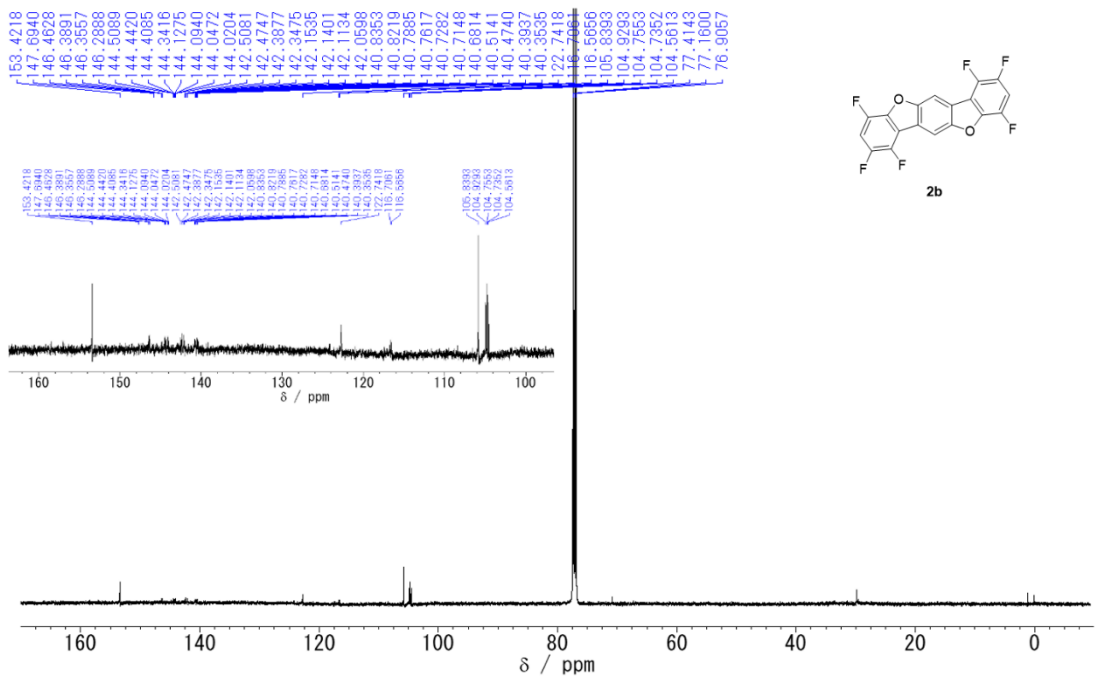

Figure S47. $^{13}C\{^{1}H\}$ NMR spectrum (125.72 MHz, $CDCl_3$) of **2b**.

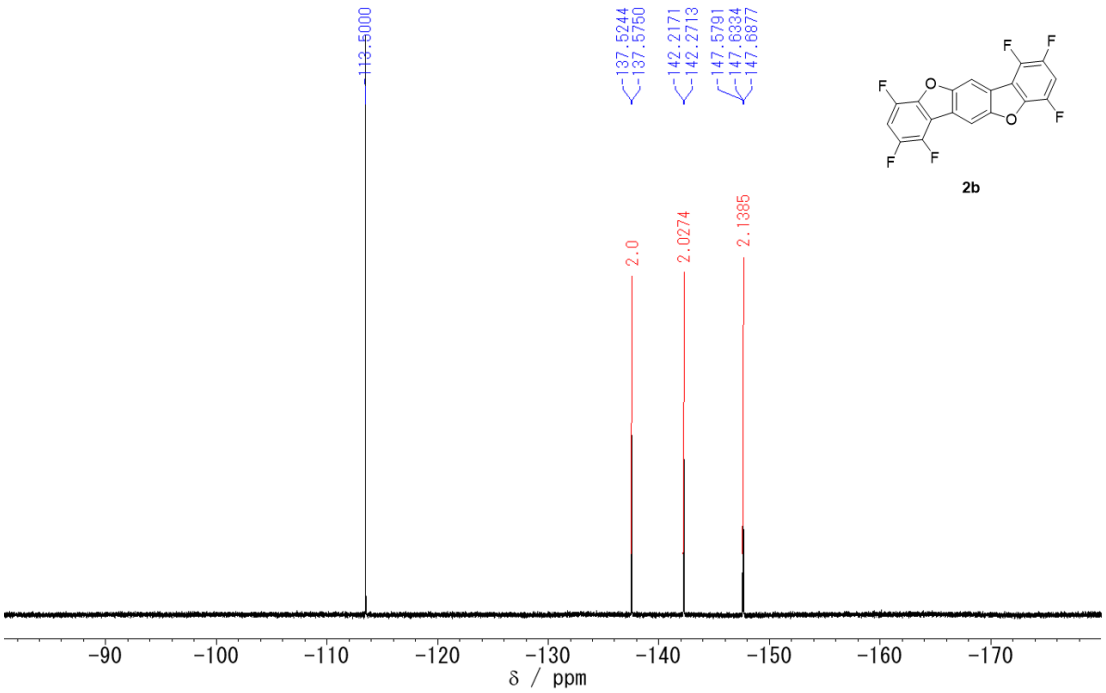

Figure S48. $^{19}F\{^{1}H\}$ NMR spectrum (376.31 MHz, $CDCl_3$) of **2b**.

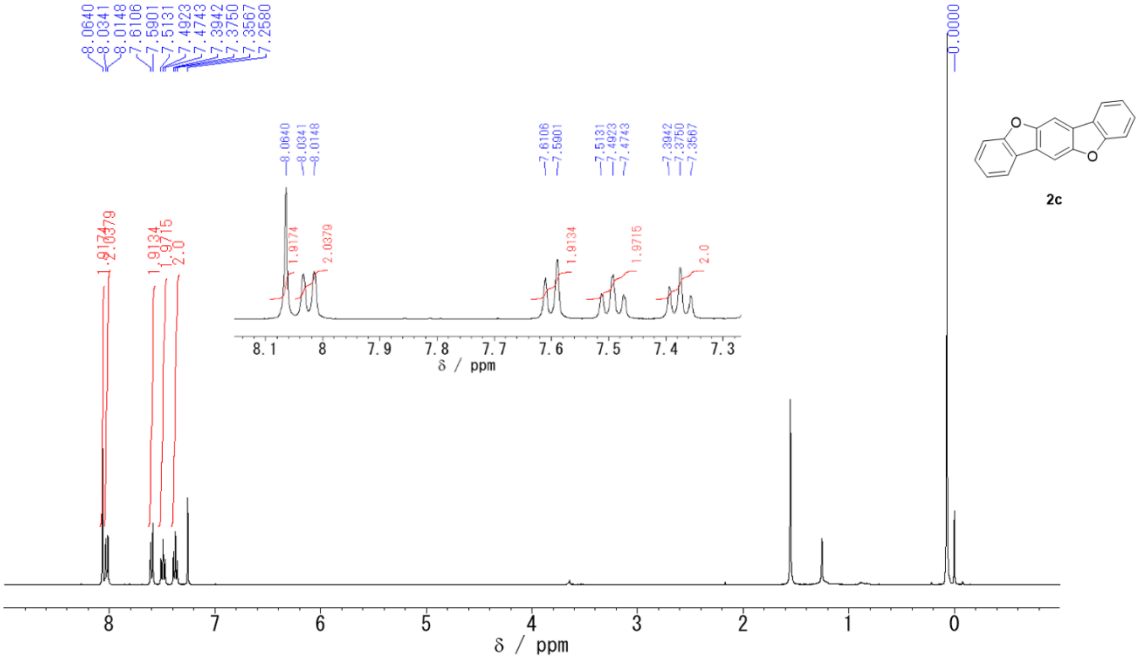

Figure S49. ^{1}H NMR spectrum (400.13 MHz, $CDCl_3$) of **2c**.

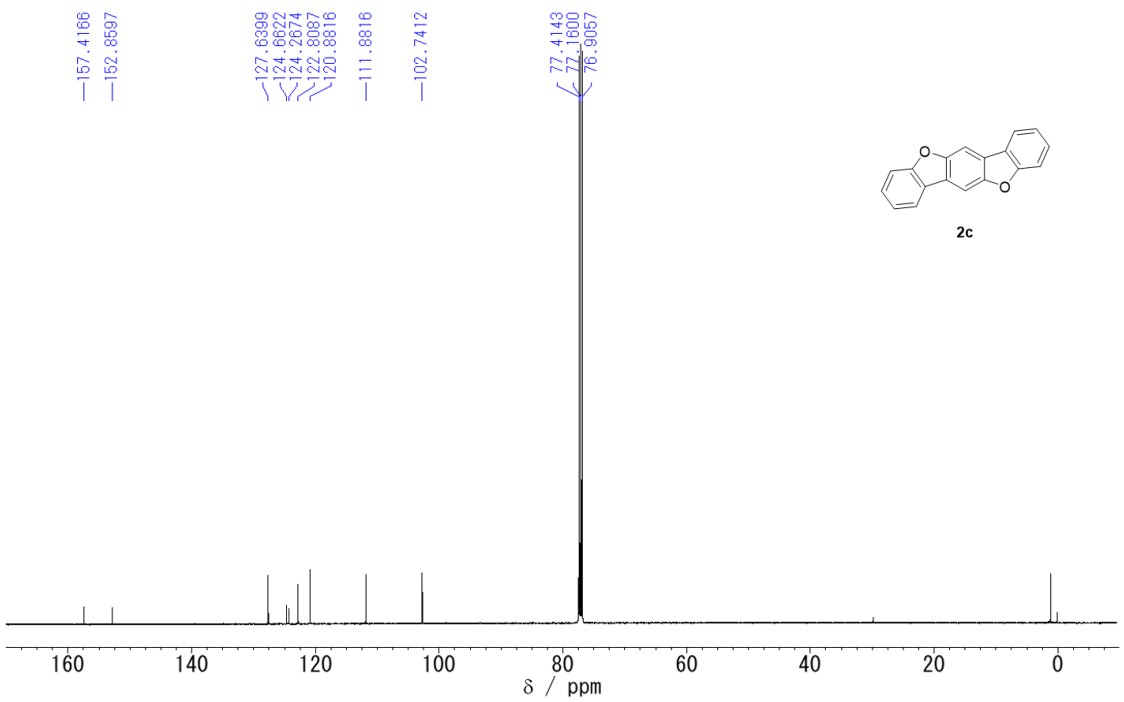

Figure S50. ^{13}C{^{1}H} NMR spectrum (125.72 MHz, $CDCl_3$) of **2c**.

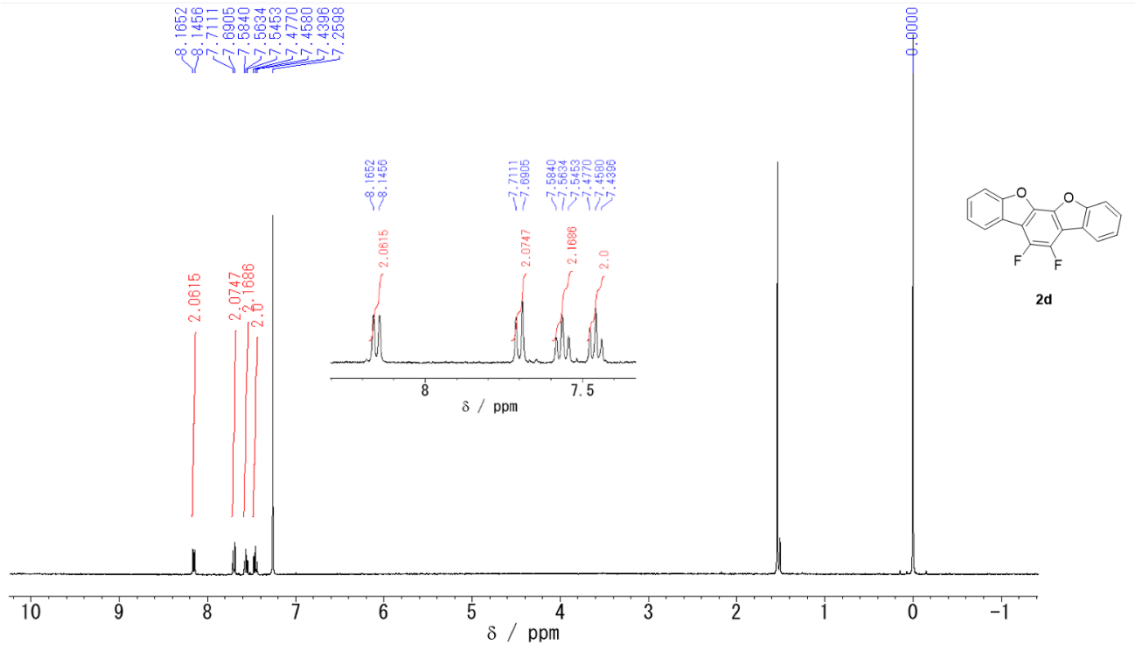

Figure S51. ^{1}H NMR spectrum (400.13 MHz, $CDCl_3$) of **2d**.

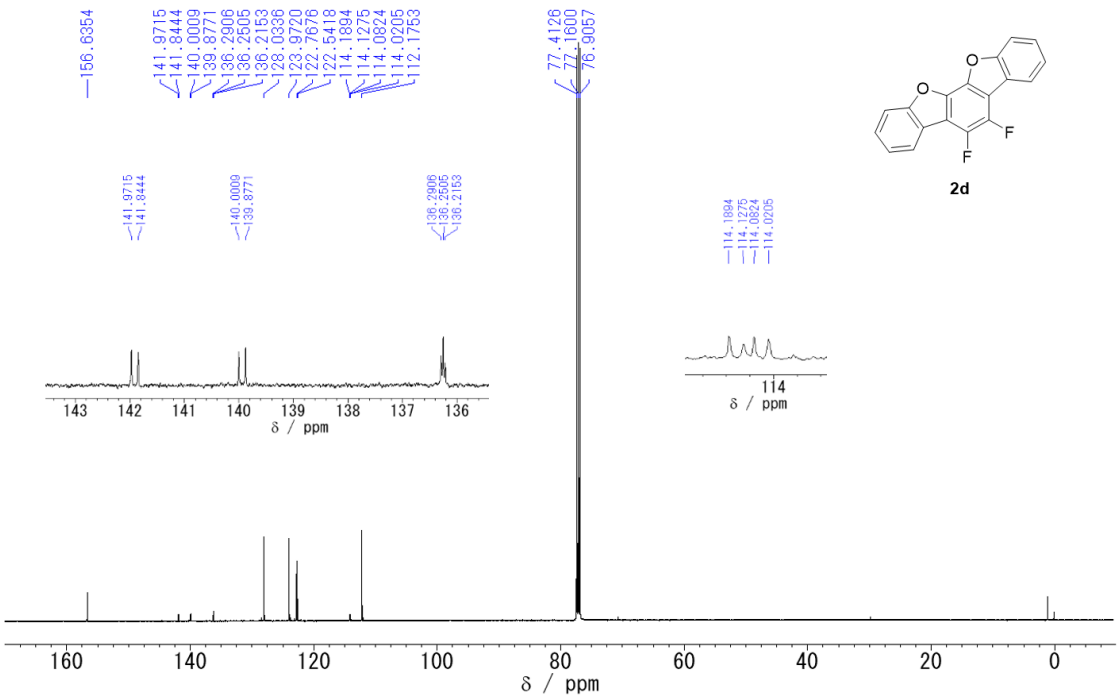

Figure S52. ^{13}C{^{1}H} NMR spectrum (125.72 MHz, $CDCl_3$) of **2d**.

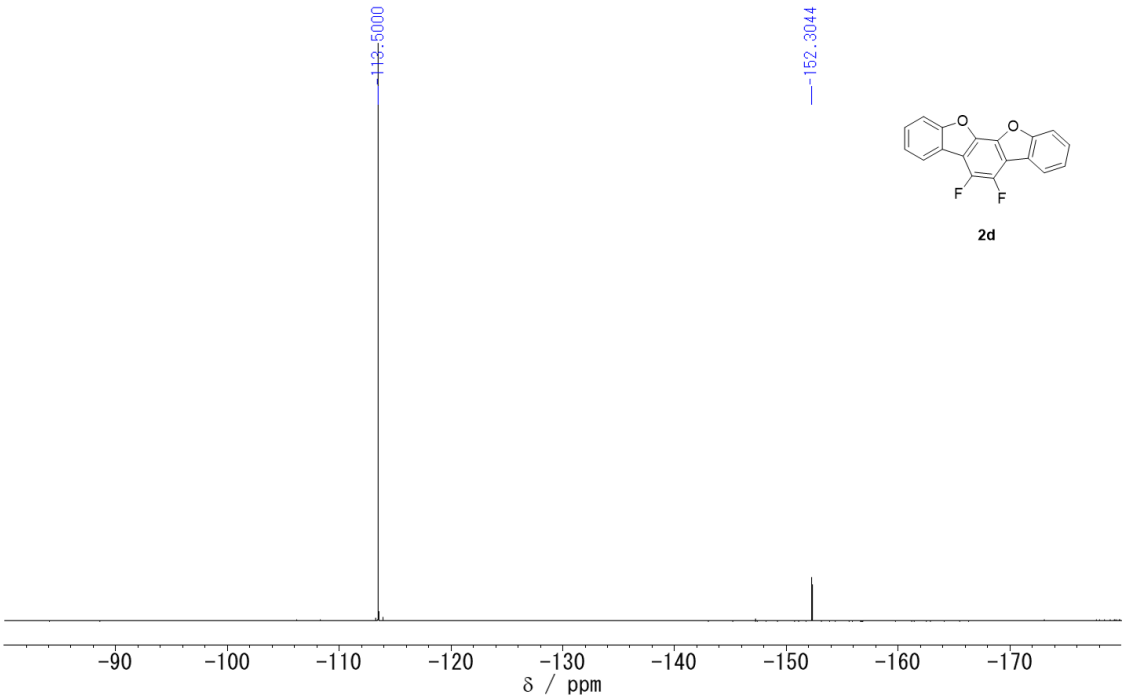

Figure S53. $^{19}F\{^{1}H\}$ NMR spectrum (376.31 MHz, $CDCl_3$) of **2d**.

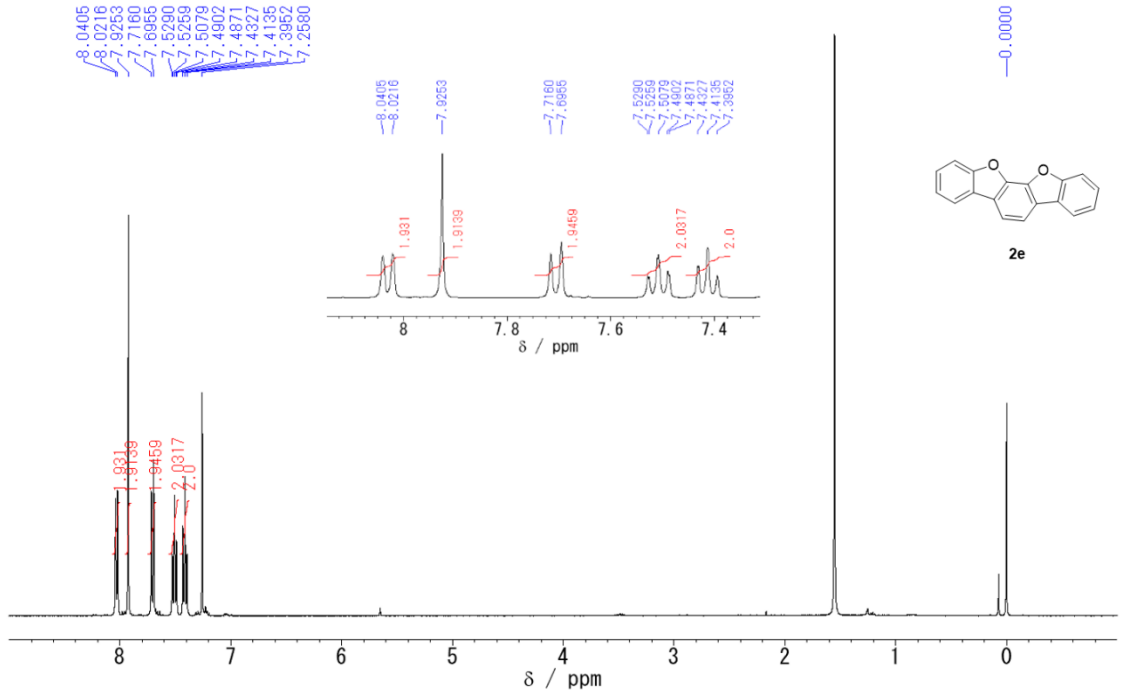

Figure S54. ^{1}H NMR spectrum (400.13 MHz, $CDCl_3$) of **2e**.

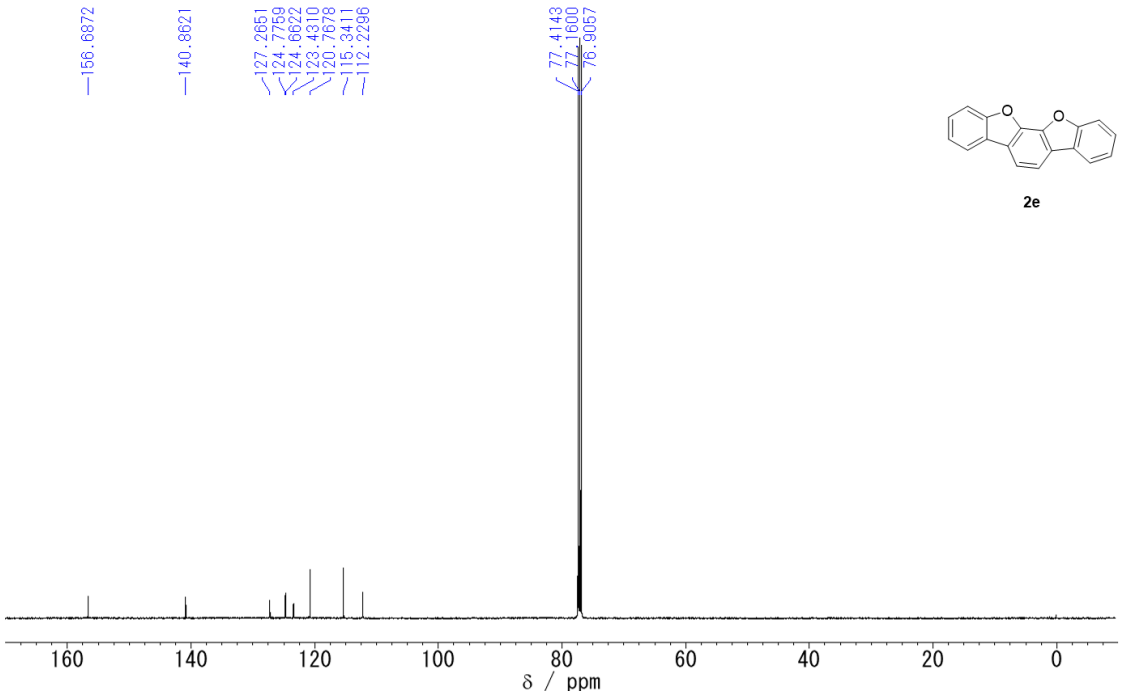

Figure S55. $^{13}C\{^{1}H\}$ NMR spectrum (125.72 MHz, $CDCl_3$) of **2e**.

13. Cartesian coordinates for simulated structures

Table S5. Cartesian coordinates of the optimized structure for *anti*-phenoxide ion (***anti*-PhO**) in Figure S4 and S6.

Symbol	X	Y	Z
C	-1.936953	-0.539568	0.59125
C	-2.46726	0.737597	0.919423
C	-1.815159	1.925399	0.62998
C	-0.569178	1.907488	0.003015
C	-0.017356	0.652826	-0.306537
C	-2.67729	-1.778017	0.87351
C	-4.713595	-3.132969	0.746402
C	-4.073537	-4.151116	1.427841
C	-2.725262	-4.029749	1.833308
C	-2.05178	-2.846249	1.539903
H	-5.749798	-3.235936	0.428851
H	-4.619779	-5.068237	1.655867
H	-2.227115	-4.832964	2.371582
H	-1.016033	-2.731292	1.858015
C	0.394535	2.884772	-0.451873
C	1.452552	2.131738	-1.008384
C	0.481485	4.283814	-0.455837
C	2.585212	2.708176	-1.565007
C	1.615871	4.881978	-1.011582
H	-0.319047	4.885659	-0.036275
C	2.653687	4.107359	-1.558376
H	3.376711	2.094719	-1.984875
H	1.69676	5.966275	-1.022449
H	3.524732	4.599214	-1.984346
F	-3.610504	0.82434	1.622522
F	-2.370658	3.11385	0.991224
O	1.213134	0.780318	-0.925829
O	-4.624096	-0.989038	-0.288606
F	-0.082739	-1.697098	-0.404877
C	-0.673875	-0.534676	-0.027914
C	-4.056794	-1.888071	0.39759

Table S6. Cartesian coordinates of the optimized structure for *anti*-Meisenheimer intermediate (***anti*-int**) in Figure S4 and S6.

Symbol	X	Y	Z
C	-1.469029	-0.908528	0.532675
C	-2.36238	0.191653	0.440848
C	-1.949355	1.42892	-0.031977
C	-0.594534	1.612467	-0.281627
C	0.306579	0.531709	-0.115169
C	-2.295508	-2.033023	0.9029
C	-4.71671	-2.31841	1.230161
C	-4.475479	-3.666285	1.521764
C	-3.171774	-4.192588	1.502554
C	-2.073912	-3.384681	1.193085
H	-5.715601	-1.893544	1.253375
H	-5.312059	-4.313713	1.775302
H	-3.014991	-5.242557	1.73966
H	-1.066709	-3.791137	1.187988
C	0.225492	2.726155	-0.713597
C	1.544974	2.227859	-0.775388
C	-0.010285	4.066486	-1.044873
C	2.632415	3.003255	-1.154284
C	1.072271	4.863386	-1.428886
H	-1.015428	4.473951	-0.995573
C	2.375666	4.339962	-1.483944
H	3.633933	2.584505	-1.186957
H	0.904153	5.906654	-1.685637
H	3.200954	4.981826	-1.783286
F	-2.214793	0.699611	2.688218
F	-2.824984	2.451005	-0.200844
O	1.607853	0.903588	-0.419715
O	-3.664289	-0.207256	0.59099
F	0.768687	-1.756556	0.392079
C	-0.113295	-0.723381	0.279809
C	-3.614991	-1.53079	0.927863

Table S7. Cartesian coordinates of the optimized structure for *anti*-transition state (***anti*-TS**) in Figure S4 and S6.

Symbol	X	Y	Z
C	-1.274115	-0.298862	0.560588
C	-0.873249	1.097757	0.553197
C	0.479662	1.384373	0.259149
C	1.410996	0.369586	0.087853
C	1.010052	-0.978412	0.201348
C	-2.69228	-0.411429	0.231358
C	-4.318742	0.80443	-1.134893
C	-5.216909	-0.252273	-0.953339
C	-4.870998	-1.380947	-0.196074
C	-3.597974	-1.462119	0.385987
H	-4.588191	1.677167	-1.724694
H	-6.20631	-0.190555	-1.405533
H	-5.58297	-2.192935	-0.064404
H	-3.311896	-2.341454	0.957158
C	2.845505	0.317795	-0.121241
C	3.185118	-1.055635	-0.117185
C	3.858478	1.2669	-0.312233
C	4.484047	-1.513314	-0.300136
C	5.172053	0.823431	-0.493655
H	3.619626	2.326185	-0.318933
C	5.481533	-0.548267	-0.488097
H	4.707064	-2.576413	-0.294118
H	5.967188	1.550365	-0.643057
H	6.51113	-0.868276	-0.631592
F	-1.399172	1.917478	1.582246
F	0.891949	2.693147	0.202373
O	2.091502	-1.853213	0.081852
O	-2.154849	1.717835	-0.586172
F	-0.702403	-2.613864	0.408565
C	-0.315468	-1.302373	0.421431
C	-3.054747	0.760709	-0.513879

Table S8. Cartesian coordinates of the optimized structure for *anti*-product **2d'** in Figure S4 and S6.

Symbol	X	Y	Z
C	-1.233678	-1.271219	0.045792
C	-1.522867	-0.050046	-0.609755
C	-0.614283	0.994689	-0.672764
C	0.623007	0.806223	-0.058595
C	0.912319	-0.415075	0.596666
C	0.003551	-1.459624	0.660104
C	-2.422529	-2.082123	-0.113462
C	-3.322662	-1.286379	-0.846628
C	-4.592301	-1.713137	-1.207055
C	-4.956284	-2.999996	-0.804422
C	-4.077284	-3.815677	-0.07187
C	-2.805412	-3.369102	0.281199
H	-5.261389	-1.07356	-1.772573
H	-5.941546	-3.376062	-1.064597
H	-4.396098	-4.811031	0.223335
H	-2.123881	-3.996014	0.846773
C	1.812097	1.616886	0.100104
C	2.712209	0.821163	0.833319
C	2.195108	2.903736	-0.294852
C	3.981731	1.248038	1.194018
C	3.467053	3.350238	0.058049
H	1.513691	3.530535	-0.860688
C	4.345913	2.534696	0.790923
H	4.650576	0.608707	1.7601
H	3.786138	4.345317	-0.237789
H	5.331092	2.910846	1.051295
F	-0.905154	2.148992	-1.299771
O	2.174104	-0.411568	1.137754
O	-2.784518	-0.053688	-1.151155
F	0.294433	-2.613938	1.287084

Table S9. Cartesian coordinates of the optimized structure for *syn*-phenoxide ion (***syn*-PhO**) in Figure S4 and S6.

Symbol	X	Y	Z
C	-1.610488	-0.807433	-0.184527
C	-1.706178	0.175855	-1.202362
C	-1.109393	1.424365	-1.126639
C	-0.370807	1.770307	0.002722
C	-0.259405	0.80725	1.022686
C	-2.290268	-2.107349	-0.282592
C	-3.750638	-3.837149	0.654035
C	-3.572836	-4.599181	-0.485182
C	-2.774304	-4.141451	-1.557487
C	-2.155451	-2.899624	-1.436415
H	-4.373401	-4.19131	1.473722
H	-4.060283	-5.573047	-0.559155
H	-2.635351	-4.745859	-2.451044
H	-1.525984	-2.539096	-2.249267
C	0.3979	2.91073	0.448858
C	0.91602	2.536489	1.708896
C	0.70189	4.180111	-0.061885
C	1.718492	3.368442	2.476944
C	1.509345	5.031049	0.69804
H	0.314932	4.492058	-1.027436
C	2.010688	4.632668	1.949533
H	2.096389	3.045238	3.442167
H	1.753102	6.019254	0.315362
H	2.634865	5.315655	2.520557
F	-2.449322	-0.079558	-2.309108
F	-1.259687	2.317007	-2.144796
O	0.528358	1.267604	2.062241
O	-3.363238	-1.812413	1.846365
F	-0.58773	-1.333311	1.919244
C	-0.843389	-0.446415	0.941425
C	-3.143683	-2.531561	0.828974

Table S10. Cartesian coordinates of the optimized structure for *syn*-Meisenheimer intermediate (***syn*-int**) in Figure S4 and S6.

Symbol	X	Y	Z
C	-1.228429	-0.936299	-0.86507
C	-1.084213	0.049699	-1.85072
C	-0.545761	1.286291	-1.566974
C	-0.180627	1.568199	-0.230483
C	-0.297219	0.587046	0.751049
C	-2.096205	-2.079227	-0.7533
C	-2.897147	-3.432096	1.144655
C	-3.684411	-4.174236	0.245166
C	-3.679545	-3.869962	-1.123619
C	-2.894082	-2.826512	-1.633008
H	-2.889009	-3.646703	2.209881
H	-4.29602	-4.992956	0.618091
H	-4.294483	-4.455041	-1.805039
H	-2.89976	-2.597484	-2.694861
C	0.307925	2.745655	0.456465
C	0.433096	2.36472	1.813277
C	0.635017	4.058248	0.087053
C	0.858523	3.237977	2.80879
C	1.072435	4.945528	1.073932
H	0.547853	4.37389	-0.948552
C	1.182754	4.541427	2.417848
H	0.939306	2.909634	3.841028
H	1.331585	5.965989	0.800311
H	1.527429	5.251865	3.165995
F	-1.585023	-0.189085	-3.103839
F	-0.38297	2.24171	-2.543948
O	0.08061	1.062307	2.002159
O	-1.328955	-1.571837	1.368064
F	0.807114	-1.572054	0.478478
C	-0.598893	-0.78598	0.446281
C	-2.120751	-2.411388	0.624771

Table S11. Cartesian coordinates of the optimized structure for *syn*-transition state (***syn*-TS**) in Figure S4 and S6.

Symbol	X	Y	Z
C	-1.333982	0.442414	0.547521
C	-0.697508	1.663111	0.274481
C	0.660223	1.775348	0.033161
C	1.428772	0.605325	0.029947
C	0.814878	-0.62139	0.321562
C	-2.726132	0.124053	0.233343
C	-3.938805	-1.587646	-1.028666
C	-5.10102	-0.820159	-0.897956
C	-5.091333	0.405289	-0.216919
C	-3.894026	0.880242	0.338175
H	-3.948429	-2.536477	-1.559662
H	-6.03114	-1.189071	-1.32942
H	-6.004507	0.989329	-0.123604
H	-3.870502	1.839126	0.84936
C	2.833939	0.305081	-0.149306
C	2.945282	-1.092823	0.033152
C	3.98477	1.047477	-0.44812
C	4.152729	-1.774461	-0.076739
C	5.206579	0.377757	-0.557324
H	3.922092	2.122155	-0.592556
C	5.289467	-1.014958	-0.374602
H	4.200318	-2.849945	0.067012
H	6.10793	0.940997	-0.788432
H	6.252627	-1.512069	-0.46584
F	-1.46344	2.79129	0.172499
F	1.249477	2.999959	-0.167768
O	1.742453	-1.662209	0.323874
O	-1.60944	-1.822111	-0.454888
F	-0.800464	-1.64758	1.706673
C	-0.554759	-0.767596	0.633712
C	-2.739515	-1.150815	-0.430653

Table S12. Cartesian coordinates of the optimized structure for *syn*-product **2d** in Figure S4 and S6.

Symbol	X	Y	Z
C	-1.582901	-0.665723	-0.488831
C	-0.582558	-0.334663	-1.413152
C	0.220115	0.774532	-1.196031
C	0.029647	1.562522	-0.052594
C	-0.974092	1.23261	0.877518
C	-1.776488	0.123595	0.660505
C	-2.571583	-1.719217	-0.400775
C	-3.273993	-1.471182	0.794261
C	-4.316416	-2.268746	1.242537
C	-4.655243	-3.361034	0.441283
C	-3.971222	-3.632282	-0.756251
C	-2.926306	-2.819351	-1.190287
H	-4.835844	-2.047848	2.168801
H	-5.465666	-4.013709	0.75271
H	-4.263704	-4.491394	-1.352846
H	-2.396281	-3.02606	-2.114141
C	0.66378	2.752198	0.474287
C	-0.014002	3.033798	1.676079
C	1.709213	3.587436	0.06335
C	0.300364	4.110918	2.49137
C	2.039567	4.674754	0.869386
H	2.242588	3.386015	-0.859738
C	1.345917	4.932173	2.064431
H	-0.243251	4.297977	3.411183
H	2.847357	5.336258	0.570336
H	1.62724	5.788026	2.671167
F	-0.403768	-1.095284	-2.510416
F	1.182868	1.09719	-2.081203
O	-1.011251	2.113052	1.926713
O	-2.794953	-0.351717	1.444191

Table S13. Cartesian coordinates of the optimized structure for *anti*-phenoxide ion (***anti*-PhO**) in Figure S5.

Symbol	X	Y	Z
C	-2.027615	-0.645063	0.601705
C	-2.557926	0.599463	1.009905
C	-1.925665	1.802657	0.75816
C	-0.707095	1.816056	0.089558
C	-0.159744	0.593676	-0.303313
C	-2.75625	-1.901995	0.848073
C	-4.749213	-3.2739	0.613711
C	-4.123579	-4.286567	1.311608
C	-2.804425	-4.150828	1.783529
C	-2.142689	-2.953574	1.533649
H	-5.767186	-3.394031	0.248213
H	-4.66463	-5.214849	1.499942
H	-2.31758	-4.952876	2.332295
H	-1.122788	-2.819852	1.894217
C	0.238807	2.821467	-0.345948
C	1.272128	2.10286	-0.969073
C	0.317728	4.213226	-0.279414
C	2.383492	2.711173	-1.530405
C	1.4277	4.842595	-0.837477
H	-0.471905	4.786126	0.195897
C	2.445969	4.10183	-1.454003
H	3.162403	2.124037	-2.005691
H	1.505888	5.925478	-0.796155
H	3.300467	4.61893	-1.881971
F	-3.682046	0.635055	1.729164
F	-2.471033	2.962168	1.182583
O	1.041593	0.757953	-0.948933
O	-4.652048	-1.10544	-0.361769
F	-0.220406	-1.742475	-0.502964
C	-0.799558	-0.610966	-0.061162
C	-4.10323	-2.016232	0.316894

Table S14. Cartesian coordinates of the optimized structure for *anti*-Meisenheimer intermediate (***anti*-int**) in Figure S5.

Symbol	X	Y	Z
C	-1.497293	-0.918322	0.967629
C	-2.395559	0.226523	1.149391
C	-2.00018	1.400538	0.410146
C	-0.696429	1.552525	0.01745
C	0.233308	0.488519	0.134948
C	-2.335928	-2.08627	1.063345
C	-4.762576	-2.438554	1.060261
C	-4.529889	-3.81954	1.103458
C	-3.226776	-4.322797	1.122311
C	-2.122806	-3.464939	1.099526
H	-5.767407	-2.027434	1.041645
H	-5.375109	-4.503159	1.127109
H	-3.06684	-5.398038	1.156514
H	-1.112179	-3.861593	1.109903
C	0.073601	2.641651	-0.562634
C	1.380629	2.145308	-0.7218
C	-0.210471	3.952005	-0.944154
C	2.411375	2.909567	-1.249937
C	0.813835	4.734545	-1.476909
H	-1.21408	4.347886	-0.825236
C	2.107512	4.218067	-1.626928
H	3.409375	2.497067	-1.360836
H	0.606808	5.757931	-1.77891
H	2.89109	4.845836	-2.044096
F	-2.449881	0.613287	2.662837
F	-2.897045	2.415926	0.243326
O	1.502415	0.860794	-0.304362
O	-3.715929	-0.247337	0.976645
F	0.654872	-1.820901	0.503724
C	-0.177718	-0.748615	0.567538
C	-3.661159	-1.604375	1.048919

Table S15. Cartesian coordinates of the optimized structure for *anti*-transition state (***anti*-TS**) in Figure S5.

Symbol	X	Y	Z
C	-1.578809	-0.799756	1.137232
C	-2.390272	0.375981	1.350186
C	-1.94276	1.58634	0.781319
C	-0.740905	1.652837	0.10095
C	0.062305	0.511356	-0.02709
C	-2.415758	-1.99731	1.203846
C	-4.700634	-2.612469	0.628005
C	-4.35737	-3.948748	0.827937
C	-3.065329	-4.321275	1.208776
C	-2.089346	-3.334928	1.383433
H	-5.706828	-2.329069	0.331121
H	-5.117602	-4.715983	0.68865
H	-2.817011	-5.368672	1.36118
H	-1.074051	-3.609319	1.656697
C	0.028151	2.717064	-0.517073
C	1.219124	2.112972	-0.959667
C	-0.168812	4.080635	-0.737522
C	2.218233	2.816144	-1.61697
C	0.826111	4.803111	-1.393334
H	-1.082763	4.560586	-0.402595
C	2.003672	4.17793	-1.827061
H	3.12455	2.318959	-1.948006
H	0.687477	5.865947	-1.573107
H	2.764947	4.762853	-2.336998
F	-2.9657	0.534238	2.611501
F	-2.69011	2.715136	0.936317
O	1.260675	0.786761	-0.66987
O	-3.975309	-0.32428	0.7361
F	0.368448	-1.819267	0.238559
C	-0.365418	-0.703542	0.470897
C	-3.744968	-1.604487	0.848741

Table S16. Cartesian coordinates of the optimized structure for *anti*-product **2d'** in Figure S5.

Symbol	X	Y	Z
C	-1.226927	-1.267338	0.04665
C	-1.520017	-0.054559	-0.606741
C	-0.615657	0.99025	-0.672063
C	0.616502	0.802097	-0.060024
C	0.909591	-0.410684	0.593372
C	0.005306	-1.455565	0.658522
C	-2.416698	-2.078385	-0.112458
C	-3.308543	-1.283351	-0.842017
C	-4.576631	-1.707215	-1.203261
C	-4.940739	-2.98875	-0.802467
C	-4.066224	-3.804571	-0.071361
C	-2.798033	-3.360919	0.281342
H	-5.243553	-1.066673	-1.768836
H	-5.925618	-3.363463	-1.063208
H	-4.386848	-4.798688	0.223059
H	-2.117869	-3.988137	0.846869
C	1.806205	1.61321	0.099242
C	2.698188	0.818033	0.828476
C	2.187388	2.8959	-0.294199
C	3.966329	1.241843	1.189598
C	3.455612	3.339517	0.058427
H	1.507096	3.52325	-0.859425
C	4.330279	2.523537	0.789173
H	4.633339	0.601207	1.754961
H	3.77616	4.333713	-0.235812
H	5.315165	2.898244	1.049899
F	-0.908362	2.135446	-1.295958
O	2.16345	-0.40628	1.130741
O	-2.773777	-0.059064	-1.144341
F	0.29802	-2.600777	1.282383

Table S17. Cartesian coordinates of the optimized structure for *syn*-phenoxide ion (***syn*-PhO**) in Figure S5.

Symbol	X	Y	Z
C	-1.233678	-1.271219	0.045792
C	-1.522867	-0.050046	-0.609755
C	-0.614283	0.994689	-0.672764
C	0.623007	0.806223	-0.058595
C	0.912319	-0.415075	0.596666
C	0.003551	-1.459624	0.660104
C	-2.422529	-2.082123	-0.113462
C	-3.322662	-1.286379	-0.846628
C	-4.592301	-1.713137	-1.207055
C	-4.956284	-2.999996	-0.804422
C	-4.077284	-3.815677	-0.07187
C	-2.805412	-3.369102	0.281199
H	-5.261389	-1.07356	-1.772573
H	-5.941546	-3.376062	-1.064597
H	-4.396098	-4.811031	0.223335
H	-2.123881	-3.996014	0.846773
C	1.812097	1.616886	0.100104
C	2.712209	0.821163	0.833319
C	2.195108	2.903736	-0.294852
C	3.981731	1.248038	1.194018
C	3.467053	3.350238	0.058049
H	1.513691	3.530535	-0.860688
C	4.345913	2.534696	0.790923
H	4.650576	0.608707	1.7601
H	3.786138	4.345317	-0.237789
H	5.331092	2.910846	1.051295
F	-0.905154	2.148992	-1.299771
O	2.174104	-0.411568	1.137754
O	-2.784518	-0.053688	-1.151155
F	0.294433	-2.613938	1.287084

Table S18. Cartesian coordinates of the optimized structure for *syn*-Meisenheimer intermediate (***syn*-int**) in Figure S5.

Symbol	X	Y	Z
C	-1.172398	-1.074564	-0.821252
C	-1.055861	-0.071675	-1.788874
C	-0.560275	1.173091	-1.49039
C	-0.228772	1.443826	-0.143366
C	-0.316374	0.456801	0.818618
C	-2.058307	-2.204794	-0.722138
C	-2.919199	-3.528506	1.157472
C	-3.69557	-4.2617	0.247756
C	-3.655864	-3.966736	-1.116207
C	-2.843831	-2.940656	-1.611611
H	-2.938888	-3.735286	2.223446
H	-4.328533	-5.067348	0.611708
H	-4.264897	-4.544635	-1.807912
H	-2.822004	-2.715752	-2.673548
C	0.187989	2.63225	0.570266
C	0.296544	2.238164	1.916551
C	0.4595	3.958765	0.224711
C	0.657591	3.114584	2.931878
C	0.830028	4.848539	1.22913
H	0.380787	4.2817	-0.808647
C	0.92759	4.431083	2.566255
H	0.728945	2.776074	3.960753
H	1.046633	5.88335	0.976213
H	1.220144	5.146346	3.330932
F	-1.535791	-0.31347	-3.038458
F	-0.405397	2.141422	-2.44484
O	0.003205	0.927716	2.078288
O	-1.33362	-1.701992	1.404929
F	0.777991	-1.661774	0.58334
C	-0.562124	-0.934895	0.503489
C	-2.117846	-2.525851	0.651066

Table S19. Cartesian coordinates of the optimized structure for *syn*-transition state (***syn*-TS**) in Figure S5.

Symbol	X	Y	Z
C	-1.32382	0.431628	0.570233
C	-0.701934	1.648942	0.272497
C	0.651209	1.768914	0.029723
C	1.421053	0.605407	0.040409
C	0.822627	-0.615732	0.342529
C	-2.716427	0.109242	0.253533
C	-3.915399	-1.547324	-1.070414
C	-5.078398	-0.798022	-0.898841
C	-5.077876	0.391021	-0.16508
C	-3.882903	0.847525	0.400916
H	-3.922284	-2.471065	-1.642927
H	-6.006775	-1.154265	-1.343175
H	-5.99474	0.961891	-0.04057
H	-3.860448	1.782297	0.95459
C	2.826466	0.308208	-0.142178
C	2.93752	-1.080084	0.050831
C	3.9681	1.050538	-0.450933
C	4.14433	-1.758831	-0.055829
C	5.186948	0.385763	-0.558191
H	3.899278	2.122975	-0.604195
C	5.272316	-1.001368	-0.363358
H	4.194682	-2.832165	0.096718
H	6.085842	0.947848	-0.797642
H	6.235938	-1.496262	-0.453981
F	-1.470719	2.760447	0.164431
F	1.228562	2.983292	-0.195015
O	1.745187	-1.646883	0.347949
O	-1.591515	-1.790312	-0.519168
F	-0.812171	-1.681519	1.652076
C	-0.546785	-0.768014	0.642279
C	-2.715682	-1.131759	-0.463543

Table S20. Cartesian coordinates of the optimized structure for *syn*-product **2d** in Figure S5.

Symbol	X	Y	Z
C	-1.576524	-0.660771	-0.491813
C	-0.579573	-0.333462	-1.415821
C	0.220572	0.772152	-1.199334
C	0.0277	1.555979	-0.057713
C	-0.968972	1.230173	0.86782
C	-1.770828	0.121944	0.650896
C	-2.566764	-1.713325	-0.40025
C	-3.26024	-1.459387	0.790043
C	-4.301855	-2.251666	1.243477
C	-4.643558	-3.34103	0.449216
C	-3.965559	-3.617533	-0.74662
C	-2.923354	-2.810928	-1.184388
H	-4.817641	-2.026463	2.169882
H	-5.454124	-3.990706	0.764185
H	-4.261825	-4.477256	-1.339014
H	-2.396459	-3.021347	-2.108359
C	0.659551	2.746086	0.472458
C	-0.019872	3.018977	1.666641
C	1.701002	3.580951	0.066183
C	0.289031	4.092621	2.485308
C	2.025848	4.663031	0.873652
H	2.236734	3.38352	-0.855557
C	1.329716	4.91386	2.064715
H	-0.257263	4.275097	3.403597
H	2.832259	5.327088	0.579447
H	1.607697	5.768054	2.674127
F	-0.403877	-1.091034	-2.505192
F	1.177967	1.09487	-2.077286
O	-1.009217	2.102255	1.911513
O	-2.781437	-0.346909	1.432028

Table S21. Cartesian coordinates of the optimized structure for phenoxide ion in Figure S7.

Symbol	X	Y	Z
C	-1.953235	-0.5275	0.587041
C	-0.59435	-0.339226	0.96642
C	0.1262	0.802855	0.655598
C	-0.48627	1.849245	-0.032885
C	-1.836972	1.696629	-0.386593
C	-2.670609	-1.768571	0.888656
C	-2.802427	-4.216328	0.934195
C	-4.071649	-4.13563	1.464504
C	-4.688907	-2.887656	1.703785
C	-3.979965	-1.73205	1.40197
H	-2.332685	-5.179717	0.743641
H	-4.612998	-5.053329	1.703224
H	-5.689222	-2.830585	2.126997
H	-4.437915	-0.763102	1.594197
C	-0.095323	3.150741	-0.516957
C	-1.249981	3.679737	-1.136024
C	1.077788	3.91412	-0.499592
C	-1.280651	4.929766	-1.734516
C	1.063027	5.175701	-1.09742
H	1.974413	3.522669	-0.029223
C	-0.097552	5.677935	-1.705906
H	-2.186664	5.302716	-2.201801
H	1.966864	5.780027	-1.092396
H	-0.081322	6.663742	-2.163684
F	0.017869	-1.245798	1.741051
F	1.413157	0.929291	1.062587
O	-2.310537	2.808805	-1.064619
O	-0.887481	-3.132841	0.034363
F	-3.839054	0.473327	-0.512563
C	-2.553838	0.548726	-0.097455
C	-2.01591	-3.046538	0.581676

Table S22. Cartesian coordinates of the optimized structure for phenoxide ion in Figure S8.

Symbol	X	Y	Z
C	-2.002916	-0.497908	0.595551
C	-1.062331	0.065724	1.498362
C	-0.361489	1.234804	1.252899
C	-0.559067	1.91433	0.052909
C	-1.488715	1.376742	-0.854689
C	-2.697838	-1.756593	0.877889
C	-3.469334	-3.982299	0.196058
C	-4.030269	-4.167093	1.440809
C	-3.931115	-3.177423	2.444055
C	-3.25953	-1.99915	2.144941
H	-3.54176	-4.749141	-0.573256
H	-4.56061	-5.096442	1.658184
H	-4.379799	-3.327196	3.42347
H	-3.186896	-1.223067	2.904949
C	-0.06711	3.127572	-0.552855
C	-0.749051	3.227946	-1.786254
C	0.852444	4.121947	-0.199481
C	-0.549585	4.273206	-2.675335
C	1.063853	5.181318	-1.083913
H	1.384805	4.060704	0.744741
C	0.374531	5.256988	-2.304115
H	-1.090991	4.316527	-3.615095
H	1.775463	5.961168	-0.823811
H	0.559598	6.091946	-2.975153
F	-0.793004	-0.568026	2.663463
F	0.528567	1.704173	2.163191
O	-1.61312	2.179328	-1.977602
O	-2.18671	-2.648146	-1.294725
F	-3.1601	-0.137585	-1.475635
C	-2.209533	0.221083	-0.602715
C	-2.74482	-2.778669	-0.17588

Table S23. Cartesian coordinates of the optimized structure for **2a** in Figure 5.

Symbol	X	Y	Z
C	-0.21805	0.003825	1.334377
C	1.036492	0.605267	1.41161
C	1.280007	1.54691	2.403799
C	0.272562	1.889123	3.31897
C	-0.990104	1.300574	3.261212
C	-0.826969	-0.984447	0.471566
C	-2.148593	-1.136993	0.959935
C	-0.378635	-1.7225	-0.62993
C	-3.085347	-1.997604	0.414626
C	-1.315482	-2.582892	-1.175423
H	0.625099	-1.627957	-1.026319
C	-2.637086	-2.735487	-0.687013
H	-4.089127	-2.09204	0.810924
C	-3.246026	-3.723708	-1.549866
C	-4.500663	-4.324932	-1.627283
C	-2.250867	-4.081416	-2.478031
C	-4.744274	-5.266351	-2.619661
C	-2.47417	-5.019998	-3.477089
C	-3.736937	-5.608312	-3.535044
O	-2.380486	-0.317557	2.048134
O	-1.083704	-3.402061	-2.263848
C	-1.213373	0.361913	2.262219
F	-1.935518	1.641255	4.143302
F	2.00504	0.283381	0.539894
F	2.475969	2.14023	2.500948
F	-5.46918	-4.003112	-0.75551
F	-5.940391	-5.859308	-2.717115
F	-1.528821	-5.36053	-4.359306
F	-4.000422	-6.517205	-4.478789
F	0.535913	2.798329	4.26245

Table S24. Cartesian coordinates of the optimized structure for **2b** in Figure 5.

Symbol	X	Y	Z
C	-0.220481	0.005201	1.3346
C	1.035132	0.605384	1.409573
C	1.268969	1.546067	2.40584
C	0.277299	1.899156	3.326669
C	-0.976687	1.303709	3.256151
H	0.491158	2.636318	4.091657
C	-0.828561	-0.983233	0.471728
C	-2.151033	-1.13633	0.960297
C	-0.377778	-1.719828	-0.629603
C	-3.085491	-1.997985	0.411945
C	-1.311975	-2.582094	-1.177439
H	0.626674	-1.622582	-1.023608
C	-2.634566	-2.734912	-0.689106
H	-4.090145	-2.094759	0.805551
C	-3.242754	-3.723095	-1.552188
C	-4.49847	-4.323038	-1.627367
C	-2.247553	-4.080695	-2.479361
C	-4.732183	-5.264008	-2.623389
C	-2.486365	-5.022033	-3.473378
C	-3.740322	-5.617547	-3.54384
H	-3.954155	-6.354773	-4.308773
O	-2.384406	-0.318944	2.047268
O	-1.078456	-3.399825	-2.26412
C	-1.215541	0.362468	2.262053
F	-1.937813	1.632092	4.132641
F	2.002006	0.280149	0.534117
F	2.477464	2.128137	2.483582
F	-5.465576	-3.997264	-0.752366
F	-5.940652	-5.84614	-2.701079
F	-1.524881	-5.351247	-4.349165

Table S25. Cartesian coordinates of the optimized structure for **2c** in Figure 5.

Symbol	X	Y	Z
C	-0.20241	0.016578	1.324677
C	1.054294	0.628833	1.39959
C	1.280259	1.568757	2.40347
C	0.272949	1.900513	3.325106
C	-0.987657	1.302683	3.269446
H	0.476634	2.636878	4.097352
C	-0.818978	-0.974288	0.463335
C	-2.136598	-1.133743	0.960872
C	-0.390322	-1.714706	-0.645056
C	-3.075016	-1.996643	0.419693
C	-1.328543	-2.578056	-1.185858
H	0.607717	-1.625959	-1.060413
C	-2.646214	-2.737392	-0.68842
H	-4.073194	-2.085069	0.834781
C	-3.26284	-3.728126	-1.549871
C	-4.51961	-4.34023	-1.62491
C	-2.273633	-4.081084	-2.487956
C	-4.745808	-5.279625	-2.629233
C	-2.477997	-5.013313	-3.49541
C	-3.738655	-5.611024	-3.551169
H	-3.942633	-6.34672	-4.323975
O	-2.362895	-0.31994	2.051034
O	-1.102214	-3.391933	-2.275959
H	1.838108	0.377347	0.69046
H	2.249684	2.053252	2.476192
H	-1.774832	1.549241	3.974112
H	-5.303268	-4.0891	-0.915482
H	-5.715148	-5.764314	-2.70179
H	-1.691091	-5.259255	-4.200592
C	-1.191673	0.369661	2.262656

Table S26. Cartesian coordinates of the optimized structure for **2d** in Figure 5.

Symbol	X	Y	Z
C	-1.582901	-0.665723	-0.488831
C	-0.582558	-0.334663	-1.413152
C	0.220115	0.774532	-1.196031
C	0.029647	1.562522	-0.052594
C	-0.974092	1.23261	0.877518
C	-1.776488	0.123595	0.660505
C	-2.571583	-1.719217	-0.400775
C	-3.273993	-1.471182	0.794261
C	-4.316416	-2.268746	1.242537
C	-4.655243	-3.361034	0.441283
C	-3.971222	-3.632282	-0.756251
C	-2.926306	-2.819351	-1.190287
H	-4.835844	-2.047848	2.168801
H	-5.465666	-4.013709	0.75271
H	-4.263704	-4.491394	-1.352846
H	-2.396281	-3.02606	-2.114141
C	0.66378	2.752198	0.474287
C	-0.014002	3.033798	1.676079
C	1.709213	3.587436	0.06335
C	0.300364	4.110918	2.49137
C	2.039567	4.674754	0.869386
H	2.242588	3.386015	-0.859738
C	1.345917	4.932173	2.064431
H	-0.243251	4.297977	3.411183
H	2.847357	5.336258	0.570336
H	1.62724	5.788026	2.671167
F	-0.403768	-1.095284	-2.510416
F	1.182868	1.09719	-2.081203
O	-1.011251	2.113052	1.926713
O	-2.794953	-0.351717	1.444191

Table S27. Cartesian coordinates of the optimized structure for **2e** in Figure 5.

Symbol	X	Y	Z
C	-0.236599	0.100408	1.362373
C	0.792871	0.977629	1.724594
C	0.645311	1.737987	2.883135
C	-0.508789	1.633852	3.677925
C	-1.548304	0.766451	3.33699
H	-0.596398	2.239256	4.575563
C	-0.46513	-0.832639	0.273227
C	-1.730395	-1.388185	0.541576
C	0.267305	-1.228947	-0.862519
C	-2.261649	-2.334254	-0.319387
C	-0.265657	-2.17804	-1.726235
H	1.242681	-0.794883	-1.060927
C	-1.531777	-2.732131	-1.455398
C	-2.378714	-3.714147	-2.109162
C	-3.533317	-3.815026	-1.309114
C	-2.284512	-4.502282	-3.262638
C	-4.595014	-4.6589	-1.600535
C	-3.339493	-5.357737	-3.57466
C	-4.478423	-5.434892	-2.755284
H	-5.285499	-6.110601	-3.023597
O	-2.294838	-0.886638	1.685621
H	1.688622	1.064489	1.115983
H	1.434819	2.423124	3.178418
H	-2.445698	0.674747	3.93961
H	-5.467666	-4.706556	-0.957821
H	-3.2821	-5.976178	-4.465818
C	-1.380115	0.019279	2.180401
O	-3.468313	-2.976336	-0.216141
H	0.289944	-2.491545	-2.60496
H	-1.407649	-4.448964	-3.901843

Table S28. Cartesian coordinates of the optimized structure for dibenzo[*a*,*h*]anthracene in Figure 5.

Symbol	X	Y	Z
C	-4.333863	-1.960936	-2.762993
C	-3.258612	-2.080366	-1.834863
C	-2.882797	-0.918662	-1.031105
C	-3.605504	0.309233	-1.197845
C	-4.681889	0.37326	-2.149088
C	-5.028494	-0.707535	-2.894079
C	-1.84492	-0.932469	-0.094791
C	-3.259342	1.4331	-0.436084
C	-2.221465	1.419294	0.500229
C	-1.498758	0.191399	0.66697
C	-0.422373	0.127372	1.618213
H	0.111511	-0.813549	1.72793
C	-0.075768	1.208167	2.363203
C	-0.770399	2.461568	2.232117
C	-1.845649	2.580998	1.303987
H	-1.268785	-1.838141	0.067287
H	-5.215773	1.314181	-2.258805
H	-5.844593	-0.64552	-3.609935
H	-3.835477	2.338773	-0.598163
H	0.740331	1.146152	3.079059
C	-2.500806	3.828611	1.206482
C	-2.118073	4.908723	1.984026
H	-2.642242	5.855456	1.885529
C	-1.056956	4.785249	2.897702
H	-0.758908	5.634434	3.506427
C	-0.396807	3.576306	3.015154
H	0.425971	3.46601	3.71781
H	-3.323289	3.954615	0.510415
C	-2.603455	-3.327979	-1.737358
C	-2.986188	-4.408091	-2.514902
H	-2.462019	-5.354824	-2.416405
C	-4.047306	-4.284617	-3.428578
H	-4.345353	-5.133802	-4.037303
C	-4.707455	-3.075674	-3.54603
H	-5.530233	-2.965378	-4.248685
H	-1.780973	-3.453983	-1.041291

Table S29. Cartesian coordinates of the optimized structure for picene in Figure 5.

Symbol	X	Y	Z
C	-8.370285	-4.605484	-0.164833
C	-7.25784	-4.340337	0.60607
C	-6.618311	-3.07879	0.552813
C	-7.124491	-2.0602	-0.308023
C	-8.268835	-2.366332	-1.086069
C	-8.877171	-3.605249	-1.017899
C	-5.466434	-2.801666	1.350085
C	-6.454891	-0.769807	-0.35019
C	-5.311256	-0.531077	0.457925
C	-4.844639	-1.589918	1.305142
C	-4.647439	0.754804	0.413485
C	-6.285177	1.498859	-1.230441
C	-6.912845	0.283262	-1.18827
H	-5.087823	-3.584347	2.003208
H	-8.853921	-5.577199	-0.116597
H	-6.852804	-5.100395	1.270208
H	-8.687666	-1.622143	-1.754072
H	-9.753384	-3.807778	-1.627861
H	-3.974884	-1.435583	1.931769
H	-6.684636	2.259748	-1.890851
H	-7.782691	0.132962	-1.817089
C	-5.138456	1.779972	-0.438606
C	-4.474252	3.073022	-0.486026
C	-3.490925	1.032977	1.214754
C	-2.863266	2.241863	1.17599
H	-3.095202	0.26968	1.873365
H	-1.988201	2.421787	1.796021
C	-3.327363	3.296424	0.332201
C	-2.669097	4.548903	0.298374
C	-4.909662	4.139053	-1.312231
C	-3.119206	5.565812	-0.517499
H	-1.796887	4.694556	0.931547
C	-4.25126	5.353981	-1.329191
H	-5.77695	4.013455	-1.950595
H	-2.60668	6.523634	-0.536068
H	-4.61094	6.151033	-1.974273

Table S30. Cartesian coordinates of the optimized structure for **2a** in Figure S13.

Symbol	X	Y	Z
C	-2.765993	0.386859	0.000045
C	-3.755834	1.359907	0.000012
C	-5.086592	0.978254	-0.000021
C	-5.432224	-0.377548	-0.000026
C	-4.458569	-1.368858	0.000003
C	-1.323301	0.396708	0.000023
C	-0.944527	-0.963813	0.000035
C	-0.360705	1.406187	0.000034
C	0.360705	-1.406187	0.000036
C	0.944527	0.963813	0.000023
H	-0.615685	2.455342	0.000035
C	1.323301	-0.396708	0.000014
H	0.615685	-2.455342	0.000033
C	2.765993	-0.386859	0.00001
C	3.755834	-1.359907	-0.000006
C	3.135267	0.966007	0.000007
C	5.086592	-0.978254	-0.000017
C	4.458569	1.368858	-0.000001
C	5.432224	0.377548	-0.00002
O	-2.049277	-1.789668	0.000032
O	2.049277	1.789668	0.000016
C	-3.135267	-0.966007	0.000031
F	-4.80671	-2.656544	-0.000006
F	-3.435505	2.660036	0.000006
F	-6.056508	1.895982	-0.000045
F	3.435504	-2.660035	-0.000008
F	6.056508	-1.895982	-0.000027
F	4.806711	2.656544	-0.000002
F	6.721047	0.717462	-0.000037
F	-6.721047	-0.717462	-0.000053

Table S31. Cartesian coordinates of the optimized structure for **2b** in Figure S13.

Symbol	X	Y	Z
C	2.777311	0.288026	0.000036
C	3.799289	1.228637	-0.000018
C	5.112244	0.789317	-0.000054
C	5.428095	-0.567353	-0.000035
C	4.413673	-1.508659	0.000021
H	6.462928	-0.877939	-0.000051
C	1.336181	0.348412	0.000035
C	0.909972	-0.999071	0.000046
C	0.411189	1.392391	0.000068
C	-0.411189	-1.392391	0.000071
C	-0.909972	0.99907	0.000051
H	0.705702	2.431171	0.000104
C	-1.336181	-0.348412	0.000041
H	-0.705702	-2.431172	0.000109
C	-2.77731	-0.288027	0.000058
C	-3.79929	-1.228637	-0.000007
C	-3.099129	1.076696	0.000066
C	-5.112244	-0.789317	-0.000058
C	-4.413672	1.508659	0.000021
C	-5.428095	0.567354	-0.000043
H	-6.462928	0.87794	-0.000068
O	1.982478	-1.863019	0.000039
O	-1.982477	1.863019	0.000049
C	3.099129	-1.076697	0.000051
F	4.702726	-2.817141	0.000011
F	3.518655	2.540175	-0.000054
F	6.105414	1.691699	-0.000113
F	-3.518656	-2.540175	-0.000045
F	-6.105415	-1.691699	-0.000128
F	-4.702725	2.817141	0.000008

Table S32. Cartesian coordinates of the optimized structure for **2c** in Figure S13.

Symbol	X	Y	Z
C	2.758729	0.491129	-0.000029
C	3.717216	1.503787	-0.000031
C	5.059223	1.148291	0.000006
C	5.44933	-0.196209	0.000041
C	4.509803	-1.222405	0.000046
H	6.502889	-0.44407	0.000072
C	1.313995	0.445937	-0.000034
C	0.982502	-0.926813	-0.000019
C	0.308327	1.412679	-0.000009
C	-0.308327	-1.412679	0.000003
C	-0.982502	0.926813	-0.000023
H	0.516277	2.473335	0.000009
C	-1.313995	-0.445937	-0.000027
H	-0.516277	-2.473335	0.000027
C	-2.758729	-0.491129	-0.000021
C	-3.717216	-1.503787	-0.000033
C	-3.179634	0.847202	0.000018
C	-5.059223	-1.148291	-0.000001
C	-4.509803	1.222405	0.00005
C	-5.44933	0.196209	0.000036
H	-6.502889	0.44407	0.000062
O	2.113593	-1.711635	-0.000007
O	-2.113593	1.711636	-0.000004
H	3.421412	2.545102	-0.000051
H	5.81755	1.920353	-0.000002
H	4.796586	-2.264832	0.000076
H	-3.421412	-2.545102	-0.000054
H	-5.81755	-1.920353	-0.000014
H	-4.796586	2.264832	0.000078
C	3.179634	-0.847202	0.000009

Table S33. Cartesian coordinates of the optimized structure for **2d** in Figure S13.

Symbol	X	Y	Z
C	-1.388995	0.535556	-0.000036
C	-0.690526	1.745058	-0.000027
C	0.690528	1.745057	-0.000029
C	1.388995	0.535553	-0.000047
C	0.68993	-0.680808	-0.000048
C	-0.689931	-0.680807	-0.000051
C	-2.78678	0.173776	-0.000026
C	-2.807863	-1.229631	-0.00001
C	-3.974107	-1.96954	0.000028
C	-5.16575	-1.251594	0.000067
C	-5.174755	0.148537	0.000065
C	-3.992359	0.875421	0.000014
H	-3.95196	-3.050278	0.000028
H	-6.105196	-1.788865	0.000101
H	-6.122192	0.671327	0.000104
H	-3.998338	1.956584	0.000007
C	2.78678	0.173771	0.000014
C	2.807862	-1.229635	-0.000024
C	3.992357	0.87542	0.00006
C	3.974108	-1.969541	-0.000002
C	5.174754	0.148539	0.000069
H	3.998326	1.956583	0.000071
C	5.165749	-1.251592	0.000046
H	3.951967	-3.05028	-0.000017
H	6.122191	0.671328	0.000094
H	6.105195	-1.788863	0.00006
F	-1.365232	2.907734	-0.000008
F	1.365237	2.907731	-0.000006
O	1.534749	-1.754874	-0.000045
O	-1.534751	-1.754871	-0.000043

Table S34. Cartesian coordinates of the optimized structure for **2e** in Figure S13.

Symbol	X	Y	Z
C	2.781963	0.52298	-0.000011
C	3.991921	1.216294	-0.000037
C	5.1742	0.488439	-0.000042
C	5.161764	-0.911595	-0.000027
C	3.966712	-1.623995	0
H	6.099495	-1.451945	-0.000037
C	1.383482	0.896539	0.000031
C	0.689832	-0.322899	0.000016
C	0.692125	2.117151	0.000043
C	-0.689832	-0.322899	0.000015
C	-0.692126	2.117151	0.000042
H	1.239965	3.050147	0.000039
C	-1.383482	0.896539	0.000029
C	-2.781963	0.52298	-0.000013
C	-2.802743	-0.879969	0.000012
C	-3.991921	1.216294	-0.000041
C	-3.966712	-1.623995	0.000003
C	-5.1742	0.488439	-0.000043
C	-5.161764	-0.911595	-0.000025
H	-6.099495	-1.451945	-0.000034
O	1.528877	-1.402375	0.000024
H	4.008787	2.298595	-0.000042
H	6.122861	1.009353	-0.000052
H	3.940232	-2.704822	0.000007
H	-3.940232	-2.704822	0.000012
H	-6.122861	1.009353	-0.000054
C	2.802743	-0.879968	0.000011
O	-1.528877	-1.402375	0.000025
H	-1.239965	3.050147	0.000037
H	-4.008786	2.298595	-0.000048

Table S35. Cartesian coordinates of the optimized structure for dibenzo[*a*,*h*]anthracene in Figure S13.

Symbol	X	Y	Z
C	-5.686672	0.468457	0
C	-5.069185	-0.761676	0
C	-3.665463	-0.87118	0
C	-2.870097	0.304941	0
C	-3.530683	1.547967	0.000001
C	-4.906856	1.632117	0.000001
C	-3.032728	-2.158598	-0.000001
C	-1.418916	0.177408	0
C	-0.835393	-1.127079	0
C	-1.686653	-2.2805	-0.000001
C	0.553354	-1.267856	0
H	0.948514	-2.274761	0
C	1.418617	-0.177591	0
C	0.834946	1.127177	0
C	-0.553168	1.267992	0
H	-3.663474	-3.039675	-0.000001
H	-6.766928	0.538239	0
H	-5.660851	-1.669639	-0.000001
H	-2.956825	2.463866	0.000001
H	-5.385653	2.603146	0.000001
H	-1.224005	-3.260393	-0.000001
H	-0.94854	2.274827	0
C	2.870417	-0.304983	0
C	3.665762	0.871181	0
C	1.686765	2.280675	-0.000001
C	3.032536	2.158887	-0.000001
C	3.530537	-1.54789	0.000001
C	4.907148	-1.632333	0.000001
C	5.686728	-0.468799	0
C	5.069022	0.761708	0
H	2.956676	-2.463806	0.000001
H	5.385535	-2.603555	0.000002
H	6.76703	-0.537965	0
H	5.661078	1.669476	-0.000001
H	3.663723	3.039706	-0.000001
H	1.223623	3.260388	-0.000001

Table S36. Cartesian coordinates of the optimized structure for picene in Figure S13.

Symbol	X	Y	Z
C	-5.704236	-0.381285	0
C	-5.024027	-1.609585	0
C	-3.648363	-1.646387	0
C	-2.879077	-0.461911	0
C	-3.575482	0.776296	0
C	-4.98617	0.789552	0
C	-1.429477	-0.457872	0
C	-0.681449	-1.661314	0
C	0.681186	-1.661446	0
H	1.192104	-2.612801	0
C	1.429468	-0.457995	0
C	0.72147	0.766277	0
C	-0.721522	0.766353	0
H	-6.786563	-0.36033	0
H	-5.58493	-2.53565	-0.000001
H	-5.49634	1.74566	0.000001
C	2.87902	-0.461999	0
C	3.575492	0.776226	0
C	1.47192	1.983447	-0.000001
C	2.828535	1.988198	-0.000001
C	3.648545	-1.646468	0.000001
C	5.024183	-1.609472	0.000001
C	5.704319	-0.381159	0
C	4.986178	0.789636	0
H	3.160863	-2.610288	0.000001
H	5.585239	-2.53546	0.000001
H	6.786641	-0.360184	0
H	5.496323	1.74575	0
H	3.367782	2.928132	-0.000001
H	0.957349	2.93196	-0.000001
C	-1.471945	1.983583	0
C	-2.828591	1.9883	0.000001
H	-0.957278	2.93204	0.000001
H	-3.367926	2.928184	0.000001
H	-1.192537	-2.612642	-0.000001
H	-3.16058	-2.610214	-0.000001

14. Supporting references

1. Truong, M. A.; Nakano, K. Syntheses of Dibenzo[*d*,*d*′]Benzo[2,1-*b*:3,4-*b*′]Difuran Derivatives and Their Application to Organic Field-Effect Transistors. *Beilstein J. Org. Chem.* **2016**, *1*, 805–812.
2. Karlsson, B.; Pilotti, A.-M.; Söderholm, A.-C. Quinone Oligomerization. V. Structure of Benzo[1,2-*b*:6,5-*b*′]Bis[1]Benzofuran, $C_{18}H_{10}O_2$. *Acta Crystallogr. Sect. C* **1983**, *39*, 1275–1277.